Department of Mechanical and Aerospace engineering

Quantitative analysis of an individual solar collector coupled borehole heat exchanger in the UK

Author: Alastair Harry Mahon

Supervisor: Ben Hughes

A thesis submitted in partial fulfilment for the requirement of the degree

Master of Science Sustainable Engineering: Renewable Energy Systems and the Environment

2019

Copyright Declaration

This thesis is the result of the author's original research. It has been composed by the author and has not been previously submitted for examination which has led to the award of a degree.

The copyright of this thesis belongs to the author under the terms of the United Kingdom Copyright Acts as qualified by University of Strathclyde Regulation 3.50. Due acknowledgement must always be made of the use of any material contained in, or derived from, this thesis.

Signed:

Date: 23/08/19

Abstract

In order to meet UK targets for reducing greenhouse gas emissions, the energy sector will have to see a rapid diversification away from fossil fuels. For this purpose, renewable energy systems are becoming increasingly viable as a means of generating energy with lower emissions. The advancement of energy storage systems is helping to further this process, as they are used to benefit the ability to match the supply and demand of intermittent renewable energy resources, whilst also reducing system efficiency and therefore cost.

This study evaluated the heating demand of UK homes, and compared this with the potential energy generated through a flat plate solar collector array. It was found that with heat loss coefficients of 65, 150, and 300 W/K the heating demand of homes in Glasgow and Brighton varied between approximately 5,000 and 30,000 kWh. The excess energy generated by 14 flat plate solar collectors was found to total approximately 5000 kWh and 8100 kWh for Glasgow and Brighton respectively when calculated against a heating demand derived from a heat loss coefficient of 150 W/K. This was sufficient thermal energy that its storage would be able to in some cases meet all, and in others partially meet the heating demand for homes throughout the winter.

By comparing the hourly heating and energy generation profiles, the quantity of excess thermal energy was then used to generate fluid temperature profiles to be imported in to ANSYS. Two methods of borehole loading were compared, the first with a constant and the second with a varying fluid flow temperature through the borehole heat exchanger. The constant temperature process managed to store 105 kWh in Glasgow and 130 kWh in Brighton. When using a varying temperature results of up to 1250 kWh were achieved.

Issues with simulations and changes made to the calculation methods provided varying results that left some uncertainty as to their accuracy, and as a result no firm conclusion was drawn, however a platform was laid that could be used to carry out investigations in this area with more time.

Contents

List of figures

List of tables

List of equations

1 Introduction

The UK government recently introduced legislation that aims to reduce CO_2 emissions to at least 80% below 1990 levels by the year 2050 [1]. To do this, the energy sector will have to be radically transformed, with the use of fossil fuels for both electricity and heating significantly declining in coming decades. As it stands, 45-47% of total UK energy consumption is used for heating, with 57% of this derived from domestic heating demand [2]. With the number of homes in the UK steadily increasing this energy demand is only set to rise, and if set CO_2 targets are to be met then new methods must be found of providing heating to homes. As it stands the majority of UK domestic heating is generated through natural gas, with approximately 310 TWh of energy generated through natural gas in 2018 [3].

The UK government's Standard Assessment Procedure (SAP) is used to evaluate the energy efficiency of homes presented on a scale between 1 and 100, where a score of 1 indicates highly inefficient and 100 indicates zero energy costs [4]. The SAP index is based upon a home's annual space and water heating costs for a standard heating routine. While the average SAP rating of homes in the UK had been steadily increasing, averaged at 58 points in 2017 for owner occupied and privately rented dwellings, the rate of increase has stalled in recent years (Figure 1). Two methods of increasing a home's SAP rating are either installing energy saving measures such as insulation and double glazing or installing more sustainable and energy efficient measures of generating heat for hot water and space heating. While improved energy efficiency measures are critical in reducing energy demand in the first place, it is difficult to bring old homes up to the standard that is now expected from new builds, meaning that SAP ratings remain lower. Therefore, renewable energy generation presents another means of reducing the environmental impact of heating homes.
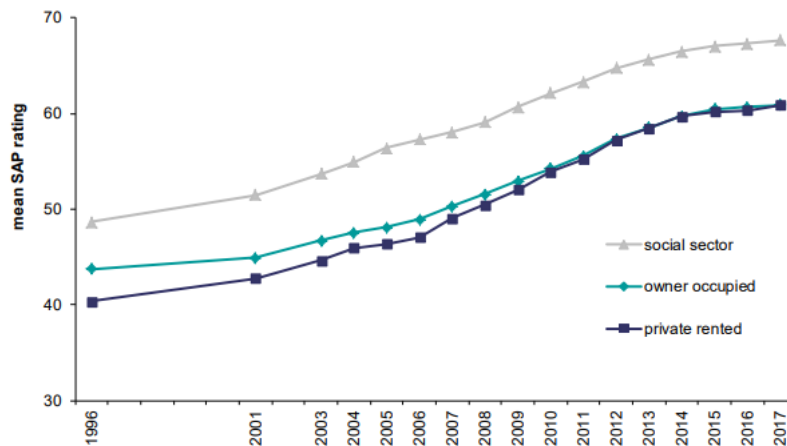
Figure 1 - Average SAP ratings for UK homes (1996 – 2017) [4]

Although renewable resources have great potential, they are limited by the intermittency or variation of supply conditions, as cloudy weather impedes solar irradiation and cold winters cool the shallow ground in which GSHP loops are often buried. As a result, renewable resources are not always suited to supplying energy on their own. By coupling a renewable energy resource with a form of energy storage, the productivity of such systems can be greatly increased, leading to improved system performance along with greater reliability and efficiency. As a result, renewable energy systems become a much more viable approach to meeting the heating demand of homes, especially as costs continue to fall as technology develops.

1.1   Project motivation

Despite being proven and embraced in a number of countries around the world, there is a distinct lack of BTESS in the UK. Upon research there is a lack of quantitative evaluation in to the potential of such systems in a UK climate despite us having similar climates to other European countries where such systems are much more prevalent. Studies have been conducted in to the potential of district scale systems, but overlook individual boreholes designed to meet the needs of a single house. Of the few published examples, the results prove promising and deserve further research. Therefore this project will seek to explore and fill this gap and evaluate the potential of an individual BHE to store and supply sufficient energy to reduce reliance on fossil fuels for heating demand.

2   Literature review

Energy storage can be an effective and efficient method of smoothing out the intermittent power supplied by renewable energy resources in addition to retaining energy that would otherwise be lost due to a lack of demand at the time of generation. Cost, size, location, and installation procedures are all deciding factors when choosing what form of TES is most suitable. TES can be split into three methods, differentiated by the way they store thermal energy.

2.1   Latent heat storage

Latent heat storage (LHS) uses thermal energy to raise the temperature of a receiving body with the intention of creating a phase change. This phase change is most commonly from solid to liquid in order to store thermal energy within the material, usually referred to as phase change materials (PCM). Solid to liquid phase change is preferred over liquid to gas as gasses require either large volumes or high pressures to be stored.

There are a number of factors that make a material an efficient medium for energy storage including its enthalpy, system operating temperature, cost, and availability [5]. Heat is stored in the PCM when it changes phase, and remains within the PCM until returned to its original state. PCM have a relatively high energy storage densities, and by virtue of this higher energy density require smaller system volumes to store the same amount of energy for latent heat storage when compared to sensible heat storage (SHS).

Extensive research has been carried out to find suitable PCMs [6, 7], but few have been commercialised. One successful example is the use of molten salts in combination with concentrated solar arrays (Figure 2). The salts are melted at high temperatures and then stored in an insulated tank where it can be stored for up to a week [8]. This stored heat can then be used to generate steam through a standard turbine and generator cycle. Large concentrated solar arrays are required to generate the heat needed to reach such high temperatures making them unsuitable for smaller applications.
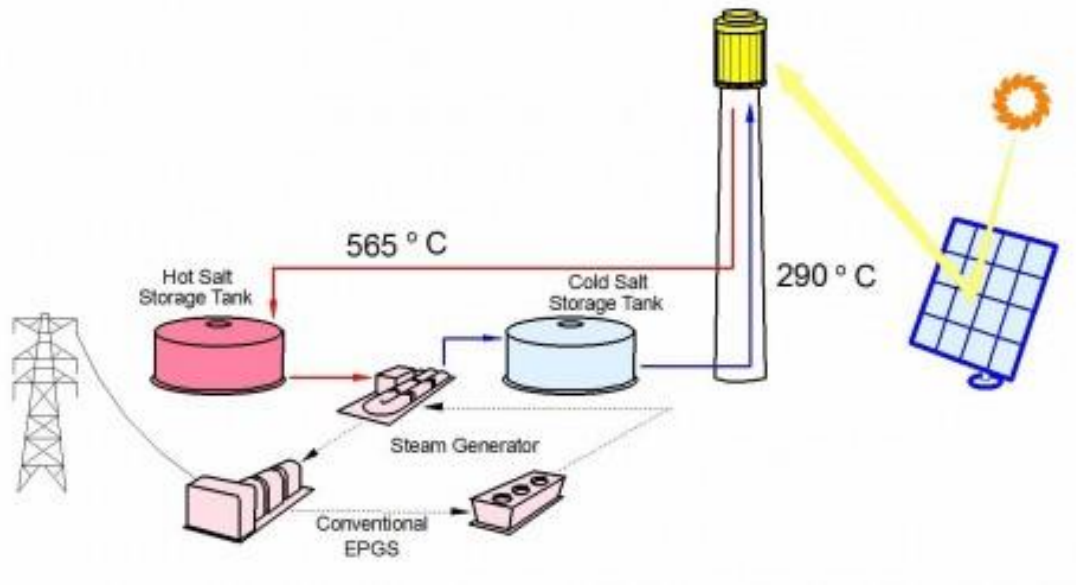
Figure 2 - Molten salt energy storage system with concentrated solar

The amount of energy that can be stored within a PCM is calculated according to Equation 1:

$$Q = m * \Delta h$$

Equation 1 - Energy stored through latent heat storage [5]

Where Q is the quantity of energy stored within the material in joules; m is the mass of the storage material and Δh is the enthalpy of phase change of the PCM.

Extracting heat from the PCM can prove difficult in some cases as a solid layer of material quickly builds up on the heat exchange surface. The solid PCM will typically have a lower heat transfer coefficient than the liquid reducing the heat transfer out of the system [9].

2.2 Thermochemical heat storage

Thermochemical heat storage (THS) uses reversible chemical reactions to store energy in separated chemical compounds. These chemical compounds are able to be stored separately and indefinitely before being re-combined to induce the reverse chemical reaction and releasing the stored heat. As the heat is stored in the form of the separated compounds there is very little

heat loss over time, making this method particularly attractive. When compared to LHS and SHS, THS has lower volume requirements, higher storage density, and lower charging temperatures [10].

There are two types of thermochemical energy storage: chemical reactions and sorption systems [5]. Chemical reactions are generally used at higher temperatures with higher volumes of energy storage required. Sorption systems use heat to separate a sorbate gas from a sorbent. This process has a much lower activation energy to start the reaction making it much more suitable for low temperature applications [11]. THS materials have a storage density approximately 8 – 10 times higher than SHS materials, and two times higher than LHS materials [11]. At the time of writing, thermochemical energy storage is still in development, however it holds great potential to be an efficient method of long term energy storage in the future. Finding the correct reversible reaction can be an issue, requiring materials with a high energy storage density that can safely and easily be stored, but are also available in a sufficient supply.

2.3   Sensible heat storage

Sensible heat storage (SHS) uses the heat contained within a body or thermodynamic system to change or raise the temperature of another body or system. This energy exchange leaves the pressure and volume of the receiving body unchanged, whilst also maintaining the original phase [5]. The amount of energy that can be stored within a body is calculated according to Equation 11:

$$Q = m * C_p * \Delta T$$

Equation 2 - Energy stored through sensible heat storage [5]

Where C_p is the specific heat capacity of the storage material in J/kg and ΔT is the difference in temperature between the two bodies or systems in degrees celsius or kelvin.

Storage materials are chosen according to their heat capacity, the space that is available for storage, and cost. Water is the most widely known and used storage material, however it is limited in that its temperature can only be raised to 100℃ before evaporating making it

unsuitable for high temperature applications. In comparison, materials like concrete can raise their temperature to over 1200℃, therefore having a much higher overall storage capacity. Appendix I lists some other possible storage materials and their thermodynamic properties. It is desirable for the storage material to have a high heat capacity as close to that of water as possible (~4.19kJ/kg-k), yet in reality most underground materials exhibit a volumetric thermal capacity of about half that [12]. At present, SHS is the most developed and utilised form of TES [4] and is generally used for space heating or domestic hot water, although some large scale commercial examples of sensible heat storage include the use of synthetic oils, liquid metals, or powders.

2.3.1   Underground thermal energy storage

Underground thermal energy storage (UTES) is a form of SHS commonly used as a form of long-term energy storage, making use of the naturally available underground sites. Thermal energy systems exist that use geothermal energy for heating and cooling such as ground source heat pumps, however UTEs differs in that it uses the ground as a storage material with the geothermal properties assisting.

UTES can be used for both space cooling and heating, with or without heat pumps, and is employed as a heat sink to help the mismatch between supply and demand of heat generation through renewable resources.

2.3.2   Aquifer thermal energy storage

Aquifers are geological formations that exist underground, consisting of water and gravel, sand, or rock [2]. Aquifer thermal energy storage (ATES) uses two wells (or two groups of wells) for the extraction or injection of groundwater [11]. During the summer, cold water is extracted from the aquifer through one well, heated above ground, and then re-injected through the other well (Figure 3). This allows the warmed water to be stored below ground until the winter when the process can be reversed and the stored heat extracted with low thermal losses in-between.
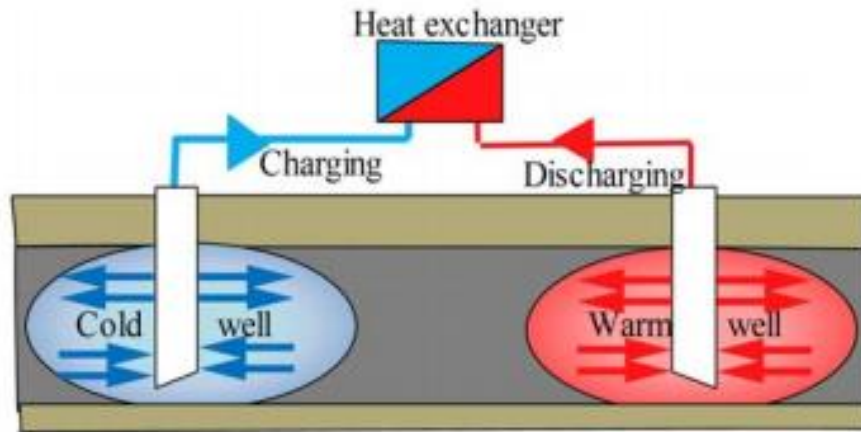
Figure 3 - Aquifer thermal energy storage system with two wells

ATES can operate either in a continuous or cyclic regime [11]. Continuous flow is used when the thermal load can be met with the extraction temperature close to that of the natural ground temperature through a continuous cycle of pumping ground water between two wells. Cyclic operation creates a hot and cold reservoir around each well, drawing or injecting from each as appropriate. Cyclic systems are disadvantaged as they are more complicated than a continuous cycle due to their operating nature, however can operate in a wider temperature range making them more suitable for a number of applications [13].

2.3.3   Hot water thermal energy storage

Hot water storage has the widest range of utilisation of the UTES methods. Due to the waters high specific heat capacity and high rate of charging and discharging, it is the most favourable in terms of thermodynamic performance. The water is contained within a large, thermally insulated tank, usually made from reinforced concrete. This tank can either be above ground or buried below the surface, and is usually insulated on at least the top and the sides [42].
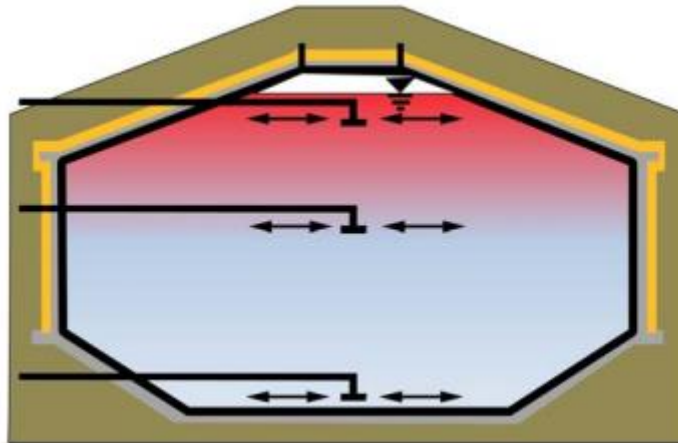
Most tanks have two levels, one at the bottom and one at the top for charging and discharging respectively. The tank pictured above in Figure 4 employs three levels, with the temperature of the stored fluid decreasing with depth from the top of the tank to the bottom. The intermediate layer allows injection and extraction of heat at different temperature points within the tank. Tanks can range in size from 270 L anywhere up to and above 10,000 L with smaller tanks usually used for short term heat storage and larger tanks for seasonal storage [5]. Most hot water tanks are not suitable for use with solar domestic hot water systems [12], with the ones that are being relatively expensive.

2.3.4   Borehole thermal energy storage

BTES makes use of underground material to directly store thermal energy for both short and long-term applications.
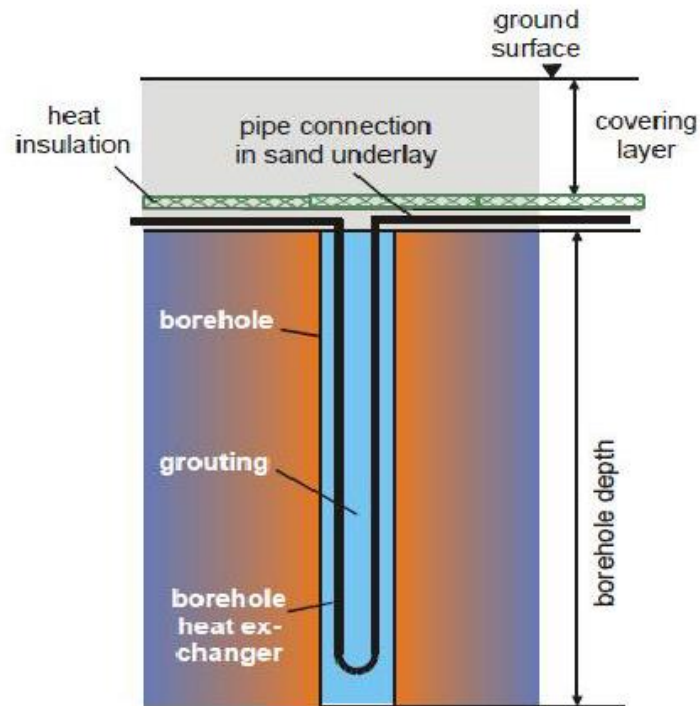
Figure 5 - Cross section of a borehole heat exchanger [46]

Figure 5 above displays a cross section of a borehole heat exchanger. The warm heat transfer fluid (HTF) is pumped through the pipe, referred to above as the heat exchanger but herein referred to as the u-tube, so that it may exchange heat with the grouting and consequently the ground material through conduction. Within approximately the first ten metres below the surface, the temperature of the ground varies throughout the year in line with the ambient temperature as it is warmed and then cooled through summer and winter. If undisturbed, below ten metres the ground temperature is much more stable, maintaining a temperature slightly above the local annual mean air temperature. As a result, heat can be pumped below ground and stored without risking excessive losses to the environment, and as the thermal conductivity of the ground material is generally low (between 1 – 5 W/K), heat does not dissipate through the ground away from the borehole extensively. Thermal losses can be reduced by having a high volume to surface area ratio, whereby the area of the surface exposed to the environment under which the thermal energy is stored is kept low in comparison to the volume of the ground material employed as a storage medium. These losses can be further reduced by installing an insulation layer just below the surface (Figure 5) as this further insulates the heated ground material from the changing ambient conditions. BTES does not have a definitive storage volume as the dissipation of heat throughout the ground cannot be controlled, but the distance it dissipates can be found and hence an estimated storage volume.

Heat is usually provided to the HTF via waste heat generated in industrial processes, or alternatively through solar collectors in domestic settings. Small solar collector arrays for use in domestic applications will operate at much lower temperate than commercial scale operations but are still capable of generating and storing enough energy for individual households.

There are three different types of heat exchanger (Figure 6): a) single u-tube pipe, b) double u-tube and c) and d) are concentric pipe
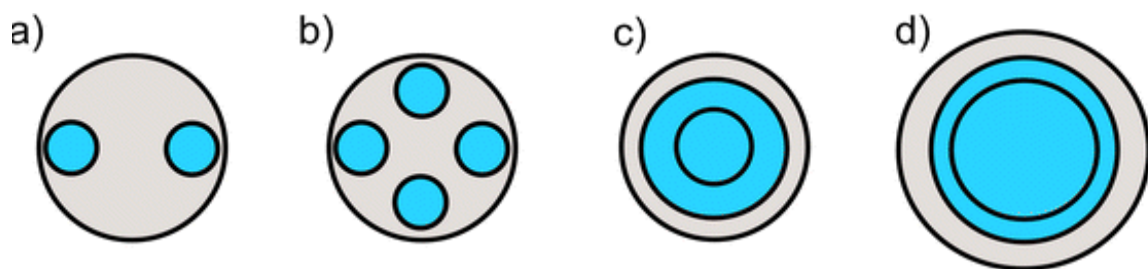
Figure 6 - Borehole heat exchanger configurations [47]

The most common heat exchanger is single u-tube, however double u-tubes are also favoured due to their ability to simultaneously inject and extract heat from the ground whilst single u-tube may operate under only one or the other. Double u-tubes offer improved efficiency and can help to reduce the required depth of the borehole, but incur more complicated system control and set-ups with two pumps needed to operate both u-tubes simultaneously.

Borehole thermal energy storage systems (BTESS) benefit from a modular approach, whereby it is easy to add additional boreholes to the system with time if the demand for energy storage grows. The heat exchangers can be arranged concentrically to create a storage field with

increasing temperature towards the centre (Figure 7). This helps to reduce losses and maintain high temperatures within the centre of the field for extraction.
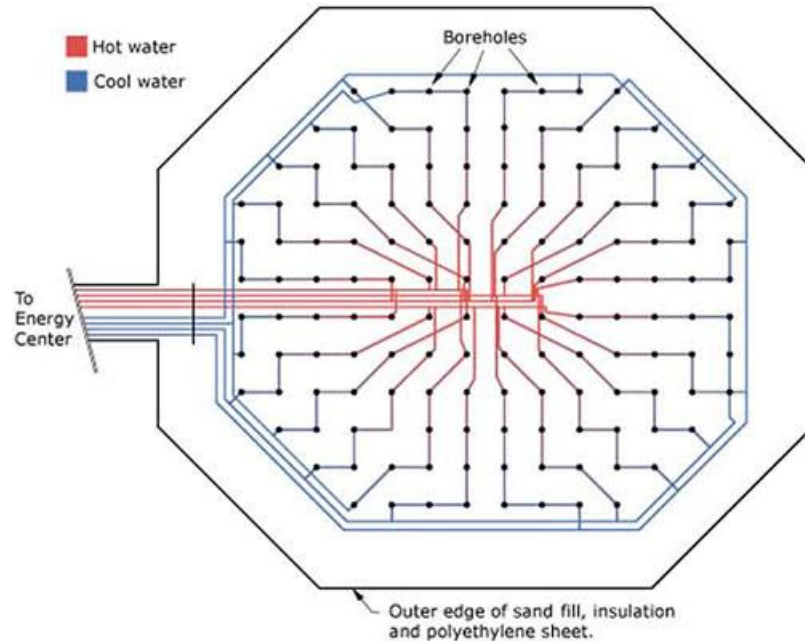
Figure 7 - Drake Landing Solar Community borehole field [14]

When extracting heat from the ground, a cold HTF is circulated through the u-tube, absorbing the heat that was previously stored. As the temperature of the exiting HTF is often much lower than the temperature required for the system application, a heat pump is used to raise the temperature of the extracted fluid to a state where it can be used.

2.3.4.1   Large scale system examples

BTES has been successfully demonstrated on both a small and large scale through a number of projects around the world. One such example is the Drake Landing Solar Community (DLSC), where a system comprised of 144, 35m deep boreholes has regularly producing an average yearly solar fraction of over 90% for the 52 homes connected to the district heating scheme [14]. Due to the success of the DLSC a number of papers have been written analysing the performance of the BTESS over its lifespan, and details how they have successfully installed and controlled the system in a particularly cold climate [52]. In 12 years of operation, only two of the solar collectors have had to be replaced, and the performance of the circulating

refrigerant has not declined, exhibiting the long term potential for such systems [15]. Whilst it is noted that DLSC itself is too small to be economically viable when compared to using natural gas to provide heating, the system design has been used to conduct feasibility studies for larger systems, reducing the cost and hence making them a viable option for district heating, even when compared to fossil fuel alternatives [16]. Figure 8 below shows the configuration of the entire DLSC system.
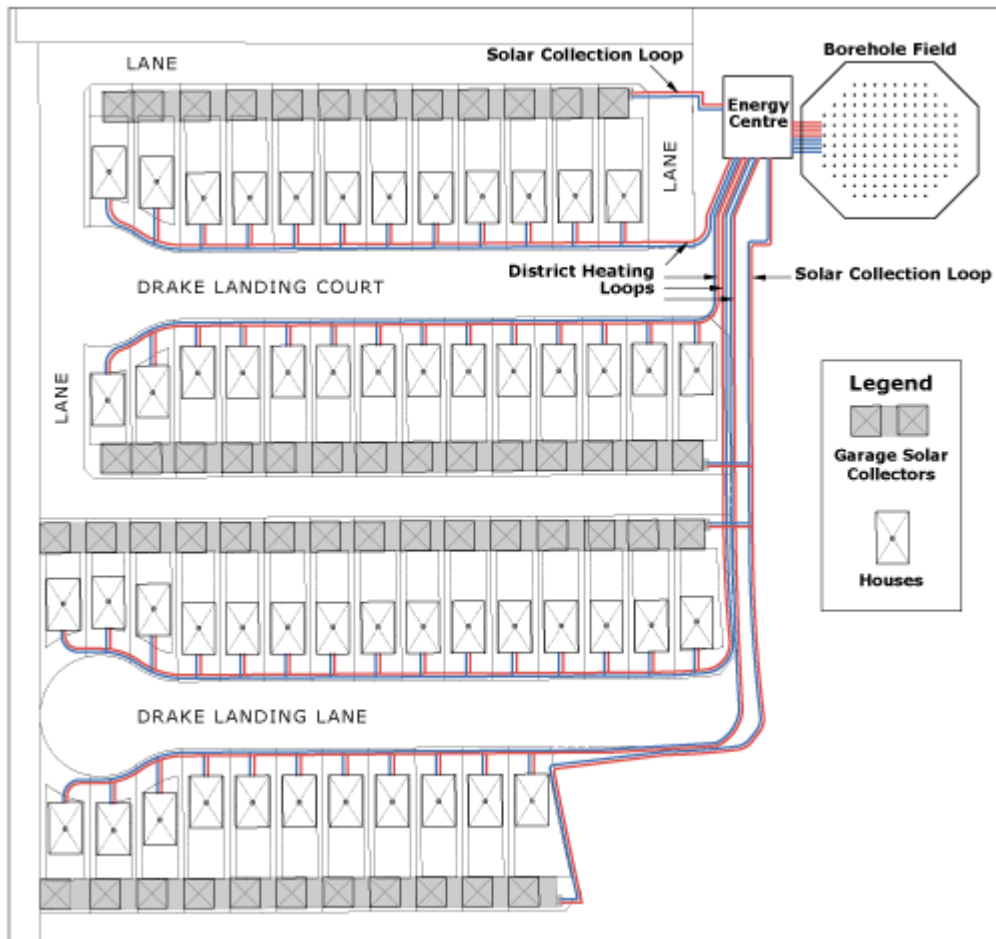
Figure 8 - DLSC solar collector and borehole heat exchanger system [K]

Another further example of BTES is the Xylem production plant in Emmaboda, Sweden. The system makes use of 140, 150m deep boreholes, recovering stored heat through two high temperature ovens and the foundry air ventilation [17]. While the system is considerable in size its performance is relatively disappointing, with the highest efficiency achieved between energy injected and extracted being only 19%. This low efficiency is attributed to the poor quality of heat supplied to the boreholes, resulting in the ground not reaching sufficient

temperatures for energy extraction. Results show a massive discrepancy between the estimated output from the plant before installation, and the actual results achieved (Figure 9), highlighting the importance of proper research and simulation prior to installation of what is still an expensive form of energy storage. The results from this project highlight the importance of accurate system analysis so that an accurate depiction of energy output may be obtained.
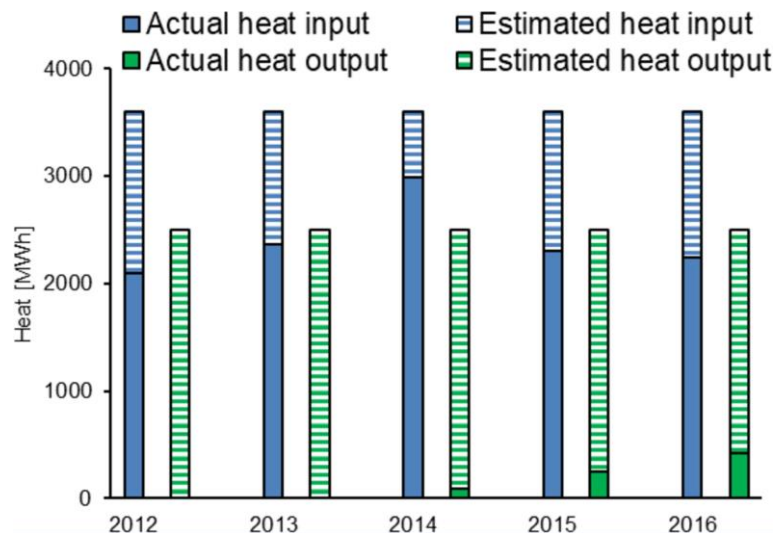
Figure 9 - Estimated vs actual heat input and output for the Xylem BTESS in Emmaboda, Sweden [17]

Gao et al [18] provide a list of large scale BTESS and their applications. The systems profiled are primarily located in Germany, Sweden, and China, and range in size from a single family house up to a 20000 m^2 borehole field, with generated solar fractions between 50 and 97%.

2.3.4.2   Small scale system examples

Trillat-Berdal et al [19] present an analysis of a single borehole coupled to a ground source heat pump (GSHP) to provide heating for a private residence. The system control sets domestic hot water as a priority for heat gained from the solar collector, with excess heat stored underground. The study concludes that while BTES was a viable option for home heating, the coefficient of performance (COP) of the GSHP was significantly impacted by continuously extracting heat from the ground, and therefore it is important to determine an efficient method of heat extraction that both meets the heating demand of the house whilst maintaining system efficiency. The pump system is switched on and off depending on the difference in temperature between the storage tank and solar collector outlet temperature. In this case, the pumps to

circulate the HTF through the borehole heat exchanger are activate when the temperature difference between the solar collector and pressure relief tank is above 18℃, and then deactivated when this temperature difference falls below 12 ℃ (Figure 10). This provides an idea of the sort of temperature range that individual borehole heat exchanger systems can be operated in when attached to a single house.
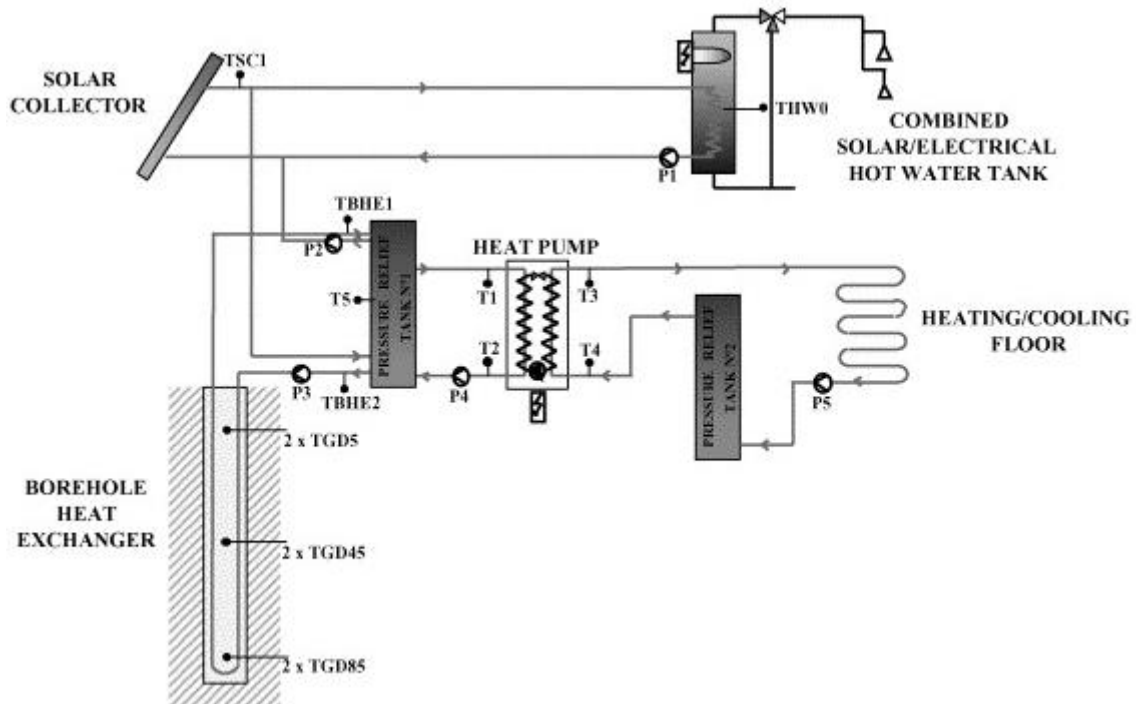
Figure 10 - System design for a solar collector coupled borehole heat exchanger as used by Trillat-Berdal et al [19]

Beier et al [20] created an actual model to generate a dataset for the validation of results for borehole analysis. The sandbox was 18.3 m long and 1.3 m long, with a u-tube buried in the centre. A schematic of the system is shown below alongside an image of the sandbox (Figure 11). Fluid was circulated through a pipe buried in the sandbox, with heat constantly applied to steadily increase the HTF temperature. The temperature of the fluid at the inflow and outflow was then measured with time and recorded. This dataset is useful for small boreholes with constant heat addition, however if this was to be attached to a domestic heating load a borehole depth of 18.3 metres is unlikely to be sufficient to store a sufficient quantity of thermal energy for a domestic heating load.
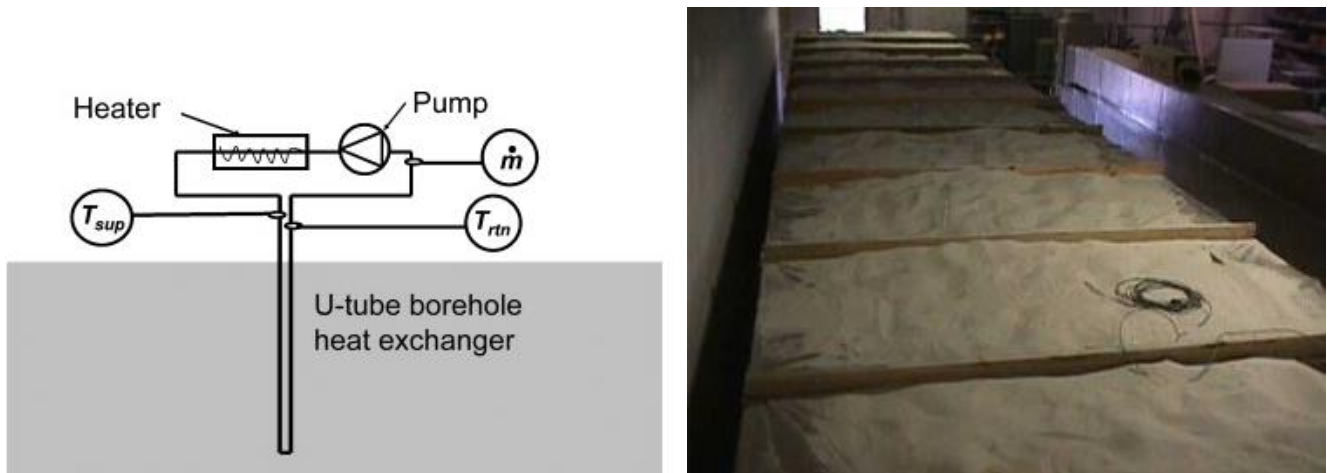
Figure 11 - System configuration (left) and sandbox frame with cover removed (right)

Kerme and Fung [21] present an analysis, simulation, and performance study of a single u-tube borehole as a method of validating numerical calculations. This study was developed in order to reduce the amount of time researchers spend exploring the impact of various parameters of performance, and also provides an analysis complete with dimensions and results of a 100m borehole. The dimensions and results from this paper were consequently used to develop and validate an ANSYS model of a single u-tube BTESS that will be further detailed later in this project.

As location, weather, and ground conditions all affect the performance of a BTESS, it is hard to accurately predict the performance of a system based upon other results. Therefore, location specific analysis is required to determine the potential of such systems before deployment in relatively untested areas.

2.3.4.3   Numerical and analytical models of borehole heat exchangers

The modelling and analysis of heat transfer through boreholes is a complex issue and as a result, numerous numerical and analytical models have been developed that aim to accurately predict the flow of heat from within the borehole to the surrounding rock or soil. The complexity of the issue is derived from the number of factors that must be considered due to their influence on exchanger performance, such as the thermal properties of the ground, water content within the receiving body, and natural ground temperature variations [22]. Other difficulties include assessing the exchange of heat between the upward and downward sections of the u-tube pipe contained within the borehole. This is because as the circulating fluid is a

different temperature in each leg of the u-tube and therefore exchanges heat with itself. As such, generating an accurate validated model is crucial to guarantee accuracy within the results obtained.

Due to the difficulties in the analysis, most numerical and analytical approaches split the problem in two, modelling heat transfer inside and outside of the borehole as separate problems. Two of the earliest approaches are the infinite line source model and cylindrical source model, both one-dimensional analytical solutions. The infinite line source model was first developed by Ingersoll et al [23], and approximates the borehole as a one-dimensional line vertical in the ground that is considered as an infinite medium. Heat transfer in the direction of the borehole axis is ignored and is therefore simplified as one dimensional, making this model only appropriate for short time steps from a few hours to months, as well as only usable for narrow pipes. The cylindrical line model was first developed by Carslaw et al [24], and then further refined by Ingersoll et al [25], and is considered a simplification of the aforementioned infinite line source model. In this model the borehole is assumed as an infinite cylinder buried in the ground which has constant properties. Both models are suitable for short term simulations, however due to their assumptions they become less accurate with increasing time as they neglect axial heat flow along the borehole depth [22]. Therefore, these models have been used and adapted to include an increasing number of parameters, hence increasing the accuracy of the models and allowing their application for a wider range of situations. Yang et al [26] lays out a much more comprehensive explanation of the workings behind the thermal analysis of boreholes, including the equations derived and developed over the years.

In more recent times the analysis of boreholes is usually conducted through computational fluid dynamic software, drastically reducing the time taken to assess the flow of thermal energy through the system. Two examples of such software are TRNSYS [27] and ANSYS [28] which are widely used for the evaluation of proposed energy systems, with ANSYS fluent used to evaluate the BHE within this project.

2.4   Solar collectors

Solar collectors use incident solar radiation to generate heat. There are two main types of solar collector, flat plate and evacuated tube. The choice of which to use depends upon the climate, roof type, wider system components, and budget. They are often used in domestic applications as they can easily be mounted on roofs and easily linked with an intermediate storage tank to provide thermal energy for space and hot water heating.

Solar collector arrays can be used in high temperature systems to further raise the temperature of the HTF following collection of waste heat, or in lower temperature systems in the range of 40 - 60°C for domestic applications.

2.4.1   Flat plate solar collector

Flat plate collectors (FPC) consist of an insulated enclosure, within which is an absorber plate and heat riser tubes (Figure 12). A glass cover over the absorber plate is used to reduce convection losses from the collector tubes, as well as reducing long wave radiation losses from the absorber plate back to the environment [29]. The glass cover also refracts the incident radiation, and therefore must be accounted for when calculating useful energy output.
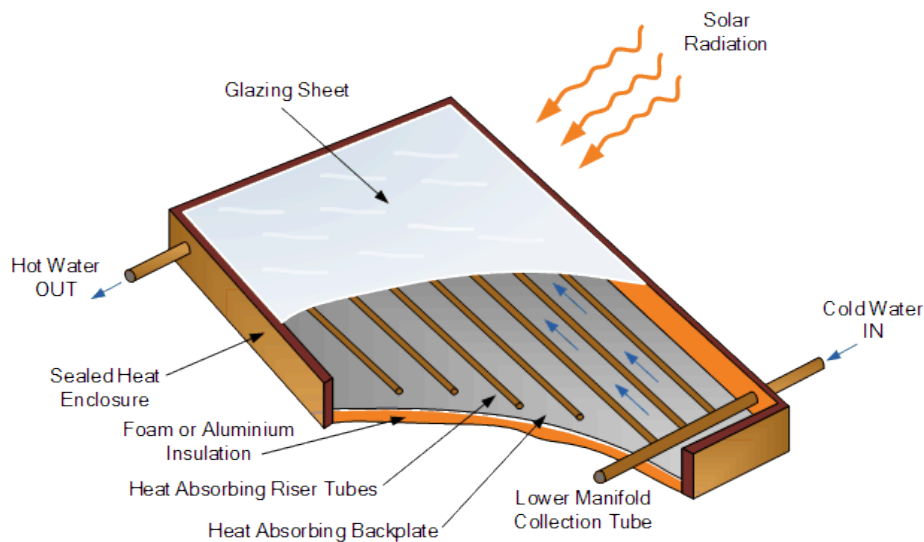
Figure 12 - Flat plate solar collector [AL]

The absorber plate is darkly coloured so that it may absorb as much radiation as possible, transferring the generated heat to the connected tubes through which the HTF circulates. The quantity of heat transferred to the fluid depends on both the thermal conductivity as well as the configuration of the riser tubes (Figure 13). Lenel [30] found that by changing the configuration of the tubes, materials with lower thermal conductivity could be used. Karim et al [31] also commented on the impact of different absorber colour, finding that black and blue absorbers outperformed red and brown.
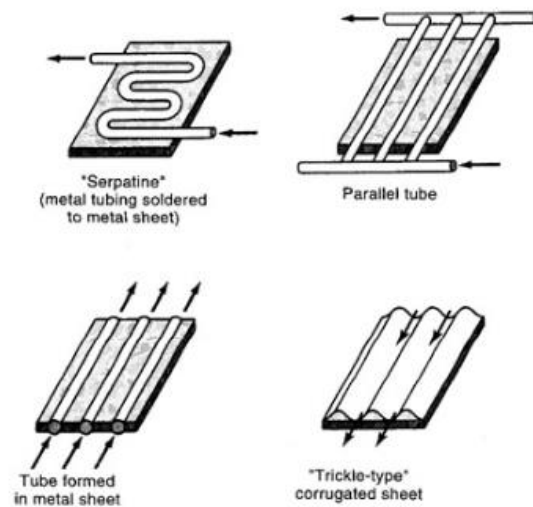
Figure 13 - Possible heat riser tube configurations within FPC [BL]

In warmer climates, water suffices as a heat carrier, however in colder climates refrigerants are often mixed in to the water to prevent freezing within the tubes. Typical refrigerants include ethylene or propylene glycol, mixed at the concentration required to prevent freezing depending on the lowest temperatures reached. The efficiency of a flat plate collector depends on the optical and thermal losses experienced due to the conduction, convection, and radiation heat transfer interactions with the environment, as well as the tilt angle and positioning of the panel relative to the path of the sun [32].

FPC tend to work in a temperature range of between $40 - 60°C$, around the same temperature as domestic hot water. Using a lower fluid inlet temperature results in reduced losses to the ambient due to smaller temperature differences, however incurs a lower quality of heat at the outflow as overall system temperatures are lower.

2.4.2 Evacuated tube solar collector

Evacuated tube collectors (ETC) work by heating a pipe within a vacuum sealed tube via incident solar radiation. The collector pipe is usually made of copper, and the HTF inside the collector tube undergoes an evaporating-condensing phase change cycle as it is heated by the solar radiation. As the fluid evaporates it travels up the collector tube to the condenser, where a flowing fluid is passed over the condenser to remove the heat gained by the HTF (Figure 14).

This causes the HTF to then condense, and sink back down the collector tube to then begin the cycle again. The vacuum serves to reduce losses through conduction and convection, meaning they are capable of operating at much higher temperatures than FPC [29].
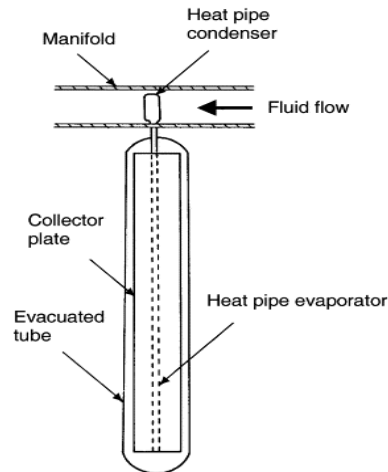
Figure 14 - Evacuated tube solar collector [29]

FPC are often preferred to ETC as they can efficiently absorb direct and diffuse radiation allowing them to be mounted stationary, whereas ETC operate primarily on direct radiation and therefore require sun tracking to generate sufficient energy making them initially more expensive [29].

3   Methodology

This paper will seek to quantitatively evaluate the operational performance of a borehole heat exchanger (BHE) coupled with a roof mounted solar collector array to meet the space and water heating demand of UK dwellings. This is not intended as a full system analysis, but will instead look at the individual performance of both solar collectors and BHE to determine if there is scope for the installation of such systems in the UK.

3.1   Space and water heating

Firstly, the heating demand of an average UK dwelling will be estimated on an hourly basis using appropriate weather and location relevant data. With access to the building, practical methods such as a co-heating test may be employed whereby an unoccupied dwelling is heated

from the inside using electrical point heaters and the amount of energy needed to maintain an internal temperature, typically 25℃, is measured. From this, the heat loss coefficient of the building can be calculated from the difference in temperature between the inside and outside of the building [53].

Alternatively, the method used by the UK government for widespread analysis is the BREDEM method [33]. The BREDEM method has been developed over 30 years and is the result of work carried out to evaluate the energy consumption of a dwelling based upon the buildings characteristics. The BREDEM method takes into account a large number of parameters such as energy consumption for lights, cooking, and heat gains through solar and internal sources. While this method generates an accurate depiction of household energy consumption, the process requires extensive data about the building and the habits of its inhabitants making it unsuitable for this project for the purpose of space heating. However, the section within this method is used to evaluate water heating requirements as this requires much less information and therefore can easily be applied.

Karacavus and Can [34] used a much more simplistic method for calculating space heating requirements as is displayed in Equation 3, with energy requirements being a function of the desired indoor temperature, the ambient temperature, and the heat loss coefficient (or U value) of the building in question only:

$$Q_{sh} = U(T_i - T_a)$$

Equation 3 - Calculation of energy required for space heating [34]

Where Q_{sh} is the energy required for space heating in joules; U is the overall heat loss coefficient of the building in watts per kelvin (W/K); T_i is the designated indoor temperature and T_a is the ambient temperature both in degrees celcius.

As the temperatures are being subtracted from one another there is no need to convert the temperatures from celcius to kelvin as this will give the same result.

3.2   Solar collector analysis

Following the assessment of heating demand, the useful energy gained from a solar collector will be determined using relevant equations from literature to develop an hourly thermal energy generation profile. A FPC will be evaluated to determine the amount of useful heat that can be gained, firstly to directly meet the combined heating demand for space and hot water, with excess heat then used for heat storage. The process of this evaluation is non-trivial and involves a number of equations based upon the location of the solar collector in question, the time of day, and the impact of the weather.

The equations required to calculate the useful heat from a solar collector can be found in 'Solar engineering of thermal processes' [35]. In addition to the equations required for the solar collector, equations for solar positioning and time are required, also be found in [35], or may also be commonly found online. These equations were incorporated in to an automatic tool used to find the useful energy present in the outgoing HTF in any location by inputting relevant weather data, panel parameters, and latitude/longitude. Appendix III details the process followed to calculate the useful energy gained in the development of the tool in question.

This energy profile will then then be compared to the hourly heating demand from the dwelling in question. Presuming that the useful energy generated from the solar collector is greater than the heating demand of the dwelling, the excess energy will then be used to heat a HTF that is then circulated through the BHE.

3.3   ANSYS model

A 3D, meshed geometry was hence created in ANSYS fluent to evaluate the performance of the borehole heat exchanger. This involved developing a 3D model from data provided in literature so the model could then be validated against published results. ANSYS is a computational fluid dynamics simulation software used to analyse the flow of fluids and thermal exchange between bodies over time. It is capable of monitoring changes over time and can be used to determine the quantity of thermal energy transferred between the HTF and the ground.

In this case it will be used to evaluate the borehole heat exchanger in situations of injection and extraction through a single u-tube. ANSYS is capable of running steady state and transient simulations. Steady state simulations use constant parameters to find the state of equilibrium

reached according the pre-determined boundary conditions. Time varying parameters can also be read by the program and used to evaluate the performance of the heat exchanger with a constant or changing fluid flow temperature. From simulations, the quantity of thermal energy that can be stored in the ground will be assessed and compared with the heating demand of a UK home to decide if such a system would be of benefit.

4   System design

While operating as separate systems, the borehole heat exchanger and solar collectors are often connected through an intermediate storage tank used as a heat exchanger for the hot and cold fluids flowing through the BHE and FPC. Figure 15 displays a setup that may be found in a domestic environment that incorporates both a solar collector and BHE. The HTF fluid is warmed through the solar collector before passing through the domestic hot water (DHW) tank. Here heat is exchanged with the water in the DHW tank before the HTF is recirculated through the solar collector to continue its cycle. The DHW tank is fed with cold water at the bottom allowing warmer water to rise to the top. Via this process the heat gained by the solar collector is stored within the DHW tank until there is a heating demand or it is stored in the ground. When hot water or space heating is used within the house, the heating circuit is activated. This draws heat from the DHW tank by circulating a cold HTF through the tank, raising its temperature to provide heating. Typically, domestic space heating is kept at approximately 21℃, with hot water in the range of 40 to 60℃. In the case that the heat output from the solar collector insufficient, heating circuits are coupled with a gas or electric boiler to make up the shortfall. All of this heat transfer is achieved through heat exchangers that incur losses through radiation and convection to the surroundings.
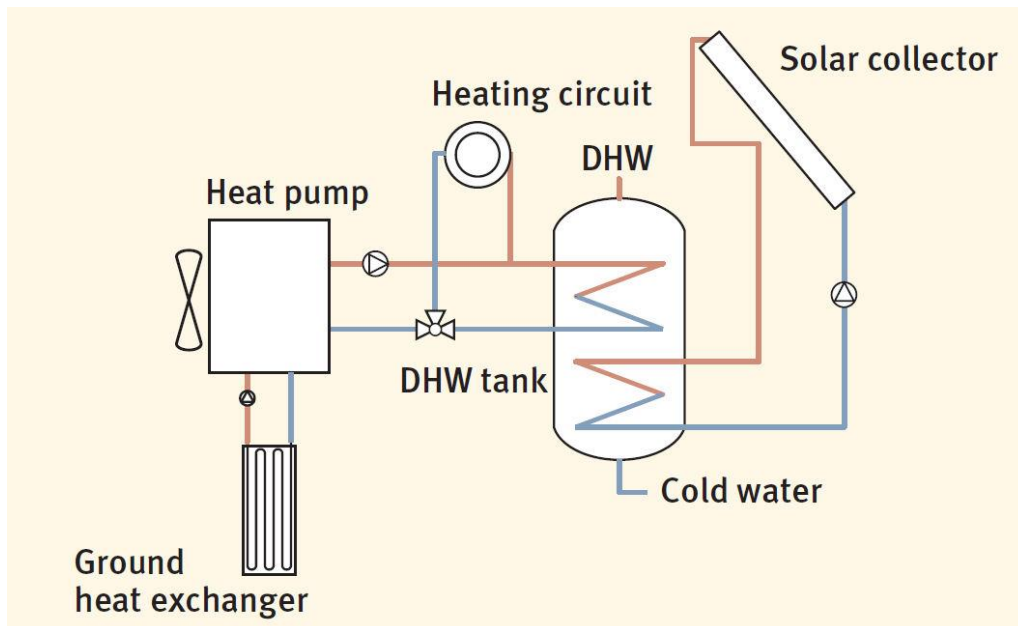
Figure 15 - System configuration for a FPC and BHE connected through a domestic hot water tank

If the solar collector array generates sufficient heat that following the extraction of heat to meet the heating demand there is an excess or thermal energy, then the ground heat exchanger system is activated to store this heat below ground. This system operates at a lower temperature than the domestic heating system, and only needs temperatures slightly above that of the steady state ground temperature to facilitate a net transfer of heat from the HTF to the ground. Typically, the borehole pump system will become active when the temperature in the DHW tank exceeds a certain temperature, indicating there is an excess of heat.

This systems is operated with the intention of storing as much energy within the ground as possible, placing a reduced emphasis on meeting heating and water demand during the summer as all excess thermal energy is circulated through the BHE.

5   Assessing heating demand

As of 2017 there were over 24 million dwellings in the UK (where a dwelling is defined as being a self-contained unit of accommodation [36]). 15.3 million of these dwellings are owner occupied and the rest either privately rented or used for social housing [21]. The most common type is semi-detached, representing just over 30% of the owner occupied housing stock, followed by detached and medium/large terraced house representing 25% and 18% respectively (Figure 16).
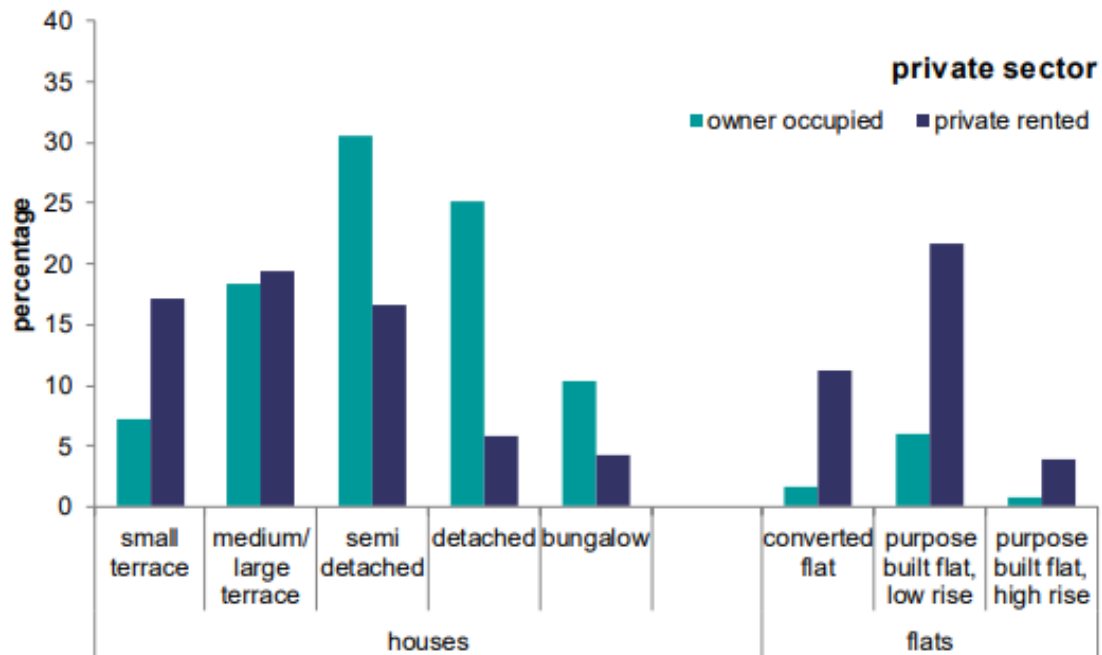
Figure 16 - UK housing stock by dwelling type [4]

As it stands, the majority of people rely on gas or electric boilers to provide heating for their homes. In a report produced by the English housing survey [4], it was found that within owner occupied homes, 45% had a boiler that was between 3 - 12 years old, and 27% had a boiler that was more than 12 years old. Old boilers are renowned to be inefficient, and lead to higher than necessary energy usage resulting in increased energy bills for the occupants as a result.

To ensure the proposed system was widely applicable, the average UK home was used for the purpose of this analysis. The average owner occupied home is represented by a semi-detached building with two occupants [37]. It is also important that the home in question would have the space necessary for the installation of a BTESS. These statistics, in addition to any further required data will be used to analyse the average domestic hot water and space heating requirements within the UK.

Heating requirements are highly dependent upon ambient temperature. Consequently, Glasgow and Brighton were chosen to be representative of both sunny and cloudy climates.

5.1 Space heating

Space heating was calculated according to Equation 3 as was laid out in the methodology. For this, research was undertaken to determine heat loss coefficients, ambient temperatures, and internal heating temperature for Glasgow and Brighton.

5.1.1 Ambient temperatures

Energy demand for heating is naturally a function of ambient temperature, with higher outdoor temperatures generally leading to reduced heating loads. Figure 17 shows the average monthly ambient temperatures. In the absence of multiple years of ground measured weather data, values were taken from Renewables.ninja [38], and were averaged between the years 2016 – 2018 to reduce the impact of irregular weather patterns. Whilst they follow much the same pattern, during the summer, Brighton is on average over 2 degrees warmer almost throughout the whole year.
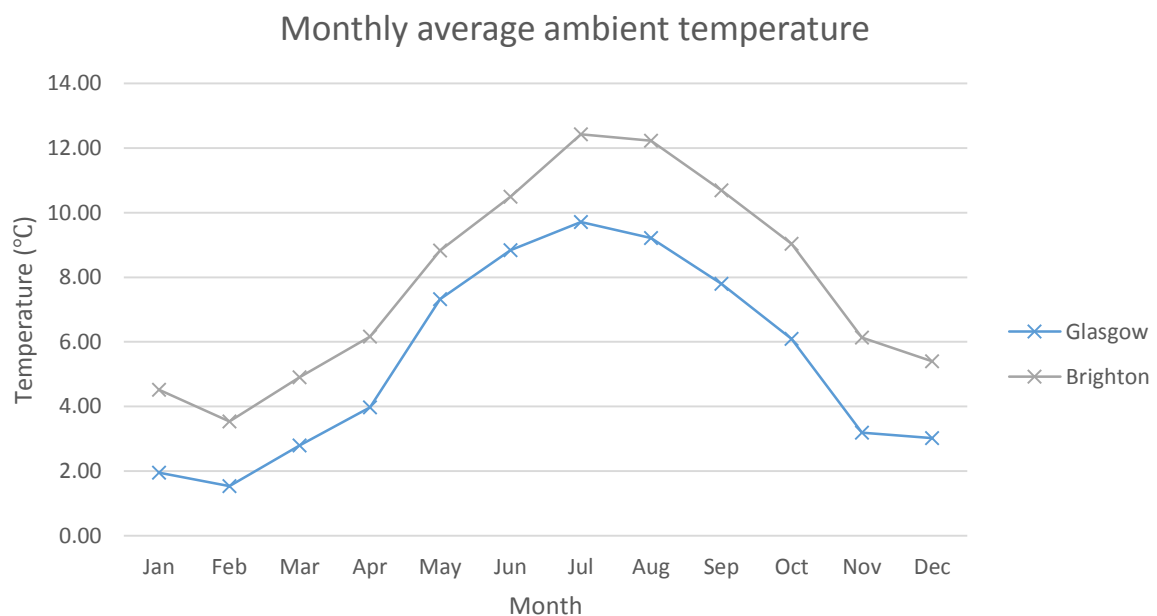
Figure 17 - Monthly average ambient temperature by location

5.1.2 Internal heating temperature

Internal temperature depends largely on personal preference, however this is usually in the region of 21℃ as is used by the BREDEM method. Shipworth et al [39] conducted a study as to the heating habits of a variety of UK dwellings, recording thermostat temperatures at forty-

five minute intervals to a resolution of 0.1℃ over a year, finding that actual indoor temperatures deviated significantly from the presumed 21℃. Estimated thermostat temperatures were often higher than actual thermostat settings, and location played a significant part in determining the average thermostat temperature over the course of a year. Figure 18, taken from Shipworth depicts the actual and estimated distribution of thermostat temperatures, and highlights that the majority of homes in fact prefer lower thermostat settings than was previously thought. This serves to reduce predicted heating demand over the year for the majority of homes.

Figure 3 Thermostat settings: estimated and reported
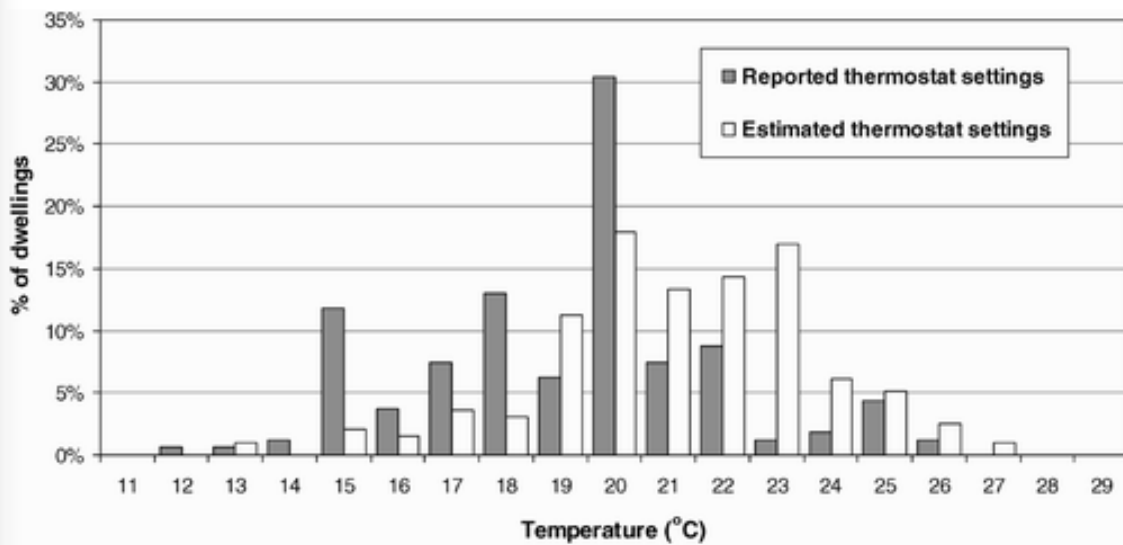
Figure 18 - Predicted vs measured thermostat temperatures [39]

These statistics can be further broken down into preference by house type and location as seen in Figures 19 and 20. From this we see that average reported temperatures are approximately 2℃ lower than the predicted, and therefore using an indoor temperature of 21℃ as in the BREDEM method is likely to lead to an overestimation of heating demand. Hence, the reported thermostat values were used when determining space heating energy demand, with reported thermostat temperatures from the South East used for Brighton, and the North West used for Glasgow in the absence of any available data for Scotland.

	Thermostat setting (°C), estimated				Thermostat setting (°C), reported [a]			
	Mean	95% CI for the mean	SD	n	Mean	95% CI for the mean	SD	n
Accommodation type [b]								
End terrace	21.2	19.6, 22.7	3.2	19	19.2	17.5, 20.8	2.7	13
Mid-terrace	21.0	20.1, 21.9	2.3	29	19.3	18.1, 20.4	2.6	22
Semi-detached	21.6	21.0, 22.3	2.3	55	18.8	17.9, 19.7	3.3	49
Detached	21.0	20.4, 21.6	2.5	70	19.3	18.6, 20.1	2.9	59
Purpose-built flat	21.6	20.3, 23.0	2.4	14	18.5	15.9, 21.1	4.3	13

Figure 19 - Predicted vs recorded thermostat settings by house type [39]

	Thermostat setting (°C), estimated				Thermostat setting (°C), reported [a]			
	Mean	95% CI for the mean	SD	n	Mean	95% CI for the mean	SD	n
Government Office Region								
North East	20.3	19.4, 21.2	1.5	14	19.3	17.2, 21.4	3.3	12
Yorkshire and the Humber	20.9	19.8, 22.1	2.5	20	17.1	15.7, 18.6	2.8	16
North West	21.2	19.9, 22.5	3.0	24	18.7	17.3, 20.0	2.4	15
East Midlands	21.5	19.8, 23.2	2.7	12	18.2	16.4, 20.0	2.5	10
West Midlands	21.2	20.5, 22.0	1.9	25	19.1	17.1, 21.1	4.7	23
South West	21.0	20.2, 21.8	2.3	33	20.2	19.0, 21.4	2.2	15
East	21.5	20.2, 22.8	2.9	21	19.3	18.1, 20.5	2.4	17
South East	21.0	19.9, 22.1	3.1	32	18.8	18.1, 19.6	2.2	36
London	21.7	20.1, 23.2	2.7	14	20.3	18.8, 21.7	3.1	20

Figure 20 - Predicted vs recorded thermostat settings by location [39]

5.1.3   Heat loss coefficient

Differing heat loss coefficients were taken in to account to represent the varying states of thermal insulation in UK housing. As building regulations have changed over time, maximum U values for new buildings have been introduced [40]. However, as homes are built to last many of them still have U values that are far greater than the new build regulations stipulate. The majority of both owner occupied and privately rented homes were built well before 1995 (Figure 21), meaning that energy efficiency is likely to be far removed from that expected from new builds. Installing insulation in walls and roofs or changing to double glazed windows can help make improvements although this is not always feasible. While new builds are prescribed a U value, the measured value often differs from the predicted. Wingfield et al [41] carried out co-heating tests on a number of new buildings, and found that measured whole house U values were much higher than predicted, in some cases by as much as 100%. The study found for

semi-detached houses, despite predicted U values of as low as 63.8 W/K, measured values were in the region to 105 - 120 W/K, predominantly due to underestimations regarding the U values of walls, floors, and ceilings. At the other end of the scale, an old building that has had little or no modification in terms of improving thermal efficiency may have a U value of up 300 W/K. This high value is commonly due to extensive heat loss through poorly insulated windows, walls, and lofts. Because of this variation, the evaluation of heating requirements for low, medium, and high U values will be considered at 65, 150, and 300 W/K respectively.
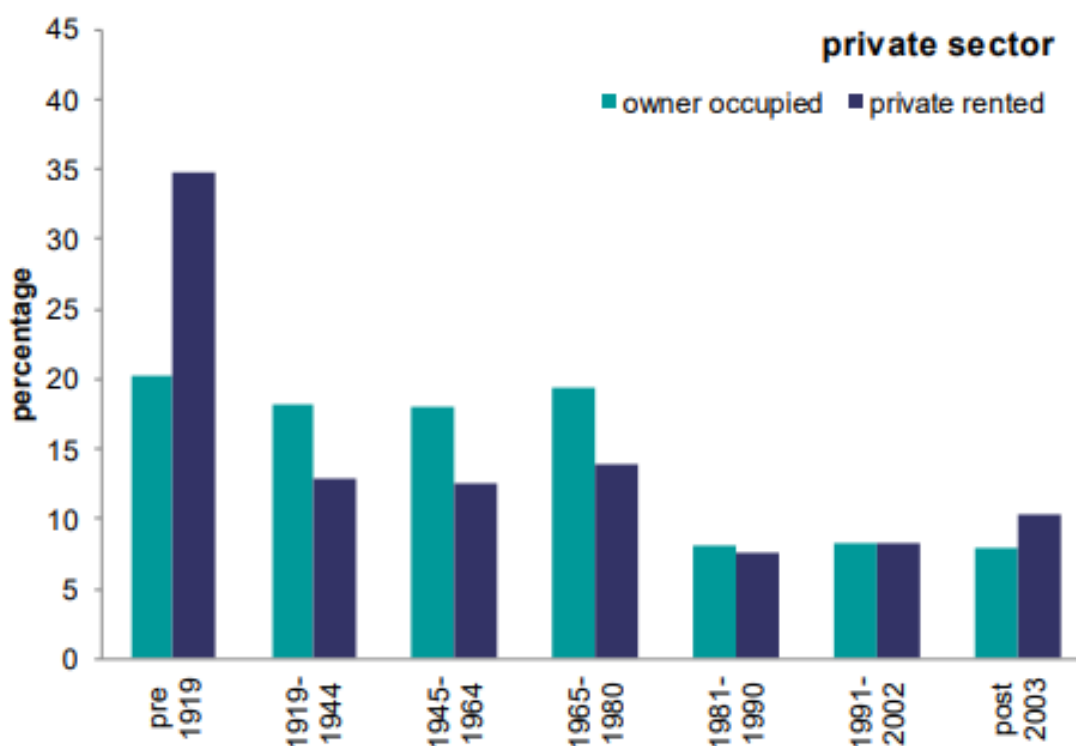
Figure 21 - Age of UK homes [4]

5.2   Water heating

UK households use on average 349 litres, or 142 litres per person [4]. Approximately 55% of water usage is hot water, with the main sources shown to be showers, baths, and washing machines (Figure 22).
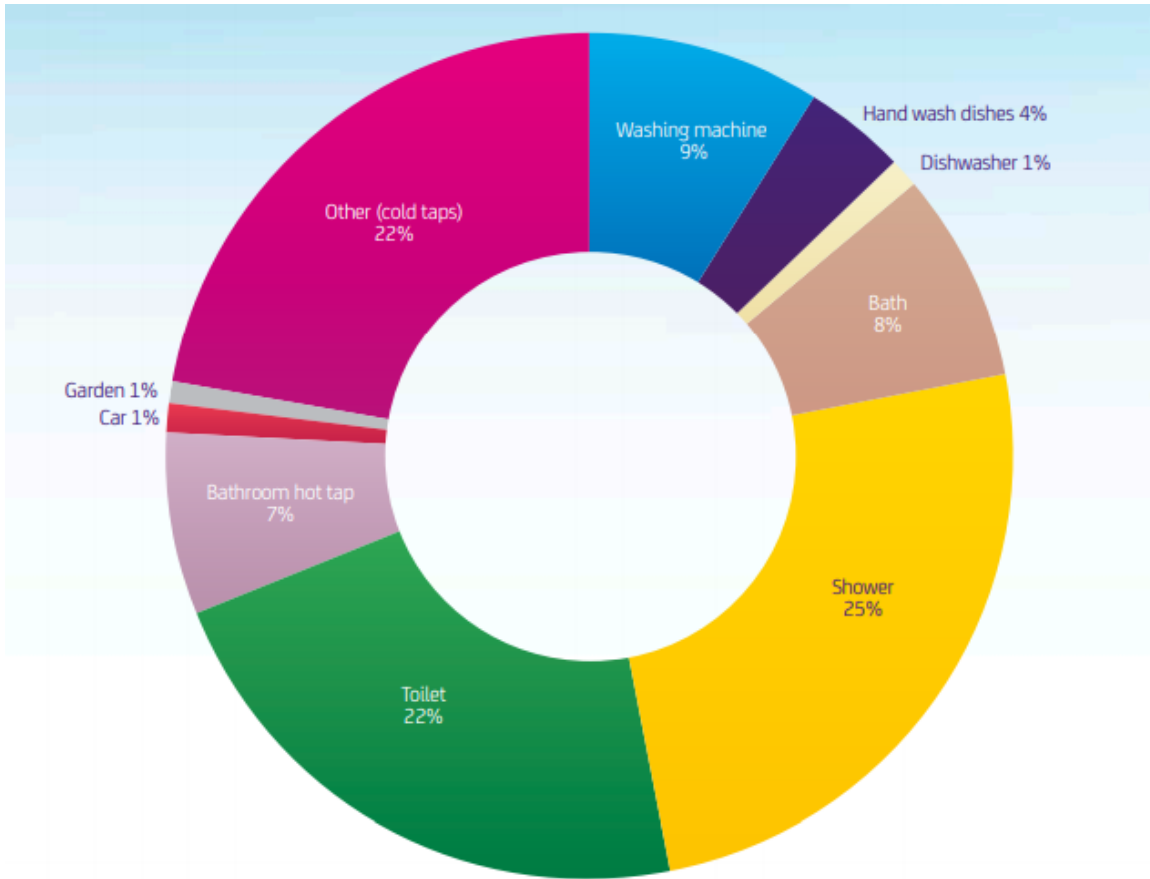
Figure 22 - Breakdown of domestic hot water usage [4]

The amount of hot water used on a day-to-day basis remains reasonably constant over the course of a year, however the amount of energy required to heat this water varies according to the cold water feed temperature. The water heating section of the BREDEM method [I] is used to estimate hot water energy demand. Factors including the number of occupants in a household and the number of baths or showers taken each day, with the process followed outlined in Appendix IV. The Energy Saving Trust [42] performed a study on approximately 120 UK households, comparing actual measured results for hot water usage with those obtained the BREDEM method. The study found that the BREDEM method was likely to overestimate the actual energy usage for hot water by up to 35%, largely due to the fact that hot water delivery temperature was estimated as 60 °C when measured hot water delivery temperature was only 51.9°C +/- 1.9°C. It was also assumed that the cold water delivery temperature was 10°C, however this is known to vary with both location and time of year, as is indicated below (

Figure 23). The midlands have the highest average cold water delivery temperature, followed by the south of England. Both Scotland and northern England's cold water delivery temperatures are on average 1 - 3 °C colder than in the south or midlands.
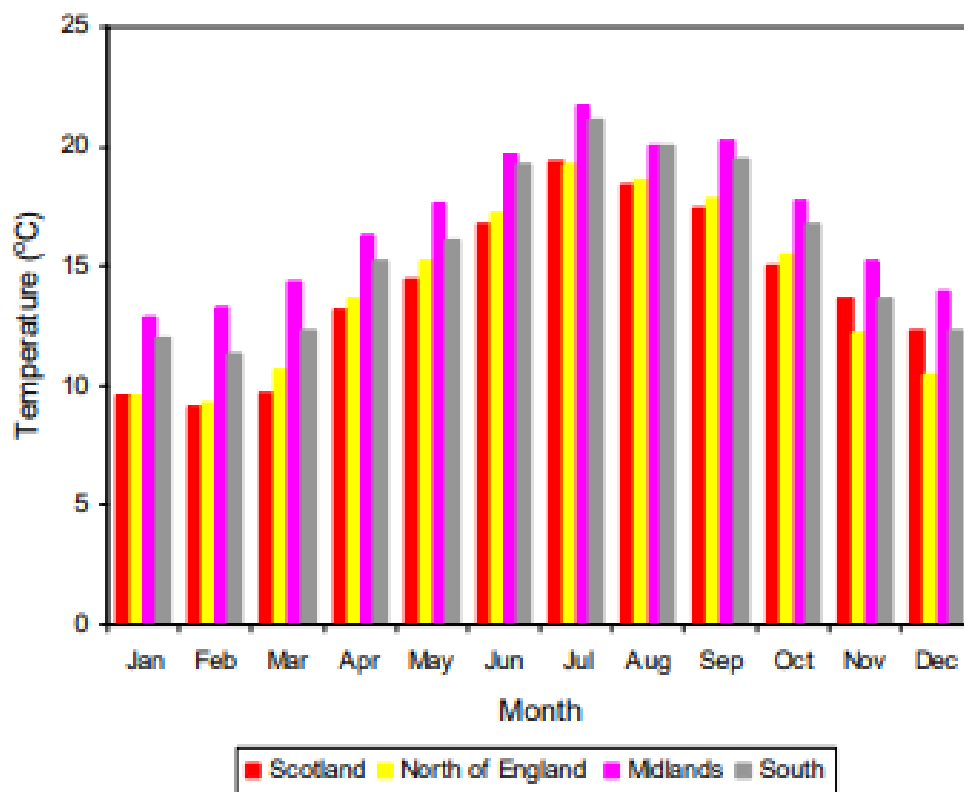
Figure 23 - Cold-water delivery temperatures by area [4]

Energy requirements for hot water also vary between boiler types. Regular boilers use water that is often stored in a water storage tank beforehand, allowing it to heat up slightly before being reaching the boiler, and so requiring less energy to reach the delivery temperature. Combi boilers which are found in many UK households do not use water storage and therefore must

heat up water from the cold water delivery temperature making the temperature range between entering and exiting the boiler slightly higher [44].

As a result of these factors, hot water usage was calculated according to the BREDEM method whilst substituting values for hot and cold water to those measured by the Energy Savings Trust in order to generate a more accurate result. Values for the number of baths and showers taken each day were taken from The Energy Savings Trust report. The results obtained are demonstrated in Figure 24 below for four different regions.
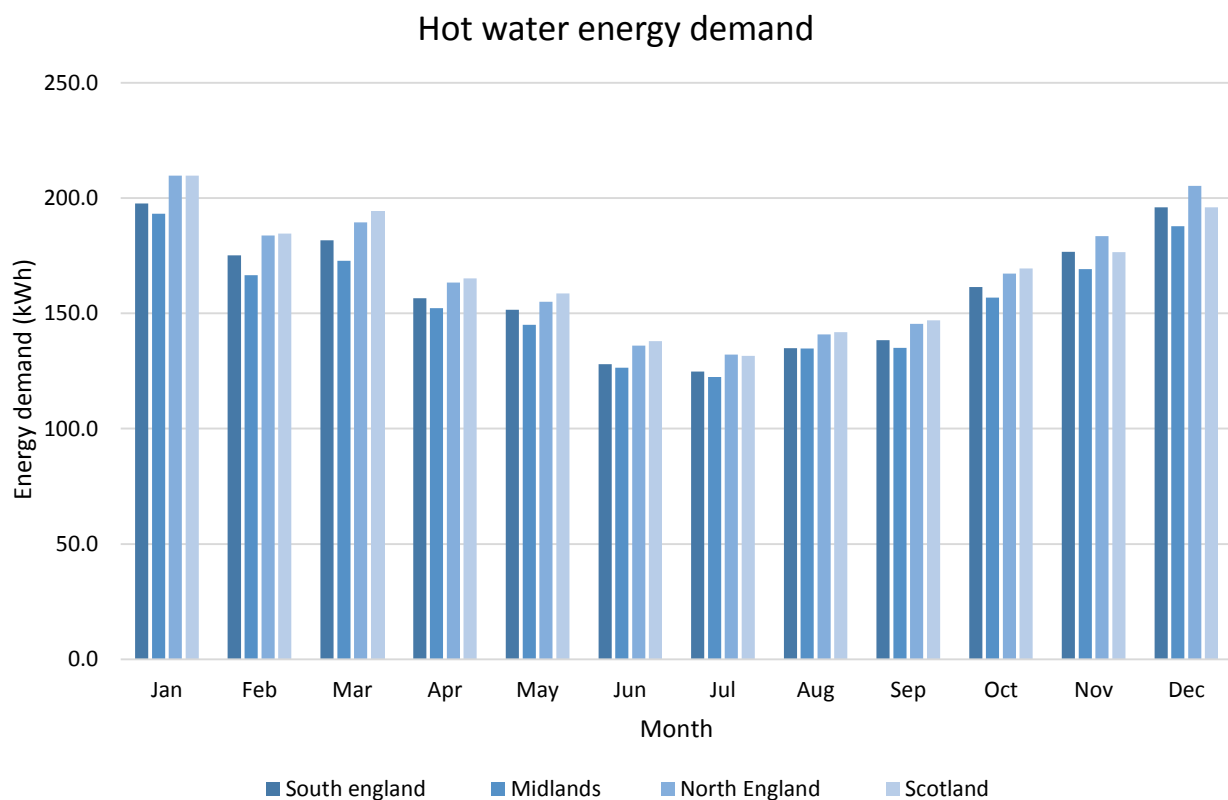
Figure 24 - Hot water energy demand per month by region

As a consequence of the cold water feed temperatures, the north of England and Scotland have the highest energy demand, yet the difference only leads to an additional 100 - 200 kWh of heating required each year when compared to the midlands and south of England.

Presuming equal hot water usage for each day, the daily average consumption can be obtained from the monthly results. This daily average demand can then be distributed according to Figure 25 to generate an hourly approximation. This hourly average is to be added to the hourly heating demand to obtain a total hourly heating demand profile.
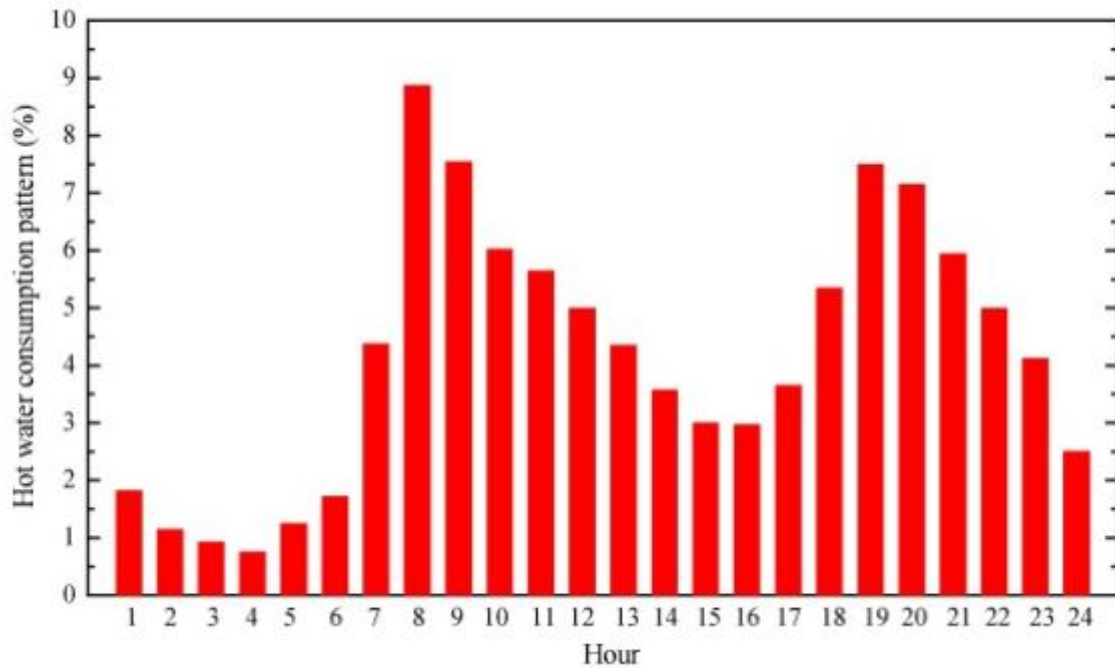
Figure 25 - Hourly hot water usage as a percentage of the daily total [4]

This means that energy needed to generate enough hot water for a day might look something like this:
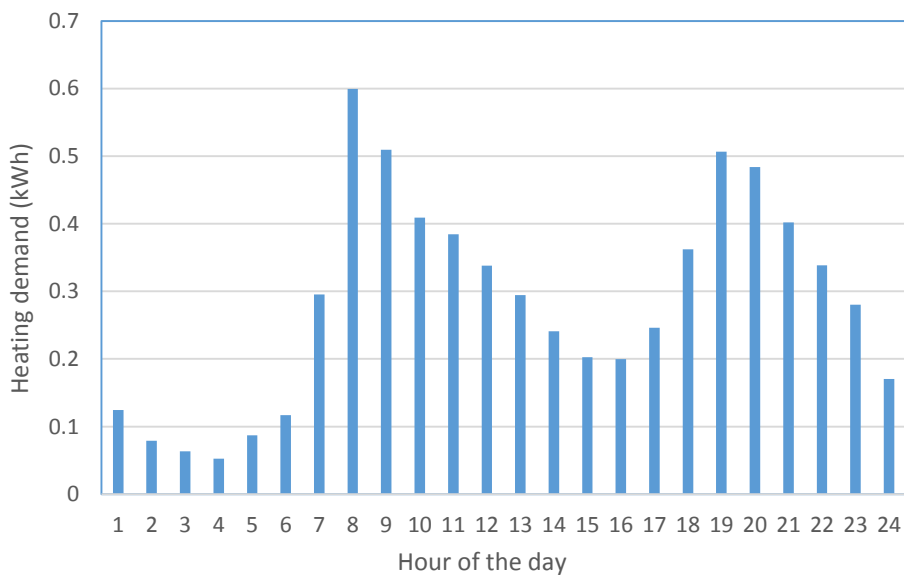
Figure 26 - Hourly water heating demand (Scotland, January)

5.2.1 Total heating demand

The total heating demand is found according to Equation 4, being the sum of the space and hot water heating requirements:

$$Q_{ht} = Q_{sh} + Q_{hw}$$

Equation 4 – Total heating demand

Where Q_{ht} is the total heating demand and Q_{hw} is the total energy demand for water heating as calculated according to Appendix IV, with both calculated in kWh.

Figure 27 below displays the predicted total energy consumption for a two person, semi-detached house in Glasgow with a heat loss coefficient of 150 W/K, with the figures for U = 65 W/K and U = 300 W/K in Appendix V. The heating demands total 8540, 17070, and 32140 kWh for U values of 65, 150, and 300 W/K respectively. Hot water accounts for 23.5% of the energy demand when the household heat loss coefficient (U = 65 W/K) is at its lowest, falling to 6.2% for the highest heat loss coefficient (U = 300 W/K).
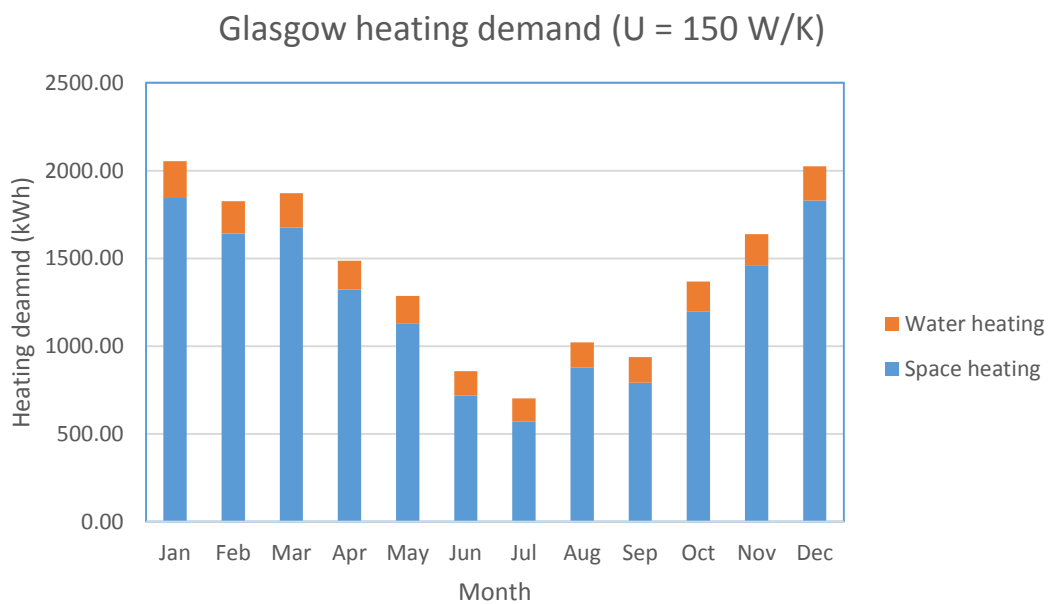
Figure 27 - Glasgow heating demand profile

The results for Brighton exhibit much the same trend (Figure 28), however in comparison total 6580, 12670, and 23410 kWh for heat loss coefficients 65, 150, and 300 W/K respectively. As the space heating demand is lower, the percentage contribution for hot water heating towards total energy demand is 41% at the lowest heat loss coefficient, falling to 8.9% at the highest. The tables for heat loss coefficients of 65 and 300 W/K can also be found in Appendix V.
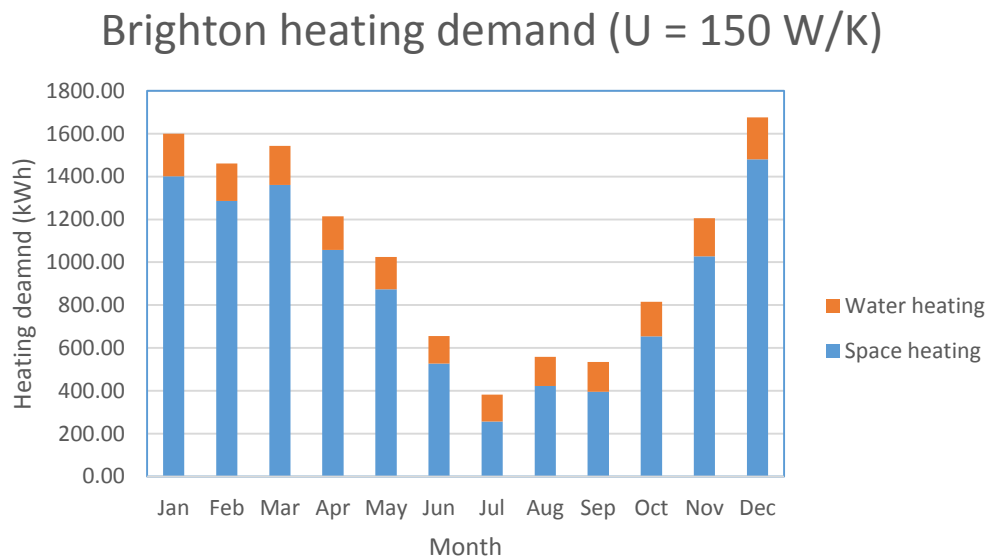
Figure 28 - Brighton heating demand profile

All of the results calculated for total heating demand fall within the expected range for a UK home [45]. From the yearly heating demands it is clear that the houses with a high heat loss coefficients would benefit more from focusing on first implementing energy efficiency measures to reduce the required energy for heating before considering installation of a renewable energy system. The results also highlight the disparity between new and old buildings, and between locations.

6   Solar collector evaluation

As was laid out in the literature review, useful heat can be generated from solar radiation through a solar collector. Here, a FPC was analysed using the process explained in the project methodology and outlined in Appendix I.

To ensure the calculation process followed gave accurate results, weather data, panel data, and useful energy output for Newcastle provided by Ma et al [43] was used to validate any results. A collector angle of 45° and a fluid inlet temperature of 30℃ were used as they were proven to generate the most useful energy. Figure 29 shows a comparison of the calculated absorbed radiation per m^2 by a FPC between this work and the results calculated by Ma et al. The results from this work follow the same profile throughout the year, however envisage marginally less energy absorbed throughout the summer months. This underestimation is carried through to Figure 30 where it is shown that the predicted useful energy generated also follows the same profile with a slight underestimation during the summer months. This underestimation could be due to slight differences in calculation methods as there are a number of possible equations for calculating solar positioning that were not laid out in the text.
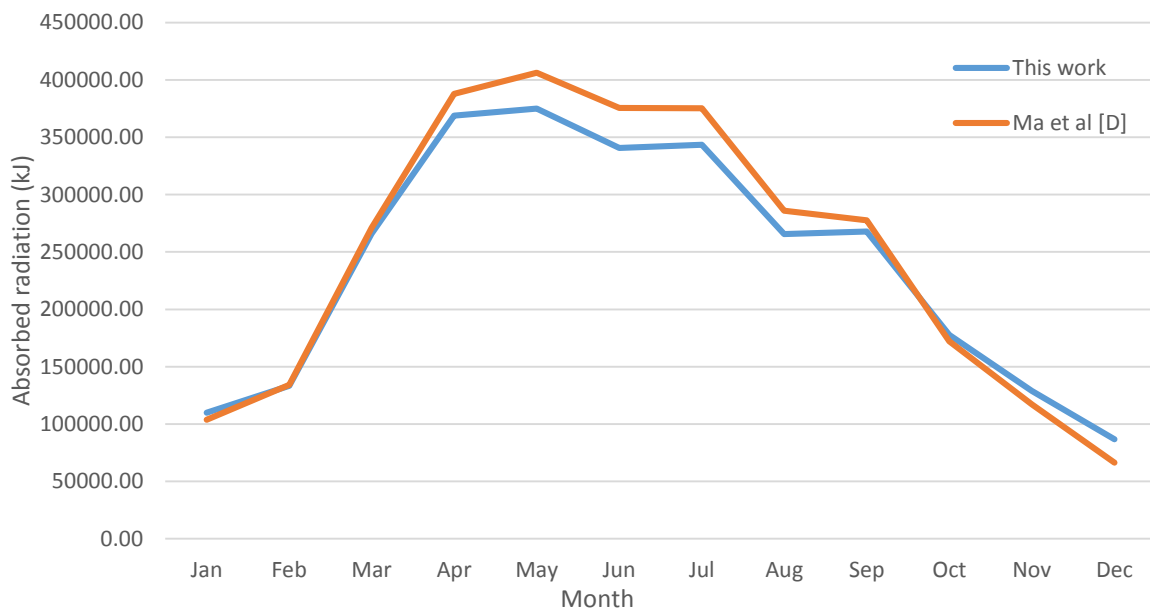
Figure 29 - Absorbed radiation by a FPC per m^2
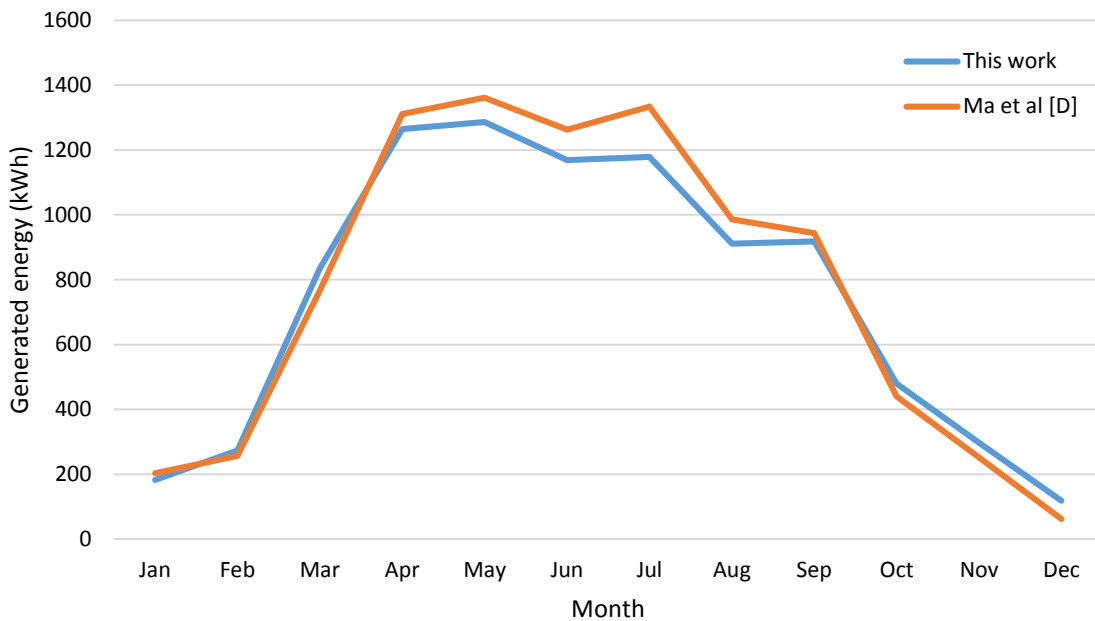
Figure 30 - Useful energy generated by a single FPC

The useful energy was calculated in kJ and then converted to kWh to allow easy comparison with heating demand. The calculated results underestimate during the summer months during which it would be expected that the majority of the borehole heat loading will take place, and therefore it must be remembered that the results that follow for each location may be slightly lower than would be anticipated in reality.

6.1 Weather data

Following the validation of the calculation method, local weather data was collected for Glasgow and Brighton. In addition to the hourly ambient temperatures previously used for calculating heating demand, hourly global horizontal irradiation values were again taken from Renewables. Ninja [38] averaged over three years between 2016 and 2018. Figure 31 displays the average monthly solar irradiation profiles over the course of a year for each location. As expected Brighton has a higher average incident irradiance, peaking at just under 200 kWh/m^2 a day in June, while the much cloudier Glasgow peaks at approximately 155 kWh in May.

Interestingly Glasgow sees a decrease in the daily incident ration in June before rising again in July.
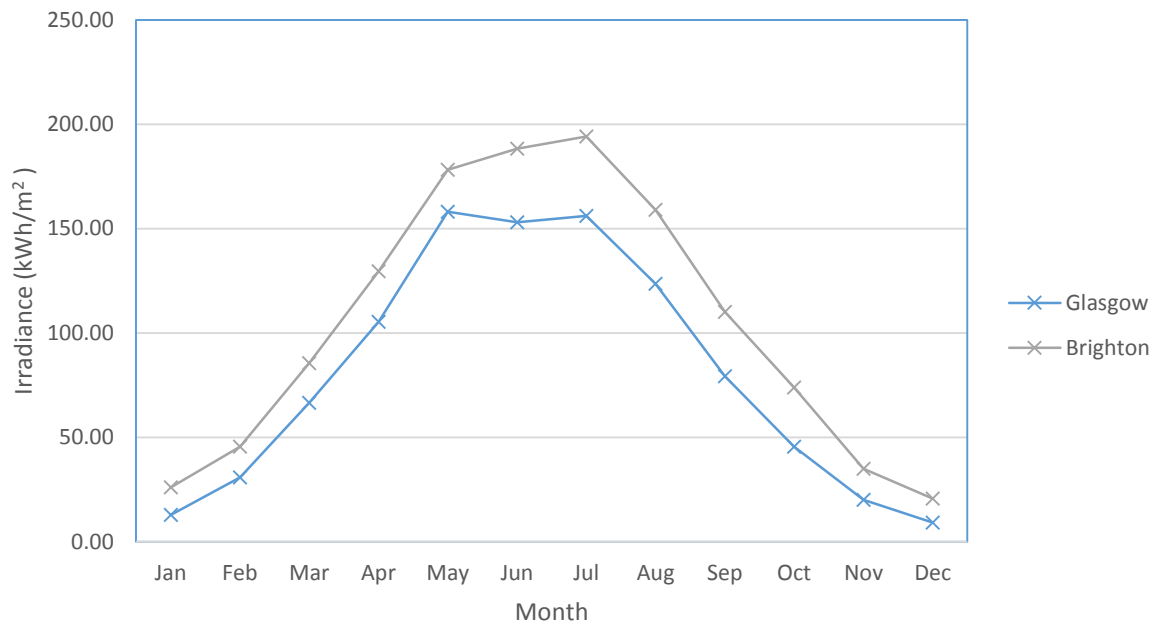
Figure 31 - Monthly average global horizontal irradiance

While Figure 31 displays the monthly average, the obtained hourly values were used in the calculations for solar collector energy output to generate an hourly energy profile to be directly compared with the hourly heating demand.

6.2   Solar collector results

A semi-detached house in the UK has an average floor area of 93.2m^2 [46]. Presuming a roof pitch of 45 degrees, this corresponds to an available roof area of just under 33m^2. As each solar collector panel has an area of 1.98m^2, there is therefore space for up to 14 panels on the roof of the house, ensuring space is left for maintenance and installation. The HTF used was water-ethylene-glycol with a specific heat of 3850 J/Kg-k, and the fluid inflow temperature was 30℃. Appendix II shows the appropriate panel data required for the calculations based upon a real panel built by SUNSYSTEM as was also used by Ma et al [43].

Figure 32 and Figure 33 below compare the amount of useful energy gained from an array of 14 solar FPC versus increasing heating demands for Glasgow and Brighton respectively. In Glasgow the energy generated by the FPC is sufficient such that for heat loss coefficients of

65 and 150 W/K, there is a reasonable excess of thermal energy generated between May and August that could reasonably be expected to contribute to winter heating demand if stored efficiently. However, for a heat loss coefficient of 300 W/K there is practically no excess energy thus agreeing with the earlier conclusion that a house with such a high heating demand would benefit more from first installing energy efficiency measures.
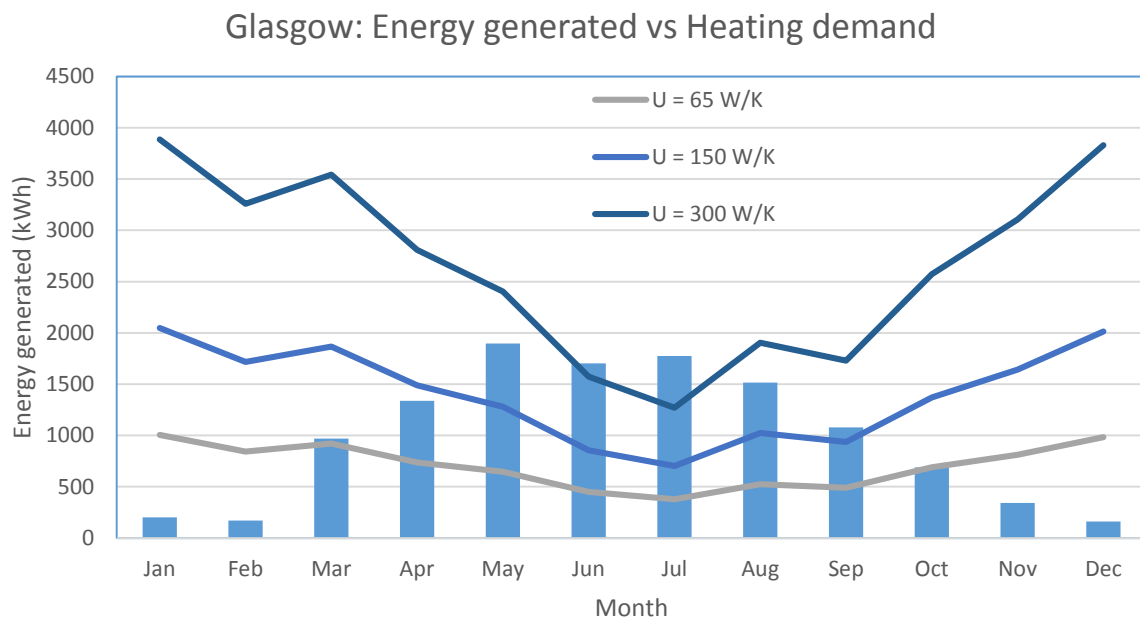
Figure 32 - Energy generated by FPC array vs heating demand for Glasgow

In contrast, a FPC array in Brighton is predicted to generate enough energy that a significant excess of thermal energy is generated throughout the summer when compared with all three heating demands, extending from April through to October. This indicates that an array of 14 panels would even potentially be surplus to requirements in Brighton, with a smaller FPC array still capable of generating enough energy for meeting heating demand. For the purpose of this analysis the energy generated by an array of 14 FPC will be carried forward, however using 10 panels would also probably suffice. As the thermal energy generated for a heat loss coefficient of 65 W/K is low enough that the FPC array generates enough energy each month to satisfy the demand, it could be inferred that in this case short term thermal energy storage as opposed to seasonal would be more suitable.
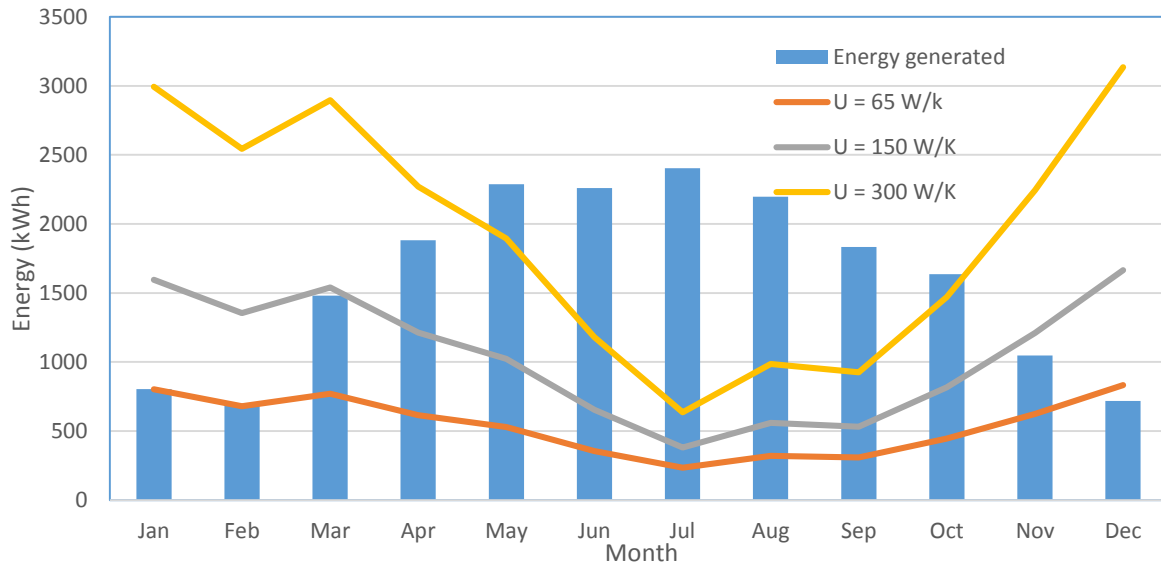
Figure 33 - Energy generated by FPC array vs heating demand for Brighton

When comparing the two locations, it is easy to see that Glasgow is impacted as it experiences both colder winters leading to higher heating demands as well as more cloudy summers.

6.3   Thermal energy available for ground storage

The thermal energy remaining for storage through the BHE is found according to Equation 5 on an hourly basis:

$$Q_{bh} = Q_{sc} - Q_{htot}$$

Equation 5 - Calculation of surplus thermal energy for ground storage

Where Q_{bh} is the quantity of thermal energy remaining for storage through the BHE measured in kWh.

Although collectively the quantity of energy generated through the solar collector is not always greater than the heating demand over a month, as the majority of the heat is generated through the middle of the day when heating demand is at its lowest there is a mismatch created. This

equation was used on an hourly basis, assuming no other demand matching controls are in operation within the system. Figures 34 and 35 show the monthly quantity of excess thermal energy for Glasgow and Brighton respectively, indicating that the quantity of excess thermal energy is significant enough to contribute towards winter heating demand if it can be efficiently stored and extracted.
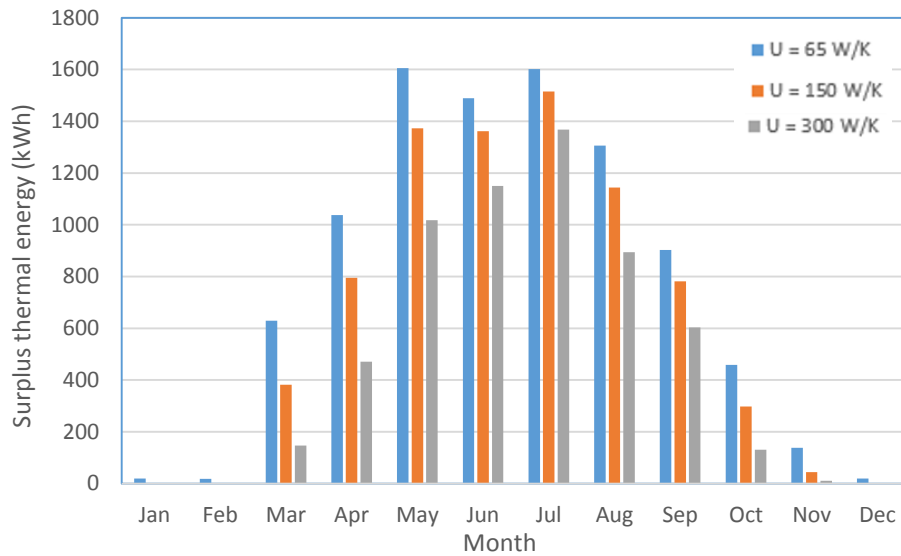
Figure 34 - Excess thermal energy generated via solar collector array (Glasgow)
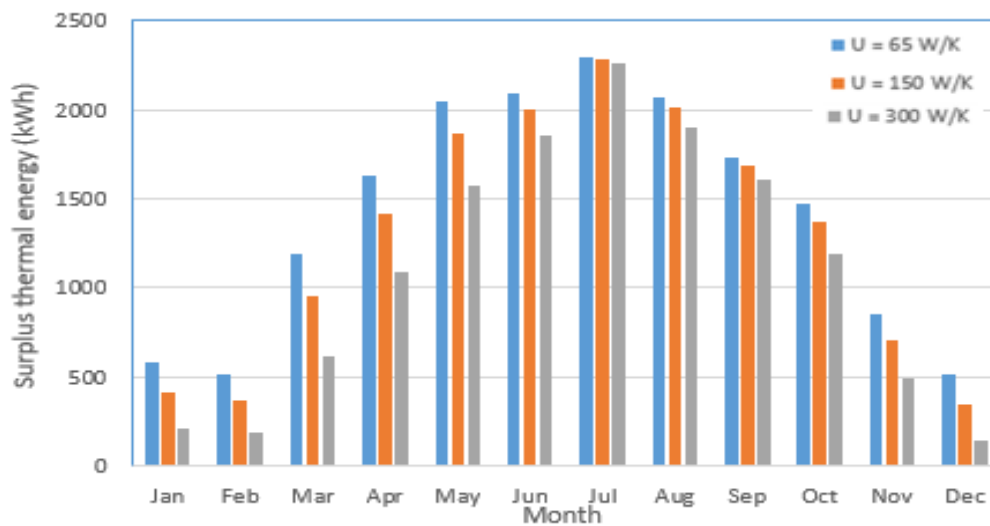
Figure 35 - Excess thermal energy generated via solar collector array (Brighton)

For the following simulations, unless stated otherwise all relevant fluid temperature profiles were generated using the quantity of excess thermal energy as calculated according to a dwelling heat loss coefficient of 150 W/K. This was done in the interest of time as performing simulations for three sets of heating demands in two different locations would be particularly time consuming.

7 Borehole heat exchanger analysis

The borehole heat exchanger system was analysed through computational fluid dynamics software ANSYS as both a steady state and transient fluid flow model. For this purpose, a 3D model was developed from 2D geometry, and then meshed to allow simulation of fluid flow and heat transfer within the created bodies. Boreholes can be anywhere from 30 to 200 metres deep depending on their application [47]. The deeper the borehole the higher the volume of storage and the lower the losses to the surroundings. Therefore, a borehole model with a depth of 100m was created, based upon the dimensions used by Kerme and Fung [21]. Table 1 contains all the relevant geometry and thermal properties required for the creation of the geometry:

Description	Symbol	Value
Borehole depth	H	100 m
Shank spacing	D	0.038 m
Borehole radius	r_b	0.10 m
Outer radius of U-tube pipe	r_{op}	0.0316 m
Inner radius of U-tube pipe	r_{ip}	0.0255 m
Thermal conductivity of U-tube (HDPE pipe)	k_p	0.39 W/(mK)
Thermal conductivity of fill material (grout)	k_b	1.5 W/(mK)
Thermal conductivity of the ground (soil)	k_s	2 W/(mK)
Circulating (working) fluid		water-ethylene glycol (20% by volume)

Average mass flow rate of circulating fluid	m_f	0.25 kg/s
Thermal conductivity of circulating fluid	k_f	0.5 W/mK
Specific heat of circulating fluid	$C_{p,f}$	3850 J/kg.K
Density of circulating fluid	ρ_f	968 kg/m3
Viscosity of circulating fluid	μ_f	$1.02 \times 10{-}3$ kg/(m.sec)
Specific capacity of soil/ground outside the borehole	C_s	2016 J/kg.K
Inlet temperature of the circulating fluid	$T_{f,in}$	40 °C
Undisturbed ground temperature	T_o	10 °C

Table 1 - Parameters used for borehole model

Meshing is the process of splitting the 3D domain into a network of smaller shapes for the purpose of analysing the movement of energy through each element. When creating a mesh it is important to ensure that its quality is high enough to accurately capture the flow of energy through the model and generate valid results whilst finding a balance with the number of elements composing the mesh to ensure computation time is not unnecessarily long. Although the program will automatically generate a mesh, for the geometry in question this resulted in a mesh with over 16 million elements, prohibitively large in this case as it resulted in computation time that was untenable. To reduce the total number of elements the vertical length of the borehole was initially split in to 1500 layers, with an applied bias that developed layers that were larger towards the centre of the model and smaller at the top and bottom.

Hexahedral elements were used to create these layers through the fluid zone, u-tube wall, grout, and soil, applying edge sizing's in the form of number of divisions. This served to significantly reducing the overall number of elements from the previous tetrahedral meshing method that was automatically applied. Figure 36 below indicates the bodies meshed in a layered pattern.
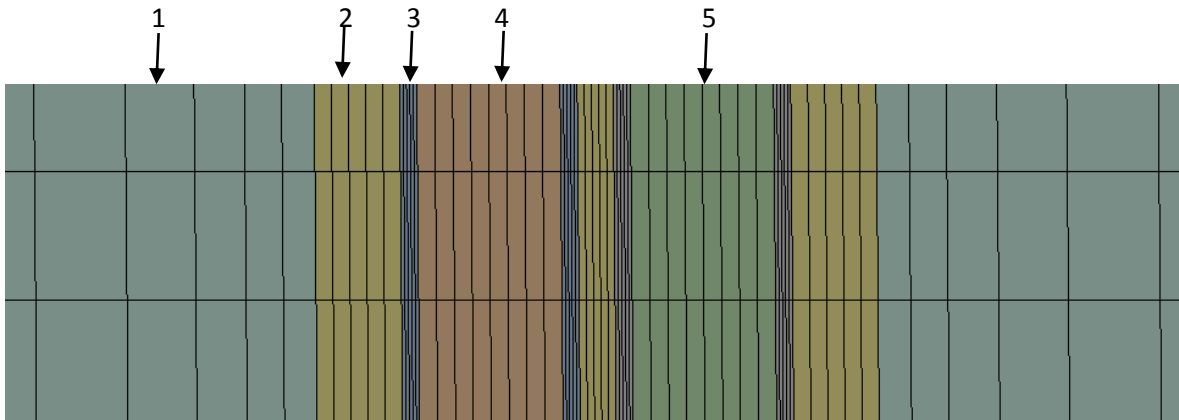
Figure 36 - ANSYS mesh cross section of vertical layers

Where the numbers above correspond with the following bodies:

1. Ground material
2. Grout
3. U-tube wall
4. Upward flowing fluid zone
5. Downward flowing fluid zone

The bottom of the u-tube was meshed separately to the legs due to the increasingly complex geometry, using a tetrahedral meshing method to allow the mesh to conform comfortably to the irregular shape of the u-tube bend while also matching up with the surrounding hexahedral layers (Figure 37). A plane of symmetry was applied along the X axis, splitting the model in half with the purpose of further reducing the computation time as only one half of the model is hence simulated.
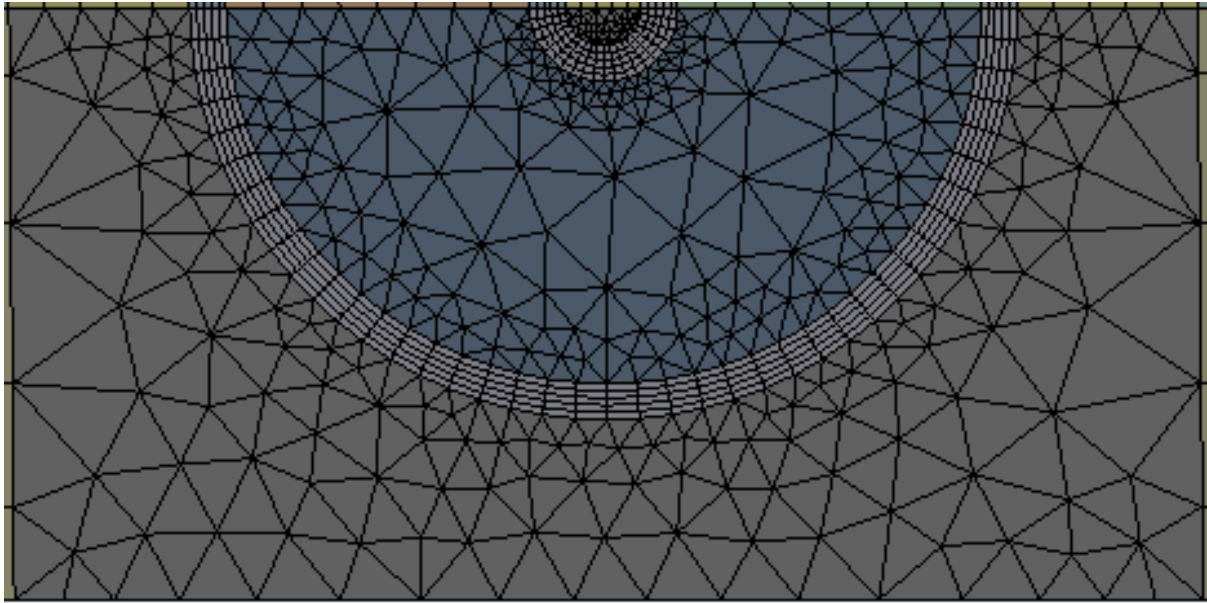
Figure 37 – Lower quality tetrahedral mesh

Following the creation of the above geometry and mesh, simulations were carried out to validate the heat transfer from the fluid to the surrounding soil. The k - ε turbulence model was used to evaluate the mean thermal flow characteristics throughout the model and relevant boundary conditions were applied. It was assumed that there was no underground water flow past the borehole and that the initial ground temperature was constant along its length. The soil body was extruded to extend 3m radially outwards from the interface with the grout. The fluid inflow temperature was set as 40℃, or 313.15 K.

7.1   Mesh independence study

The quality of the mesh generated within ANSYS can have a significant impact upon the accuracy of the results obtained. Therefore, it is important to carry out a mesh independence study to ensure that any results are independent of the quality of the mesh and are solely based on simulation parameters.

To carry out a mesh independence study, an initial simulation is run with the first mesh generated until convergence of residual errors falls below a certain factor, in this case 10^{-4}. Once the model has converged, the results at a point of interest can be recorded the mesh refined, and the simulation repeated. A point of interest may be the velocity of the fluid at a critical point or the temperature at the outflow of a pipe for example. With the simulation repeated, the results at the same point from the second simulation can then be compared to the first, evaluating if the chosen parameter measurement at the monitor point is either the same,

or falls within an allowable tolerance. If this is true then the resolution of the mesh in the first simulation was acceptable and may be used for further studies, however if the difference in results falls outside the acceptable tolerance then the quality of the mesh must be improved further and the process repeated. The quality can be improved by increasing the number of elements in the mesh, or locally refining points. This process is repeated until the result at the monitor point stops changing or falls within an allowable tolerance.

For this study a point was placed at the apex of the u-tube, the approximate location of which is shown below in Figure 38 by the red dot, and used to measure the velocity of the fluid. Table 2 contains the settings that were used to develop the mesh at each iteration. The relevance and relevance centre are used to refine the global mesh quality, whereas the global meshing method determines how the it is developed. In this case initially the curvature size function was applied meaning that mesh elements were generated according to the curvature of each entity within the specified maximum element size or curvature normal angle. In later iterations, this was changed to proximity and curvature. This forms elements on the basis of both the curvature of the body, as well as its proximity to any other nearby bodies. Other functions such as smoothing were also altered to reduce the size ratio between elements closer and further away from important areas of the model.
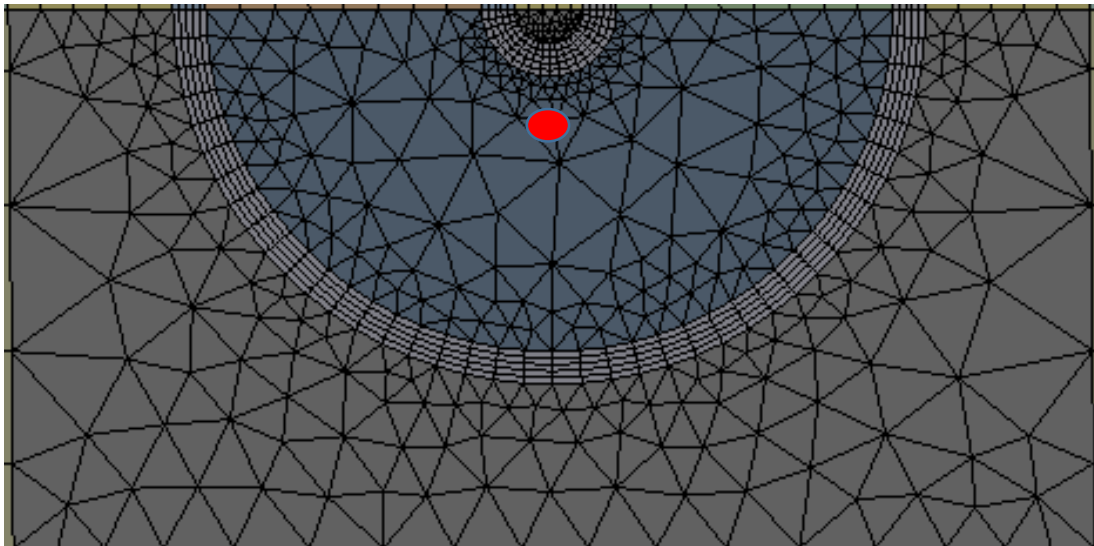
Figure 38 - location of point to measure velocity for mesh independence study

For this case it was found that a mesh with 4,116,574 elements was suitable for the simulation. Increasing the number of elements in the mesh beyond this resulted in a minimal reduction in

the measured velocity, but also it was noted that the simulation time was increased considerably. As many of the elements were constrained with enforced number of divisions, changing the global mesh settings only resulted in small increases in the overall number of elements and so local areas were also refined by increasing the number of divisions imposed on the geometry.

Iteration	Number of elements	Number of nodes	Meshing method	Relevance centre	Relevance	Smoothing	Measured velocity (m/s)
1	2,946,865	3,015,788	Curvature	Medium	0	Medium	0.1689
2	3,289,422	3,401,796	Curvature	Fine	0	Medium	0.1622
3	3,795,282	3,874,142	Curvature	Fine	100	Fine	0.1548
4	4,116,574	4,245,169	Curvature and proximity	Medium	50	Fine	0.1521
5	5,014,392	5,174,291	Curvature and proximity	Fine	50	Fine	0.1507

Table 2 - Settings used for mesh development during mesh independence study

7.2   Model validation

Following the mesh independence study, steady state simulations were performed with the above mentioned boundary conditions. Monitors were created through the centre of the fluid domain within the upward and downward u-tube legs to measure the temperature of the fluid along the length of the borehole. The results were compared with analytical and numerical results presented by Kerme and Fung [21] and Lamarche et al [48], as is shown in Figure 39. The downward leg is found to have a reduced rate of heat transfer from the fluid to the u-tube, grout, and soil, resulting in an apex temperature marginally higher than that of the other studies. On the upward leg there is an increased rate of heat transfer resulting in an outflow temperature equal to that of Kerme and Fung and marginally below Lamarche. This possibly stems from the fluid exchanging heat with itself between the u-tube legs, causing a temperature increase in

the upward leg and hence an increased rate of heat transfer when compared to the downward leg.

Overall, there is a strong agreement between this work and the numerical and analytical studies, resulting in a very similar degree of heat transfer from the fluid to the borehole along the combined length of the upward and downward u-tube legs.
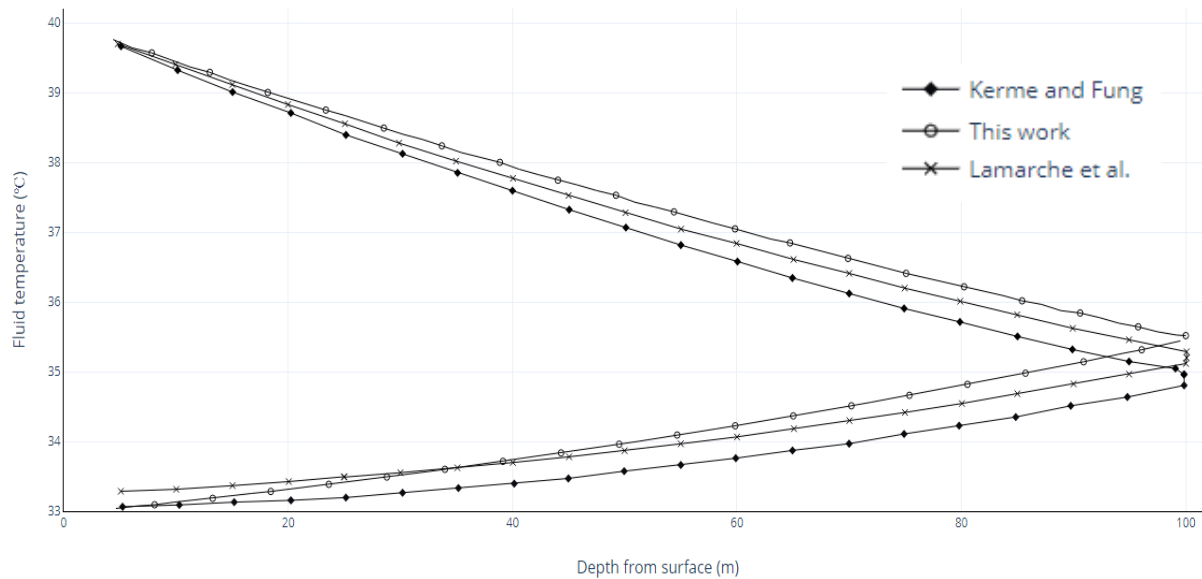
Figure 39 - Validation of fluid temperature profiles for this work vs published data

7.3   BHE performance in UK conditions

Following the validation of the borehole heat exchanger model, simulations were then undertaken to evaluate the performance of the BHE in a UK environment. To do this relevant soil and fluid flow properties were determined from literature and the following calculations respectively.

7.3.1   Soil properties

Soil type has little influence on the short-term capabilities of a borehole system, however when used as a seasonal thermal storage medium the impact of the soil properties becomes much more apparent [49]. Renaldi [49] identified three main soil types found in the UK, displayed below in Table 3. The study concluded that loam was the best ground material for thermal energy storage, but also that it was important to identify location specific soil types to ensure accuracy within simulations.

Properties	Unit	Sand	Loam	Clay
Thermal conductivity	W/m-K	1.56	1.15	1.81
Specific heat capacity	kJ/kg-K	1.014	1.267	1.398
Density	kg/m$_3$	1520	1280	1250

Table 3 - Thermal properties of common UK soil types [49]

It was therefore important to identify the most prevalent soil types for both Glasgow and Brighton. Using Scotland Soils maps [50] the common soil types surrounding Glasgow were brown soils (brown) and mineral gleys (blue) as is indicated in Figure 40 (Full legend in Appendix VII). Both of these soil types consist of a high percentage of sand, along with traces of clay, and therefore the soil type for Glasgow was approximated as sand. Brighton was found to consist mainly of shallow loamy soils over chalk or sandstone (yellow) [51] as indicated below in Figure 41 (Full legend in Appendix VII), and hence loam characteristics were applied to all Brighton based simulations.
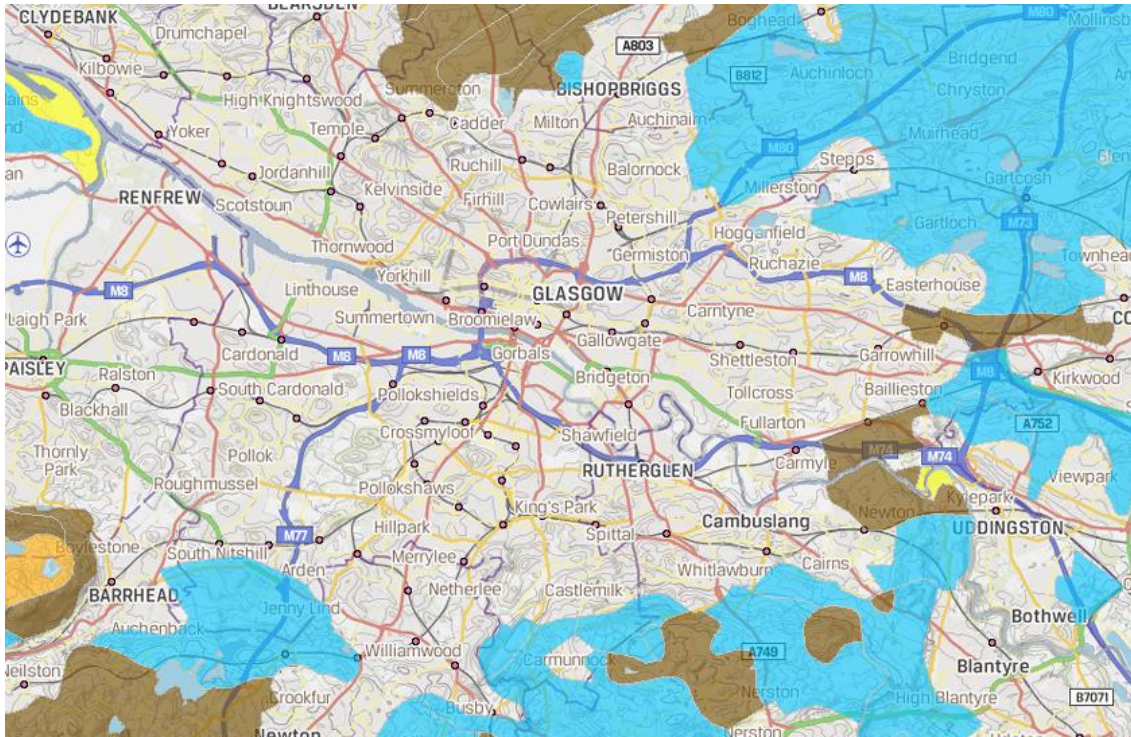
Figure 40 - Soil types surrounding Glasgow[50]
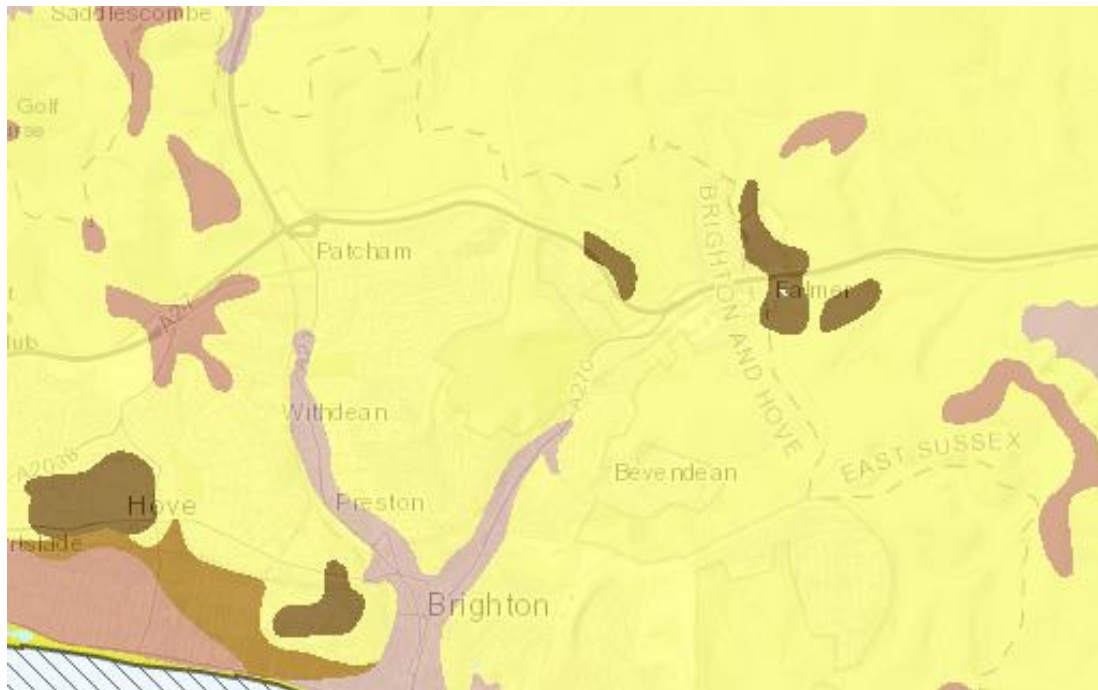
Figure 41 - Soil types surrounding Brighton [51]

7.4   Mass flow rate

The mass flow rate of the HTF through the u-tube is known to impact the rate of heat transfer from the fluid to the ground. Increasing the mass flow rate has the effect of increasing borehole loading per unit depth, however also increases the amount of power required by the pump to circulate the fluid. Increased mass flow rate also reduces the operating temperature of the HTF as more thermal energy is needed to heat to fluid. Reducing the mass flow rate has the opposite effect, thus it is important to find a balance where borehole loading remains high, generating high enough temperatures within the borehole whilst also keeping in mind the power that will be required to circulate the fluid.

Steady state simulations were undertaken with the same parameters as the model validation for changing mass flow rate to explore the impact this would have on a single borehole heat exchanger. Within ANSYS, mass flow rate is converted to litres per second (l/s). Results for borehole loading with depth were compared for mass flow rates of 0.15, 0.25, and 0.35 kg/s, or 0.0735, 0.122 and 0.171 l/s when the internal diameter of the u-tube is 0.0255 m.

The following figures display the impact of varying the HTF mass flow rate on fluid temperature in the upward and downward legs of the u-tube (Figure 42), the temperature of the soil with radial distance from the borehole wall (Figure 43), and the temperature of the soil with vertical depth from the surface (Figure 44). From this it may be inferred that the rate of heat transfer from the HTF to the ground directly correlates with the mass flow rate. It was decided to use a mass flow rate of 0.25 kg/s moving forward as increasing the mass flow rate to 0.35 kg/s would incur larger amounts of thermal energy to raise the temperature of the HTF to the desired temperature, and reducing the mass flow rate results in a reduced rate of heat transfer away from the HTF.
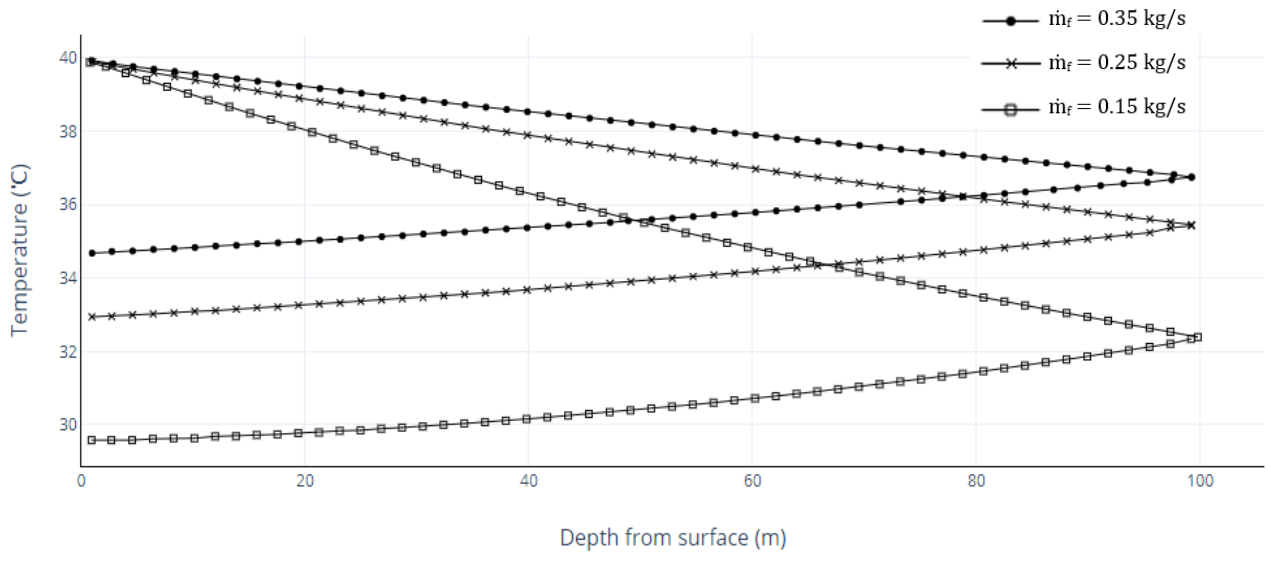
Figure 42 - Effect of HTF mass flow rate on fluid temperature
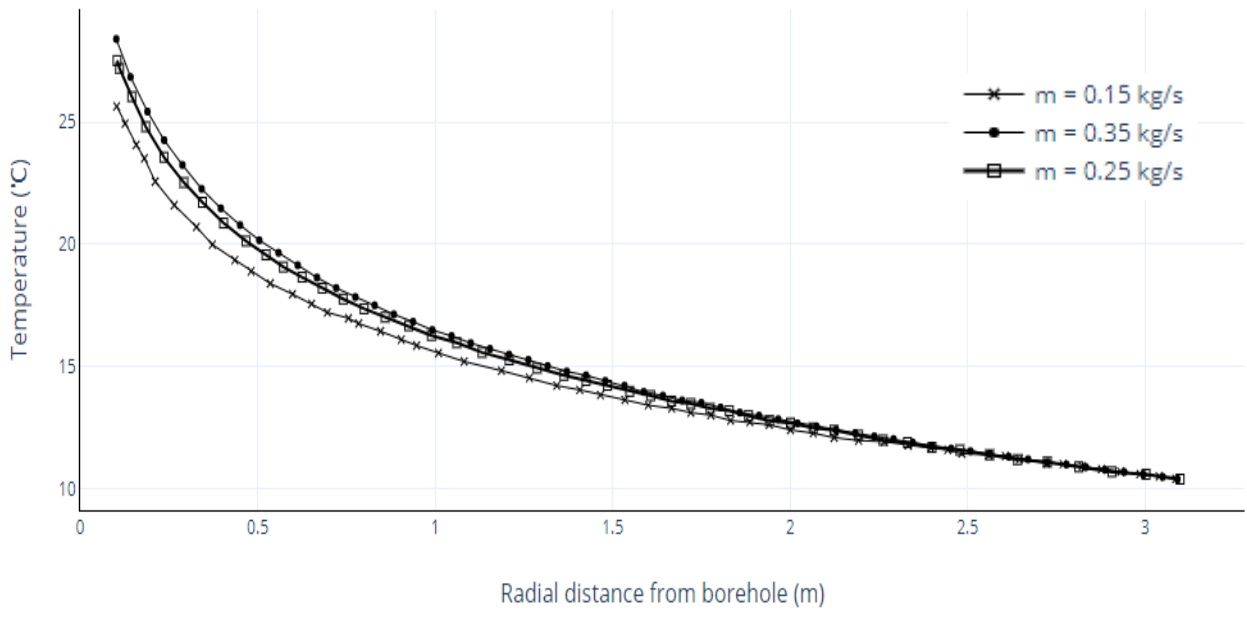
Figure 43 - Soil temperature with radial distance from borehole wall
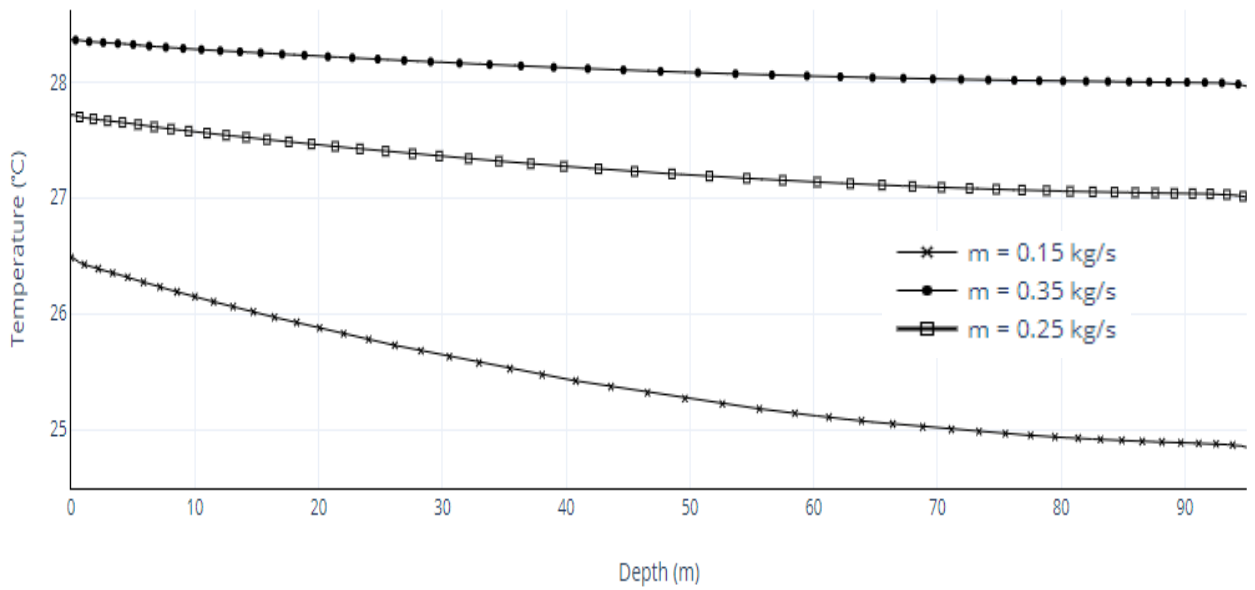
Figure 44 - soil temperature with vertical depth from surface

7.5   Transient modelling

Following the determination of the impact of mass flow rate on heat transfer, transient simulations were carried out to mimic expected conditions during borehole loading, during which heat is transferred from the HTF being circulated through the u-tube to the surrounding ground. Summer months of pure loading and no energy extraction were evaluated to estimate the quantity of thermal energy that could be expected to be stored within the ground via the BHE. Simulations were carried out with one-hour long time steps, with a maximum of 20 iterations at each time step to allow the result time to converge. Initially, a HTF momentum equal to 0.25 kg/s through the u-tube was used when excess heat was being generated by the solar collector, with the momentum of the HTF set to zero otherwise to indicate switching off the pump and stopping the fluid circulation. Figure 45 below indicates the intended fluid momentum profile over a 48-hour period. Fluid temperatures were kept constant during the testing of the model at 40℃.
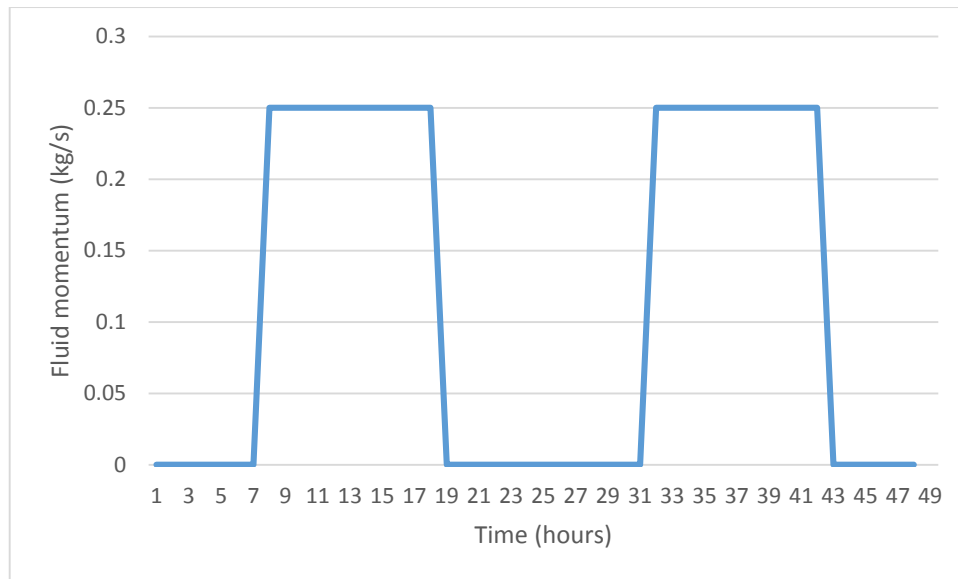
Figure 45 - Example fluid momentum profile over a 48 hour period

The variation of fluid momentum was found to cause issues within the model simulation. Although ANSYS registered the fluid flow temperature and momentum profiles, the model detected divergence within the solver when the fluid momentum was reduced to zero after periods of loading, consequently ending the simulation prematurely. This could have been caused by a number of issues including too large time steps or the fact that there was no fluid flow taking place within the model. In an attempt to solve this the fluid momentum was increased from zero to 0.00001 kg/s during periods when the solar collectors were not generating excess heat. While having the fluid momentum not equalling zero would result in a small amount of heat transfer from the fluid to the soil, it was predicted that this would be negligible in comparison to the overall heat transfer occurring otherwise. In conjunction with registering fluid momentum as non-zero, smaller time steps of 30 minutes and 15 minutes were also tested with a reduced number of iterations per time step to keep simulation times down.

After making these changes the simulation still returned the error of detecting divergence. Further increasing the momentum of the fluid when there was supposed to be no flow would result in heat transfer either to or away from the ground that would be indiscernible from the intended heat transfer during loading. In addition, further reducing the simulation time would result in excessively long computation time. Therefore, to work around this, simulations were instead run with only the hours during which excess heat from the solar collectors was available. This meant that there was no down time creating a continuous cycle of borehole

loading over the whole month. This is predicted to negatively impact the rate of heat transfer from the HTF to the ground as constant loading temperatures do not allow time for the transferred heat to dissipate and the rate of heat transfer will be slowed.

7.5.1 Initial ground conditions

Prior to simulation, the energy content of the ground was calculated so that the change experienced following simulation could be quantified in terms of an increase in energy within the ground body.

The volume of the ground within the model is 1507 m^3. Using the densities for sand and loam, this translates to a mass of approximately 2290 and 1930 tonnes respectively. Within the ANSYS solver, the volume integral function can be used to find the internal energy within a body. The volume integral is measured in j/kg-m^3, and therefore the value provided must be multiplied by the total body volume to obtain the overall energy. For sand this resulted in an energy content of 34.58 GJ, and for loam 43.19 GJ within the entire body. When converted to kWh, this equates to approximately 9580 and 11,690 kWh already contained within the bodies of sand and loam respectively.

These values were hence used to compare the energy within the soil prior to and following the activation of the BHE.

7.5.2 Transient loading

The first method of borehole loading was simulated with a constant fluid temperature, with the number of hours of loading possible determined by the excess of thermal energy generated by the solar collectors. This was first undertaken with ground and energy conditions determined by parameters attributed to Brighton.

For the activation of the pump to circulate the HTF through the BHE, the quantity of excess thermal energy generated in one hour must greater than the quantity of energy needed to raise the temperature of the fluid to the desired temperature. In this case, the desired HTF loading temperature is initially set as 25℃ and was then increased to 35℃ to determine if a higher HTF temperature with fewer loading hours resulted in an overall greater quantity of energy stored within the ground.

T$_1$ (°C)	T$_2$ (°C)	Energy required (kWh)
10	25	14.4
10	35	24.1

Table 4 - Energy required to raise the temperature of the HTF for one hour

The energy required to raise the HTF to the required temperature is indicated above in Table 4 as calculated according to Equation 1:

$$Q_{bh} = \dot{m} * Cp * (T_2 - T_1)$$

Equation 1 - Energy stored through latent heat storage

Where $\dot{m}$ is the mass flow rate of the HTF through the borehole heat exchanger; C_p is the specific heat capacity of the HTF; T$_1$ is the temperature of the HTF prior to entering the DHW tank and T$_2$ is the temperature of the HTF leaving the DHW tank. In this case the mass flow rate is 0.25 kg/s. The HTF used is water-ethylene-glycol at 20% refrigerant concentration by mass, with a specific heat capacity of 3850 J/Kg-K.

In the case that the excess energy generated by the solar collectors is not sufficient to produce a 15°C or 25°C temperature rise, then the sum of excess thermal energy is then carried through to the next hour, being set to zero at the end of each daily solar collector generation cycle with the presumption that any thermal energy still present within the DHW tank would then be used to meet evening heating demand. Table 5 below indicates a one-day cycle for a 25°C HTF temperature, with a 1 or a 0 in the BHE loading column indicating whether the HTF is pump active or inactive respectively.

Hour	Excess thermal energy (kWh)	Hourly summation (kWh)	BHE loading (yes/no)
1	0.00	0.00	0
2	0.00	0.00	0
3	0.00	0.00	0
4	0.00	0.00	0
5	0.00	0.00	0
6	0.00	0.00	0
7	1.66	1.66	0
8	4.76	6.42	0
9	7.28	13.70	0
10	8.68	7.95	1
11	8.35	1.86	1
12	7.93	9.79	0
13	6.63	1.99	1
14	5.37	7.36	0
15	3.80	11.16	0
16	1.79	12.94	0
17	0.00	0.00	0
18	0.00	0.00	0
19	0.00	0.00	0
20	0.00	0.00	0
21	0.00	0.00	0
22	0.00	0.00	0
23	0.00	0.00	0
24	0.00	0.00	0

Table 5 - One day cycle for 25℃ borehole loading

Using this process, the number of hours of loading between the beginning of May and the end of August were calculated according to the excess thermal energy available with a dwelling heating demand attributed to an overall home heat loss coefficient of 150 W/K. This was found to be a total of 568 hours across the four months for a desired HTF temperature of 25℃, with 130, 139, 159, and 140 hours of loading in May, June, July, and August

respectively. For a HTF temperature of 35℃ a total of 336 loading hours were possible, with 77, 82, 94, and 83 hours in May, June, July, and August respectively. For this to occur, it is presumed that the quality of heat within the DHW is sufficient that this temperature rise can be realised.

7.5.2.1 Results

Using the calculated number of loading hours simulations were then run within ANSYS, saving the results at the end of each month, again using radial ground temperature as an indicator of quantity of thermal energy stored before calculating the actual energy increase through the volume integral function.
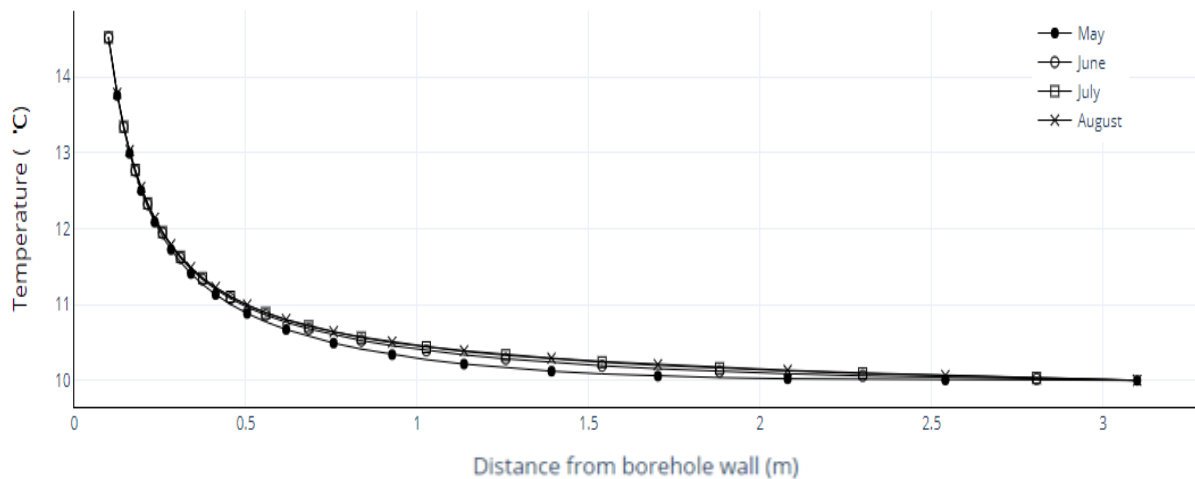
Figure 46 - Monthly radial ground temperature in Brighton using a HTF temperature of 25 ℃

Figure 46 above shows the radial ground temperatures measured at the end of each month for a HTF temperature of 25℃. It is shown that while initially the ground temperature increases, reaching approximately 14.5℃ at the borehole wall, following May the temperature increase within the ground is limited and only detectable further away from the borehole wall. This temperature increase translates to a total of 43.4 kWh of energy stored within the ground between the beginning and the end of May, a further 59.7 kWh between the beginning of June and end of July, and only 2.9 kWh in august, totalling approximately 106 kWh in total.

This comes from a total of around 8100 kWh used to raise the HTF temperature between the beginning of May and end of August. The results of using a HTF temperature of 35℃ proved to follow the same pattern of an initial increase in ground temperature until the end of May,

followed by a marginal increases in the following months resulting in a ground temperature profile at the end of August marginally higher than that achieved through using a HTF temperature of 25℃ (Figure 47). This translates to a total of 135 kWh of heat transferred to the ground compared to the 106 kWh achieved using 25℃.
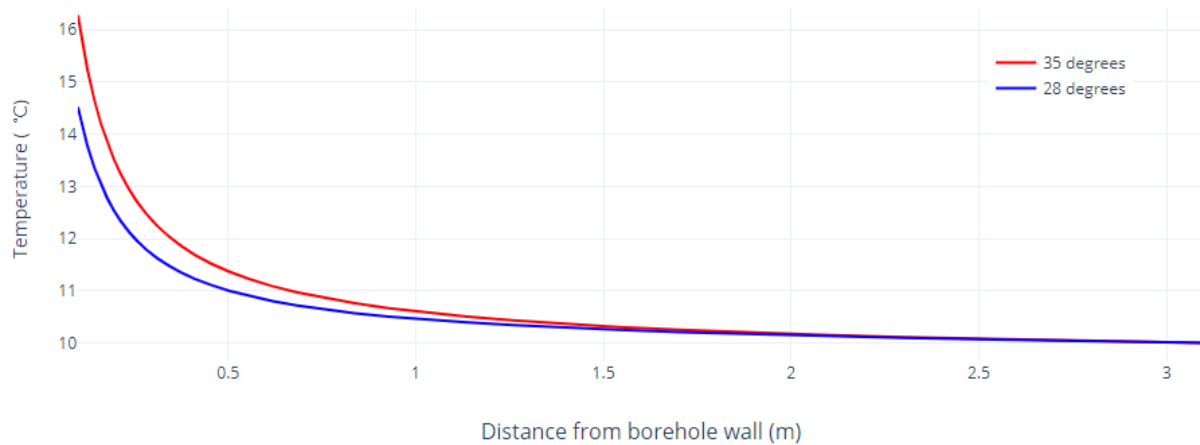
Figure 47 - Radial ground temperature following summer borehole loading at 25℃ and 35℃

To understand why the rate of heat transfer is poor, the temperature distribution from the u-tube wall through the grout and in to the soil was examined. As is shown below in Figure 48, the temperature within the grout is almost 4℃ warmer than that of the ground. This serves to significantly slow the rate of heat transfer away from the u-tube wall due to the decreased temperature difference between the HTF, u-tube wall, and grout. This is compounded by the fact that each hour of loading was run concurrently was the last. As a result, no time was allowed for the heat to dissipate through the ground and high temperatures within the u-tube wall and grout are consistently maintained. Without any way to perform the simulations with intermittent gaps between loading hours, the affect that this has had could not be quantified.
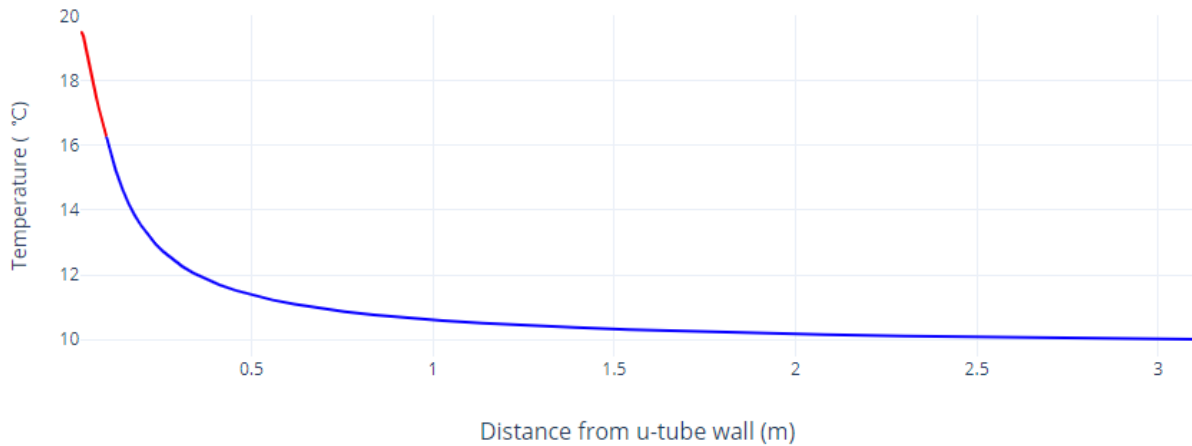
Figure 48 - Radial temperature from u-tube wall

A final possibility is that as the heat the heat remaining within the fluid following its exit from the BHE is not considered for recirculation through the DHW tank, and therefore a large quantity of energy is going to waste as the current model accounts for the HTF being heated from 10°C at each time interval. This could be recirculated to allow more heating hours, but as has already been proven, many hours at one temperature serves very little temperature increase throughout the ground.

7.5.3   Alternate loading method

As a consequence of the poor results achieved through constant temperature loading, varying temperature fluid profiles were generated.

7.5.3.1   Fluid temperature profile

Fluid temperature profiles were calculated according to the quantity of thermal energy available following the subtraction of the heating demand on an hour by hour basis. Fluid temperature profiles were generated for both Glasgow and Brighton, calculated according to Equation 6, which is generated by re-arranging Equation 1 to find T_2:

$$T_2 = T_1 + (\frac{Q_{bh}}{\dot{m}C_p})$$

Equation 6 - Eq. 1 re-arranged to calculate outgoing fluid temperature

66

Where in this case Q_{bh} has previously been calculated in section 7; ṁ, C_p, and T_1 values are unchanged

The outgoing temperature of the fluid changes each hour, generating a higher HTF during the months in which there is a higher excess of thermal energy. The mass flow rate is 0.25 kg/s, or 900 kg/hr. This means that 0.925 kWh is required to raise the temperature of the HTF by 1℃.

Using Equation 6 and the data generated in Section 7 the fluid temperature profiles shown in Figures 49 and 50 were created for Brighton and Glasgow respectively for the month of May, and subsequently and imported in to ANSYS along with the relative profiles for June, July, and August. Once again the periods of time when there is no excess thermal energy available have been omitted to allow the simulation to run continuously. There is a total of 278 hours of borehole loading during May for Brighton, with 1165 between May and August. For Glasgow, there are 252 hours of loading in May, with 1058 total between May and August. It must also be noted that if the temperature of the fluid was calculated to be lower than 12℃ then it was also omitted to prevent heat transfer towards the HTF instead of away from it.

Figure 49 - Fluid temperature profile for Brighton in May using a 10℃ inflow temperature
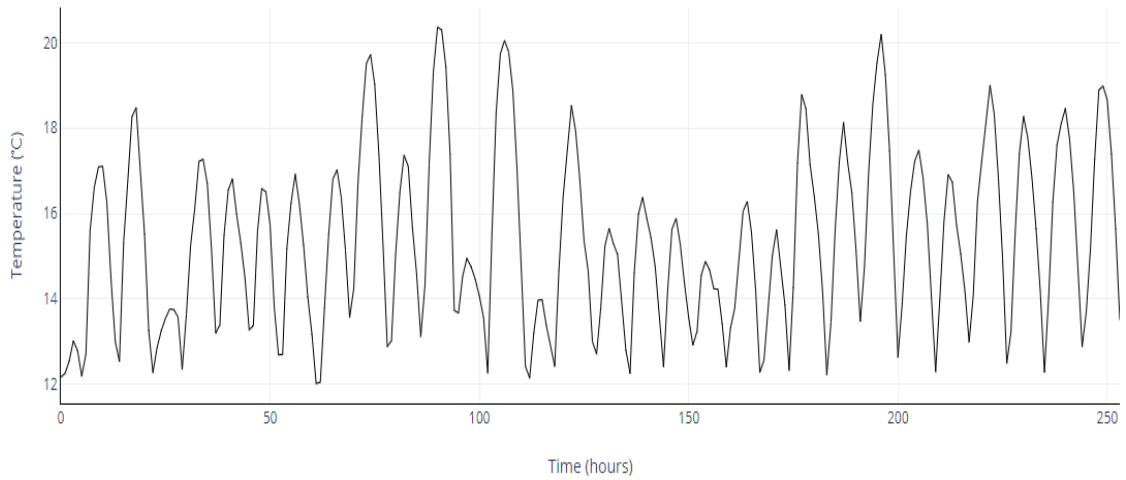
Figure 50 - Fluid temperature profile for Glasgow in May using a 10℃ inflow temperature

7.5.3.2   Results

The results at the end of each month were saved and compared so that the change in the ground temperature and quantity of energy could be found. Figure 51 below shows the radial ground temperature in Brighton at the end of each month, starting at the borehole wall. It I shown that the ground temperature increases between the beginning of May and the end of June, resulting in a net transfer of 848 kWh to the ground from the fluid. However, following this the temperature of the ground then decreases through July, resulting in a net transfer of heat away from the ground of 346 kWh, before then again increasing slightly to end with a total of 525 kWh stored within the ground.
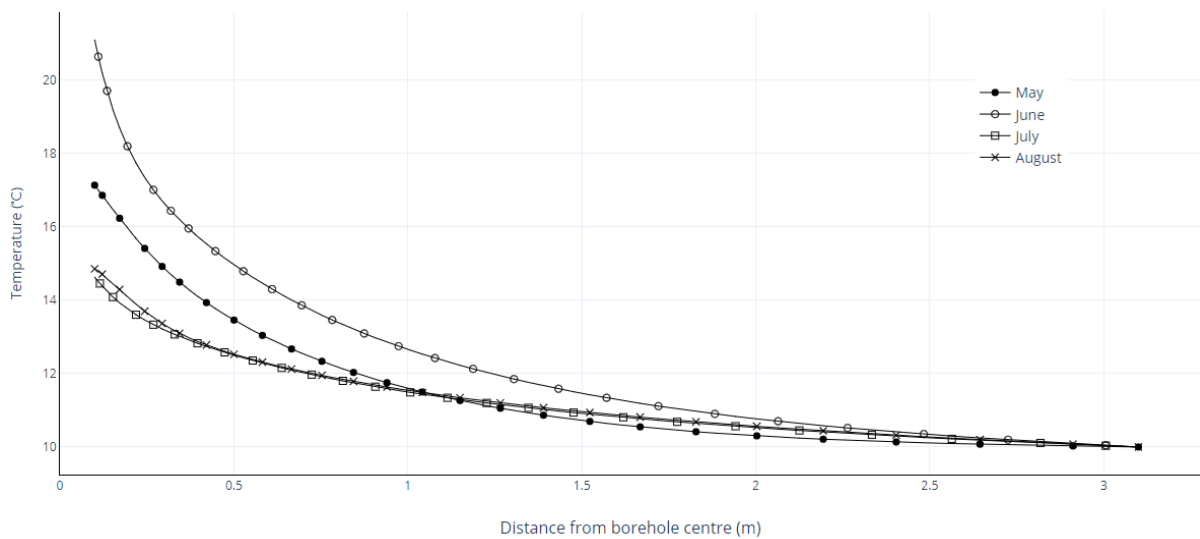
Figure 51 - Brighton radial soil temperature with 10℃ inlet temperature

68
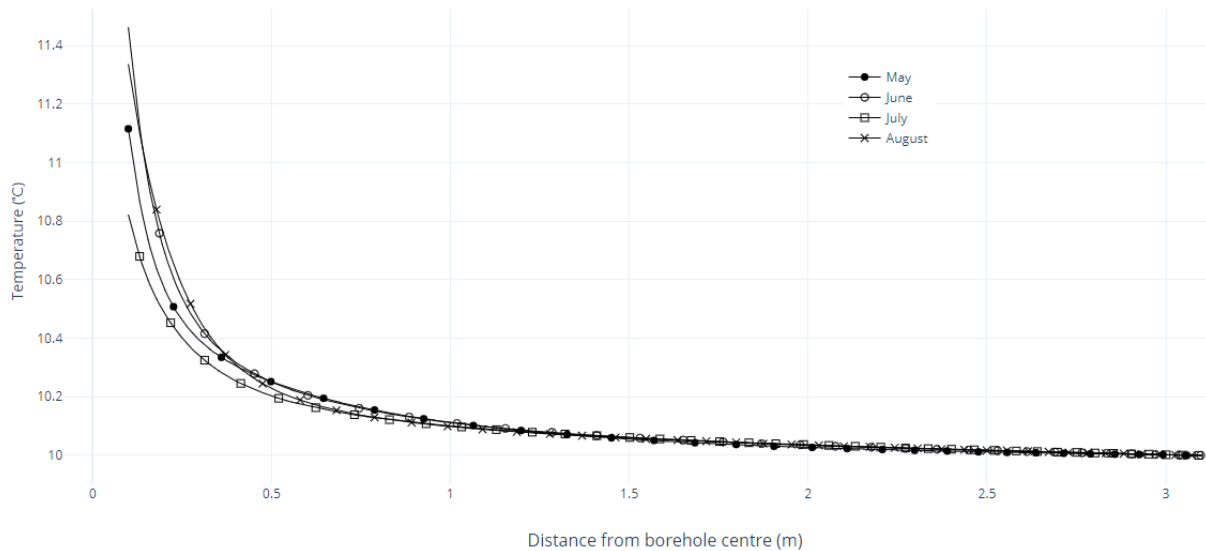
Figure 52 - Glasgow radial soil temperature with 10℃ inlet temperature

Differing from the results seen in Brighton, the quantity of energy stored within the ground was significantly lower in Glasgow, only totalling 20.2 kWh. This is very low and is mirrored in the very low radial ground temperatures seen within the soil. This is most likely due to the lower fluid flow temperatures achieved through the solar collector, although when comparing the HTF temperatures to that of Brighton they are not so much lower

7.5.4   Increased inlet temperature

The simulation above was then repeated with all variables kept the same apart from the fluid inflow temperature to the DHW which was raised to 15℃. The fluid temperature profiles were then re-calculated using an inflow temperature of 15℃ to evaluate the impact higher fluid flow temperatures had on thermal storage. As a result, the following fluid temperature profiles were developed for Brighton (Figure 53) and Glasgow (Figure 54) for May. Fluid temperature profiles were also generated for Jun, July, and August, and imported in to ANSYS as was done previously.
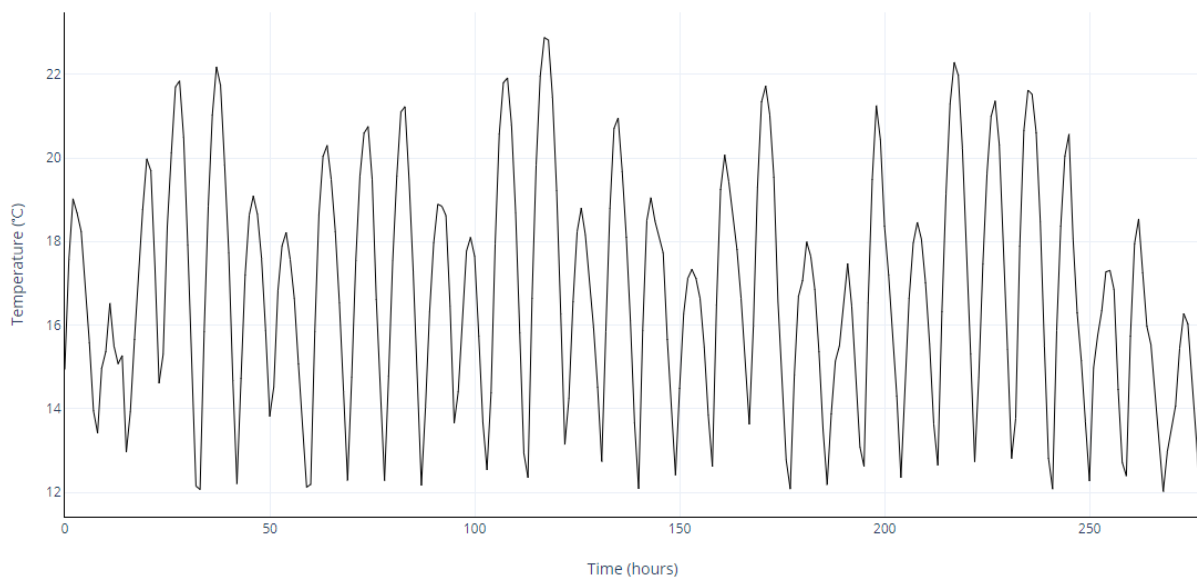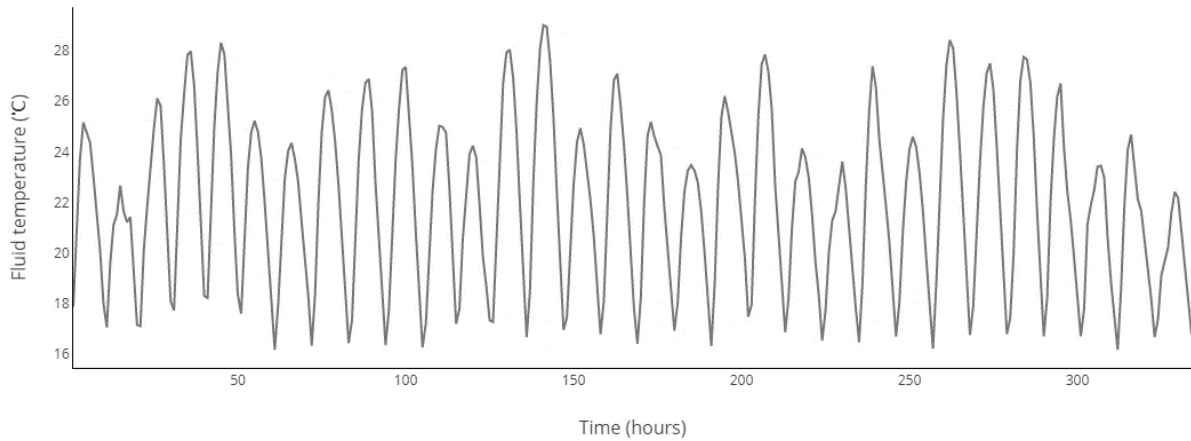
Figure 53 - Fluid temperature profile for Brighton in May using a 15℃ inflow temperature
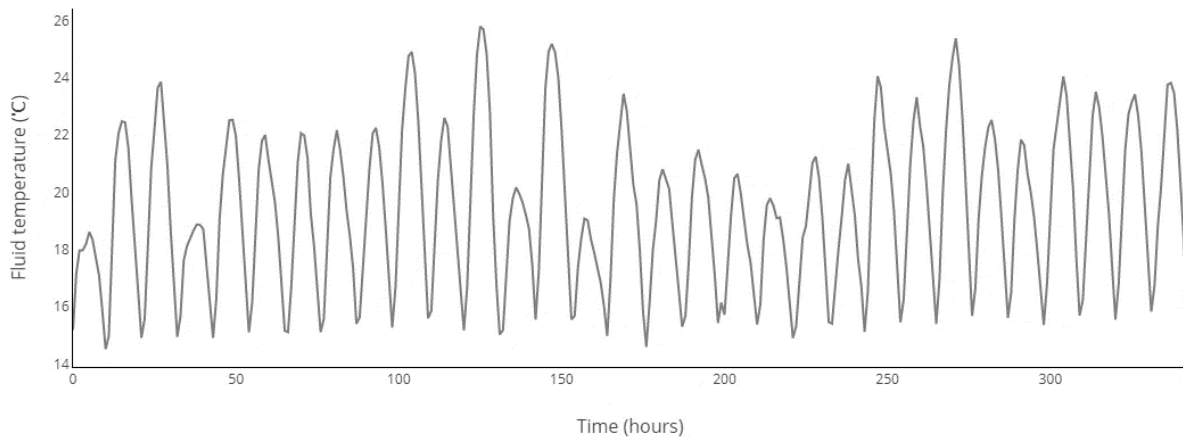
Figure 54 - Fluid temperature profile for Glasgow in May using a 15℃ inflow temperature

7.5.4.1 Results

Figure 55 shows the monthly resulting radial ground temperatures for Brighton. From this the stead increase in ground temperature is monitored, peaking at around 21.5℃ at the borehole wall. Although this temperature is reached by the end of June, the temperature further within the ground continues to rise whereas previously it remained fairly static. This is evidence that a ranging temperature profile is more efficient at transferring heat from within the HTF to the ground, and the results returned display a steady increase throughout the four month period instead of the up and down nature that was exhibited before. By the end of august, there is a net transfer of heat to the ground of approximately 1240 kWh from a total of 8100 kWh

transferred to the HTF. Considering that the recirculation of remaining heat is not considered, this is a much more promising result for the ability of a BHE to be used as a seasonal thermal energy store.
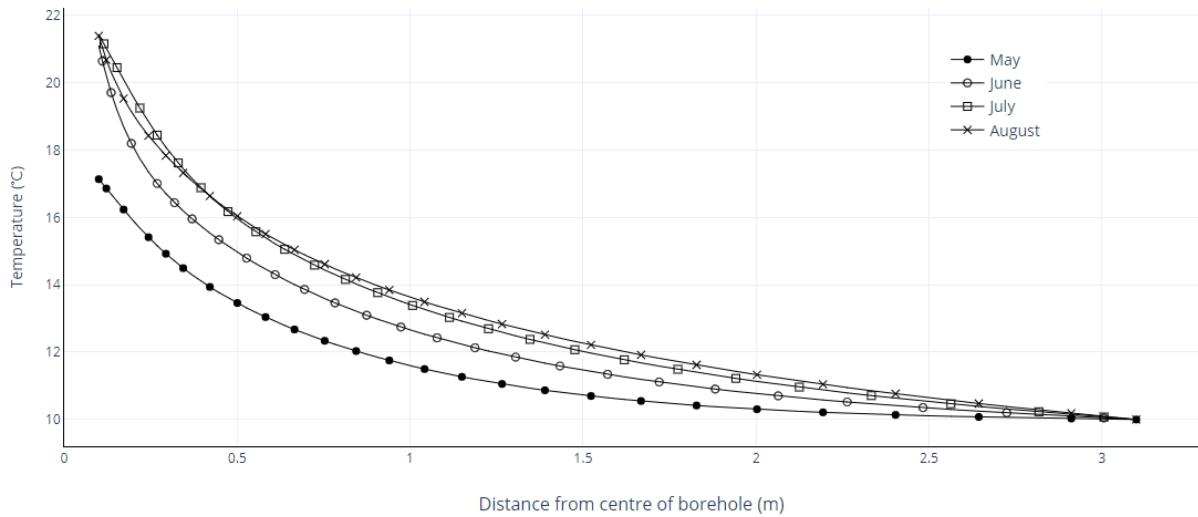
Figure 55 - Brighton radial ground temperature with 15℃ inlet temperature

The results for Glasgow are also much more favourable, resulting in approximately 715 kWh of thermal energy stored within the ground from a total of nearly 5400 kWh between May and August. This represents a total storage efficiency of 15.3% for Brighton and 13.2% for Glasgow, although it is anticipated that this would be higher if loading hours were not run continuously and the recirculation of remaining heat was accounted for.
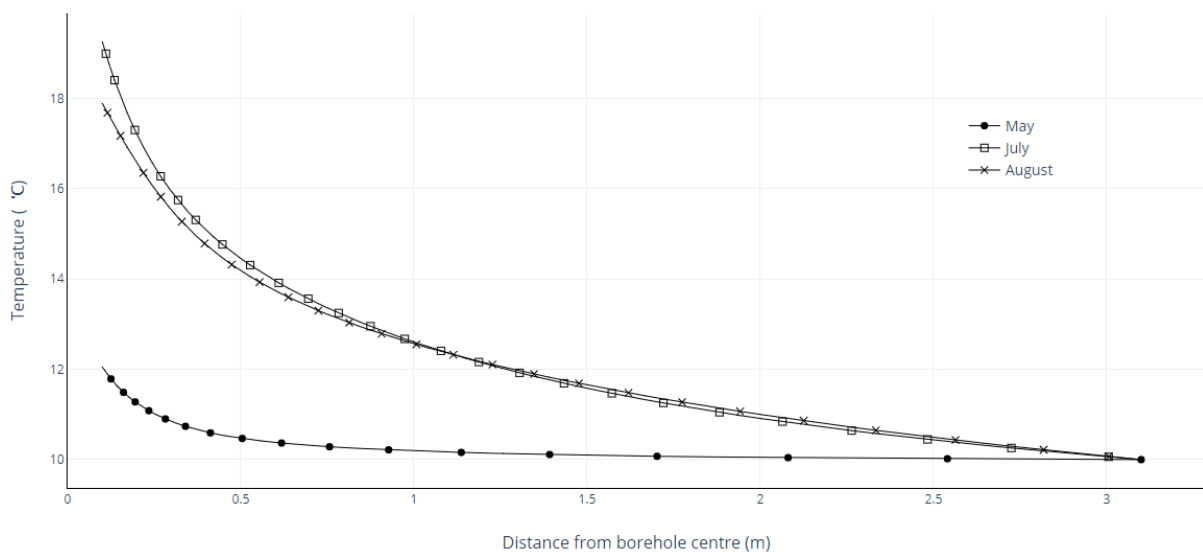
Figure 56 - Glasgow radial ground temperature with 15℃ inlet temperature

71

By raising the temperature of the fluid inflow by only 5℃, the efficiency of the system was improved radially. For both Glasgow and Brighton the results indicate that with some refinement to minimum temperatures allowed through the borehole, as well as the flow pattern, this could be a viable form of energy storage although the results concluded here are not enough to say.

When compared to the heating demand of each relevant home, the quantity of stored thermal energy is not high enough to make a significant contribution towards the heating demand experienced throughout the winter months as it currently stands. Due to time limitations, no further simulations were run and so the efficiency of thermal energy storage over time and the efficiency of energy extraction remains to be found.

8 Conclusion

To conclude, this study did not manage to definitively determine if an individual BHE would be suitable to provide thermal energy storage for a UK home.

The heating demand for space and water heating was assessed on an hourly basis and found to vary dramatically depending on the heat loss coefficient of the home, highlighting the importance of installing energy efficiency measures where possible to reduce thermal losses from the building. The useful energy generated by a FPC was then evaluated and compared with the heating demand and was found to generate varying quantities of excess thermal energy depending upon the heating demand of the household. The FPC array in Brighton performed particularly well, so much so that even short term thermal energy storage in the form of a hot water tank would possible suffice to store and provide enough thermal energy for heating all year round.

A comparison was made between two methods of borehole loading, with a constant and varying loading temperature and from this it was shown that a varying loading temperature generated much better results for the storage of thermal energy. The results that were gathered indicate that such a system may have the potential to store sufficient energy below the ground to be used during the winter, however longer simulations over a number of years would have to be carried out

8.1   Further work

This project has conducted the work to set up and evaluate a BHE, but fell short of providing definitive answers. There is a considerable amount of further work that could be conducted, carrying on the process which was started here.

Firstly, it would be beneficial to be able to run simulations for multiple years as it is known that the performance of BHE improves with time as the temperature within the ground gets steadily higher. As well as this, creating a user defined function that allowed the inlet temperature to a function of outlet temperature as well as the excess thermal energy would be beneficial to model the re-circulation of the HTF through a closed loop system.

For the analysis of an entire system, the use of TRNSYS would prove more beneficial to account for all of the components within the system.

9 References

[1] Gov.uk. (2019). *Welcome to GOV.UK*. [online] Available at: https://www.gov.uk/ [Accessed 13 Aug. 2019].

[2] Gao, L., Zhao, J., An, Q., Wang, J. and Liu, X. (2017). A review on system performance studies of aquifer thermal energy storage. *Energy Procedia*, 142, pp.3537-3545.

[3] GOV.UK. (2018). *Digest of UK Energy Statistics (DUKES): natural gas*. [online] Available at: https://assets.publishing.service.gov.uk/government/uploads/system/uploads/attachment_data /file/820685/Chapter_4.pdf [Accessed 16 Aug. 2019].

[4] Energysavingtrust.org.uk. (2019). [online] Available at: https://www.energysavingtrust.org.uk/sites/default/files/reports/AtHomewithWater(7).pdf [Accessed 18 Jul. 2019].

[5] [5] Cabeza, L., Martorell, I., Miro, L., Fernandez, A. and Barreneche, C. (2015). Introduction to thermal energy storage (TES) systems. *Advances in thermal energy storage systems*, [online] pp.1-28. Available at: https://www.sciencedirect.com/science/article/pii/B9781782420880500018 [Accessed 10 Aug. 2019].

[6] Kenisarin, M. (2010). High-temperature phase change materials for thermal energy storage. *Renewable and Sustainable Energy Reviews*, 14(3), pp.955-970.

[7] Liu, M., Saman, W. and Bruno, F. (2012). Review on storage materials and thermal performance enhancement techniques for high temperature phase change thermal storage systems. *Renewable and Sustainable Energy Reviews*, pp.2118 - 2132.

[8] Ehrlich, Robert (2013). "Thermal storage". *Renewable Energy: A First Course*. CRC Press. p. 375

[9] Blanco, M. and Santigosa, L. (2017). *Advances in concentrating solar thermal research and technology*. Woodhead Publishing Series in Energy, pp.213 - 246.

[10] Aydin, D., Casey, S. and Riffat, S. (2015). The latest advancements on thermochemical heat storage systems. *Renewable and Sustainable Energy Reviews*, 41, pp.356-367.

[11] Socaciu, L. (2011). Seasonal Sensible Thermal Energy Storage Solutions. *Leonardo Electronic Journal of Practices and Technologies*, (19), pp.49 - 68.

[12] Reuss, M. (2019). The use of borehole thermal energy storage (BTES) systems. *Advances in thermal energy storage systems*, [online] pp.117-147. Available at: https://www.sciencedirect.com/science/article/pii/B9781782420880500067 [Accessed 10 Aug. 2019].

[13] Lee, K. (n.d.). Numerical Simulation on the Continuous Operation of Aquifer Thermal Energy Storage System. [online] Available at: http://cdn.intechopen.com/pdfs/11909/InTech-Numerical_simulation_on_the_continuous_operation_of_aquifer_thermal_energy_storage_system.pdf [Accessed 16 Aug. 2019].

[14] Dlsc.ca. (2019). *Drake Landing Solar Community*. [online] Available at: https://www.dlsc.ca/homes.htm [Accessed 10 Aug. 2019].

[15] Sibbitt, B., McClenahan, D., Djebbar, R., Thornton, J., Wong, B., Carriere, J. and Kokko, J. (2011). *MEASURED AND SIMULATED PERFORMANCE OF A HIGH SOLAR FRACTION DISTRICT HEATING SYSTEM WITH SEASONAL STORAGE*. [online] Available at: https://www.dlsc.ca/reports/bjul15/ISES_SWC_2011_final.pdf [Accessed 10 Aug. 2019].

[16] Mesquita, L., McClenahan, D., Thornton, J., Carriere, J. and Wong, B. (2017). Drake Landing Solar Community: 10 Years of Operation. *ISES Solar World Congress 2017*. [online] Available at: https://www.dlsc.ca/reports/swc2017-0033-Mesquita.pdf [Accessed 1 Aug. 2019].

[17] Nilsson, E. and Rohdin, P. (2019). Performance evaluation of an industrial borehole thermal energy storage (BTES) project – Experiences from the first seven years of operation. *Renewable Energy*, 143, pp.1022-1034.

[18] Gao, L., Zhao, J. and Tang, Z. (2015). A Review on Borehole Seasonal Solar Thermal Energy Storage. *Energy Procedia*, 70, pp.209-218.

[19] Trillat-Berdal, V., Souyri, B. and Fraisse, G. (2006). Experimental study of a ground-coupled heat pump combined with thermal solar collectors. *Energy and Buildings*, 38(12), pp.1477-1484.

[20] Beier, R., Smith, M. and Spitler, J. (2011). Reference data sets for vertical borehole ground heat exchanger models and thermal response test analysis. *Geothermics*, 40(1), pp.79-85.

[21] Mainwaring, N. (2019). *Dwelling Stock Estimates: 31 March 2018, England*. Ministry of Housing, Communities, and Local Government.

[22] Yang, H., Cui, P. and Fang, Z. (2010). Vertical-borehole ground-coupled heat pumps: A review of models and systems. *Applied Energy*, 87(1), pp.16-27.

[23] Ingersoll LR, Adler FT, Plass HJ, Ingersoll AC. Theory of earth heat exchangers for the heat pump. ASHVE Trans 1950;56:167–88.

[24] Carslaw HS, Jaeger JC. Conduction of heat in solids. Oxford UK: Claremore Press; 1946

[25] Ingersoll LR, Zobel OJ, Ingersoll AC. Heat conduction with engineering, geological, and other applications. New York: McGraw-Hill; 1954.

[26] Yang, H., Cui, P. and Fang, Z. (2010). Vertical-borehole ground-coupled heat pumps: A review of models and systems. *Applied Energy*, 87(1), pp.16-27.

[27] Resources, e. (2019). *Welcome | TRNSYS : Transient System Simulation Tool*. [online] Trnsys.com. Available at: http://www.trnsys.com/ [Accessed 22 Aug. 2019].

[28] Ansys.com. (2019). *ANSYS Fluent Software | CFD Simulation*. [online] Available at: https://www.ansys.com/products/fluids/ansys-fluent [Accessed 22 Aug. 2019].

[29] Kalogirou, S. (2004). Solar thermal collectors and applications. *Progress in Energy and Combustion Science*, pp.231 - 295.

[30] Lenel, U. R. (1984). A REVIEW OF MATERIALS FOR SOLAR HEATING SYSTEMS FOR DOMESTIC HOT WATER (Vol. 32).

[31] Nakoa, K., Karim, M., Mahmood, S. and Akhanda, M. (2011). Effect of Colored Absorbers on the Performance of a Built-In-Storage Type Solar Water Heater. *International journal of renewable energy research*, 1(4), pp.232 - 239.

[32] Rodríguez-Hidalgo, M., Rodríguez-Aumente, P., Lecuona, A., Gutiérrez-Urueta, G. and Ventas, R. (2011). Flat plate thermal solar collector efficiency: Transient behavior under working conditions. Part I: Model description and experimental validation. *Applied Thermal Engineering*, 31(14-15), pp.2394-2404.

[33] Bre.co.uk. (2019). *BRE Group: BRE Domestic Energy Model (BREDEM 2012)*. [online] Available at: https://www.bre.co.uk/page.jsp?id=3176 [Accessed 18 Jul. 2019].

[34] Karacavus, B. and Can, A. (2009). Thermal and economical analysis of an underground seasonal storage heating system in Thrace. *Energy and Buildings*, 41(1), pp.1-10.

[35] Duffie, J. and Beckman, W. (2013). *Solar Engineering of Thermal Processes*. Somerset: Wiley.

[36] GOV.UK. (2019). *Definitions of general housing terms*. [online] Available at: https://www.gov.uk/guidance/definitions-of-general-housing-terms [Accessed 4 Aug. 2019].

[37] Horscroft, D. (2019). *Families and households in the UK - Office for National Statistics*. [online] Ons.gov.uk. Available at: https://www.ons.gov.uk/peoplepopulationandcommunity/birthsdeathsandmarriages/families/bulletins/familiesandhouseholds/2016 [Accessed 2 Aug. 2019].

[38] Renewables.ninja. (2019). *Renewables.ninja*. [online] Available at: https://www.renewables.ninja/ [Accessed 4 Aug. 2019].

[39] M. Shipworth, S.K. Firth, M. Gentry, J.A. Wright, D. Shipworth, K.J. Lomas. Central heating thermostat settings and timing: building demographics. Building Research & Information, 38 (2010), pp. 50-69

[40] Homemicro.co.uk. (2019). [online] Available at: http://www.homemicro.co.uk/download/lzc_uvalue.pdf [Accessed 7 Aug. 2019].

[41] Wingfield, J, Bell, M, Miles-Shenton, D, South, T and Lowe, R J (2009) Evaluating the impact of an enhanced energy performance standard on load-bearing masonry construction: final report. PII Project CI39/3/663. Leeds: Leeds Metropolitan University.

[42] Schmidt, T., Mangold, D. and Müller-Steinhagen, H. (2004). Central solar heating plants with seasonal storage in Germany. *Solar Energy*, 76(1-3), pp.165-174.

[43] Ma, Z., Bao, H. and Roskilly, A. (2018). Feasibility study of seasonal solar thermal energy storage in domestic dwellings in the UK. *Solar Energy*, 162, pp.489-499.

[44] Assets.publishing.service.gov.uk. (2019). [online] Available at: https://assets.publishing.service.gov.uk/government/uploads/system/uploads/attachment_data /file/48188/3147-measure-domestic-hot-water-consump.pdf [Accessed 18 Jul. 2019].

[45] Ovoenergy.com. (2019). *How much energy do you use to heat your home? | OVO Energy*. [online] Available at: https://www.ovoenergy.com/guides/energy-guides/how-much-heating-energy-do-you-use.html [Accessed 4 Aug. 2019].

[46] Socaciu, Lavinia. (2012). SEASONAL THERMAL ENERGY STORAGE CONCEPTS. 55. 775-784.

[47] Media.springernature.com. (2019). [online] Available at: https://media.springernature.com/lw785/springer-static/image/art%3A10.1186%2Fs40517-015-0027-3/MediaObjects/40517_2015_27_Fig1_HTML.gif [Accessed 23 Aug. 2019].

[48] L. Lamarche, B. Beauchamp. New Solutions for the Short-Time Analysis of Geothermal Vertical Boreholes, vol. 50 (2007), pp. 1408-1419

[49] Renaldi, R. and Friedrich, D. (2019). Techno-economic analysis of a solar district heating system with seasonal thermal storage in the UK. *Applied Energy*, 236, pp.388-400.

[50] Map.environment.gov.scot. (2019). *Scotland's Soils - soil maps*. [online] Available at: http://map.environment.gov.scot/Soil_maps/?layer=1 [Accessed 14 Aug. 2019].

[51] Landis.org.uk. (2019). *Soilscapes soil types viewer - National Soil Resources Institute. Cranfield University*. [online] Available at: http://www.landis.org.uk/soilscapes/ [Accessed 14 Aug. 2019].

[52] Mesquita, L., Mcclenahan, D., Thornton, J., Carriere, J. and Wong, B. (2017). Drake Landing Solar Community: 10 years of operation. [online] Available at: https://www.dlsc.ca/reports/swc2017-0033-Mesquita.pdf [Accessed 22 Aug. 2019].

[53] Johnston, D., Wingfield, J., Miles-Shenton, D., 2010. Measuring the fabric performance of
UK dwellings. In: Proceedings of 26th Annual ARCOM Conference, 6–8 September

10 Appendix

Appendix I – FPC calculation process

The following process is used to calculate the useful thermal energy generated by a flat plate collector. This used a number of equations that can be found in 'Solar engineering of thermal processes' [35]. These equations are collected, ordered, and explained by Ma et al [43], and the write up of the process which follows is taken from this paper with the omission of a few equations that are not required but were provided anyway. Solar positioning equations can easily be found online.

Equations for the calculation of useful energy gained by a FPC

The angle of incidence, θ, is the angle between the beam radiation and the normal to the surface should be calculated first by the following equation

$$\cos\theta = \sin\delta\sin\phi\cos\beta - \sin\delta\cos\phi\sin\beta\cos\gamma + \cos\delta\cos\phi\cos\beta\cos\omega + \cos\delta\sin\phi\sin\beta\cos\gamma\cos\omega + \cos\delta\sin\beta\sin\gamma\sin\omega$$

where ϕ is the latitude of the location; β is the angle of the surface; γ is the surface azimuth angle with due south zero, west positive and east negative; ω is the hour angle, with noon zero, morning negative and afternoon positive; δ is the solar declination that can be calculated by the following:

$$\delta = \frac{180}{⍰}(0.006918 - 0.399912\cos B + 0.070257\sin B - 0.006758\cos 2B + 0.000907\sin 2B - 0.002697\cos 3B + 0.00148\sin 3B)$$

B = 360(n-1)/365

Where n is the number of the day of the year.

The figure below is provided to help visualise the angles that either are known or have to be calculated:
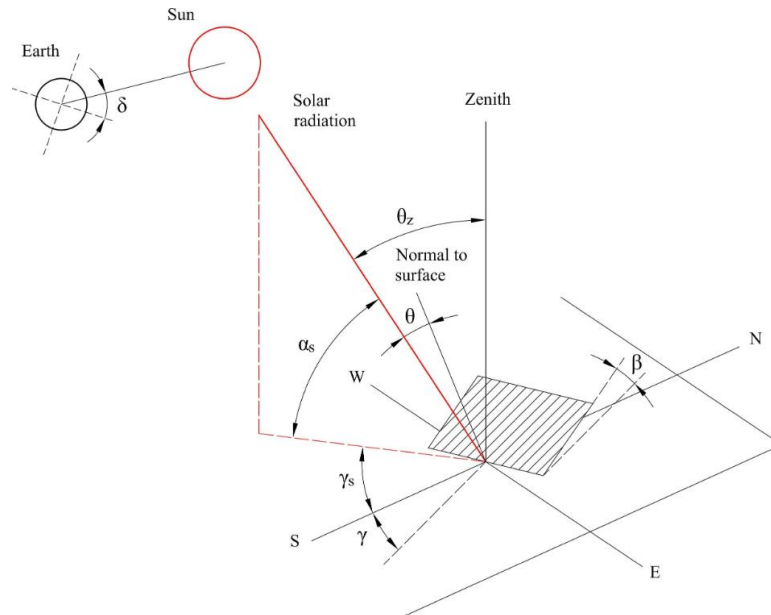
To find the surface azimuth angle, use the following equation:

$$\cos\theta_z = \sin\delta\sin\phi + \cos\delta\cos\phi\cos\omega$$

And therefore the extraterrestrial radiation on a horizontal surface between any interval of solar angle ω_1 and ω_2:

$$I_{oH} = \frac{12*3600}{\pi} G_{sc}\left(1 + 0.033\cos\frac{360n}{365}\right)(cos\phi\cos\delta\,(\sin\omega_2 - \sin\omega_1) + \frac{\pi(\omega_2 - \omega_1)}{180}\sin\phi\sin\delta)$$

Where G_{sc} is the solar constant equal to 1367 W/m^2.

Beam and diffusion components

The value of solar radiation provided through a pyranometer or satellite data is the sum of the beam and diffuse components. The ratio of these two components can be found through the hourly clearness index, K_T:

$$K_T = \frac{I_H}{I_{oH}}$$

Where I_H is the hourly solar irradiance measured on a horizontal surface, commonly available as pyranometer measurement data. Then the diffuse fraction can be calculated by the following:

$$\frac{I_{dH}}{I_H} = \begin{cases} 1 - 0.09K_T & for\ K_T \leq 0.22 \\ 0.9511 - 0.1604K_T + 4.388K_T - 16.638\ K_T + 12.336K_T & for\ 0.22 \leq K_T \leq 0.80 \\ 0.165 & for\ K_T \geq 0.80 \end{cases}$$

Where I_{dH} is the hourly diffusional irradiance on a horizontal surface. From this the <u>beam radiation</u> I_{bH} can be calculated as:

$$I_{bH} = I_H - I_{dH}$$

Solar radiation on a tilted surface

From the provided values for hourly horizontal solar irradiance and the calculated diffuse and beam components, the total solar radiation on a tilted surface is found:

$$I_T = I_{bH}R_b + I_{dH}\left(\frac{1 + \cos\beta}{2}\right) + I_H\rho_g\left(\frac{1 - \cos\beta}{2}\right)$$

$$R_b = \frac{\cos\theta}{\cos\theta_z}$$

Where ρ_g is the ground reflectivity, with values for different surfaces available commonly online.

Solar thermal energy absorbed by a FPC

100% of the incident radiation is not absorbed by the absorber due to the transmission, reflection and absorption by different parts of the solar collector. As shown below if the figure, transmittance-absorptance product, τα, is calculated as the ratio of absorbed radiation to the total incident radiation by the following equation:

$$\tau\alpha \cong 1.01\,\tau\alpha$$

Where:

$$\tau \cong \tau_a\tau_r$$

and:

$$\tau_a = \exp(-\frac{KL}{\cos\theta_2})$$

Where K is the extinction coefficient of the panel; L is the thickness of the glass cover; θ_2 is the incident angle to the absorber plate following refraction from the glass as found by the following equation:

$$n_1 \sin\theta_1 = n_2 \sin\theta_2$$

Where n is the refraction index, with glass having an average value of 1.526 and air having a value near 1.

The following are used for reflectance transmittance:

$$\tau_r = \frac{1}{2}\left(\frac{1 - r_1}{1 + r_1} + \frac{1 - r_2}{1 + r_2}\right)$$

$$r_1 = \frac{sin^2(\theta_2 - \theta_1)}{sin^2(\theta_2 + \theta_1)}$$

$$r_2 = \frac{tan^2(\theta_2 - \theta_1)}{tan^2(\theta_2 + \theta_1)}$$

The absorptance of the plate can be found through:

$$\frac{\alpha}{\alpha_n} = 1 - (1.5879 * 10^{-3}\theta) + (2.7314 * 10^{-4}\theta^2) - (2.3026 * 10^{-5}\theta^3)$$
$$+ (9.0244 * 10^{-7}\theta^4) - (1.8 * 10^{-8}\theta^5) + (1.7734 * 10^{-10}\theta^6) - (6.9937 * 10^{-13}\theta^7)$$

Where α_n is the solar absorptance at normal incidence for a flat black surface independent of incident angle.

For a tilted flat-plate solar collector, the absorbed radiation, S, is given based on the total incident radiation I_T and the transmittance-absorptance products:

$$S = I_{bH}R_b\tau\alpha_b + I_{dH}\left(\frac{1 + \cos\beta}{2}\right)\tau\alpha_d + I_H\rho_g\left(\frac{1 - \cos\beta}{2}\right)\tau\alpha_g$$

where the subscript *b*, *d* and *g* represent beam, diffusion and ground reflection respectively. The beam incident angle is used straightforwardly to determine the value of $\tau\alpha^{-}b$; however, effective incident angles should be calculated by the following equations to determine $\tau\alpha_d$ and $\tau\alpha_g$ for diffusion and ground reflected radiation of a tilted surface.

$$\theta_{ed} = 59.7 - 0.1388\beta + \beta^2$$
$$\theta_{eg} = 59.7 - 0.1388\beta + \beta^2$$

The useful thermal energy output from a flat-plate solar collector can be calculated by the following equation.

$$Q_u = A_{sc}F_R[S - U_L(T_i - T_a)]$$

where A_{sc} is the collector surface area; U_L is the heat loss coefficient; T_i is the inlet HTF temperature; T_a is the ambient temperature; F_R is the collector heat removal factor, which can be estimated based on following equations with the collector dimensions shown in the figure below:

$$F_R = \frac{\dot{m}C_p}{A_{sc}U_L}\left[1 - \exp\left(-\frac{A_{sc}U_LF'}{\dot{m}C_p}\right)\right]$$

$$F' = \frac{1/U_L}{W\left[\frac{1}{U_L[D + (W - D)F]} + \frac{1}{C_b} + \frac{1}{\pi D_i h_{fi}}\right]}$$

$$F = \frac{\tanh[\frac{m(W - D)}{2}]}{\frac{m(W - D)}{2}}$$

$$m = \sqrt{\frac{U_l}{k\delta_p}}$$

where ṁ is the mass flow rate of HTF; c_p is the specific heat of HTF; k is the thermal conductivity of the absorber plate; C_b is the bond conductance; h_{fi} is the HTF heat transfer coefficient, which can be calculated by the classical heat transfer correlations.
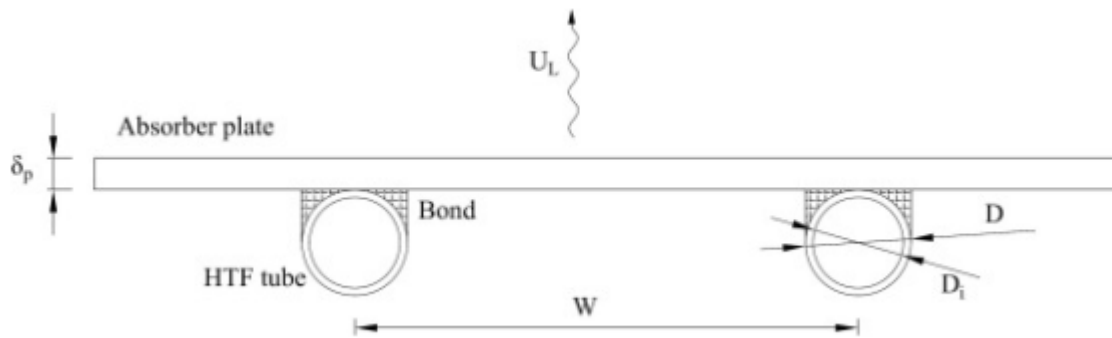
Appendix II – FPC panel data used for calculating useful energy output.

Parameter	Value
K	$16\,\mathrm{m}^{-1}$
L	$4.2\,\mathrm{mm}$
α_n	0.93
$^b A_{sc}$	$1.94\,\mathrm{m}^2$
U_L	$6\,\mathrm{W/(m^2\,K)}$
$^c \dot{m}$	$50\,\mathrm{kg/(h\,m^2)}$
k	$400\,\mathrm{W/(m\,K)}$
C_b	$\infty\ \mathrm{W/(m\,K)}$
W	$114\,\mathrm{mm}$
D	$10\,\mathrm{mm}$
D_i	$8\,\mathrm{mm}$
δ_p	$0.5\,\mathrm{mm}$

Appendix III - Table of possible storage materials for sensible energy storage and their thermal properties.

Material	Thermal conductivity (W/mK)	Volumetric heat capacity (MJ/m^3)	Density (10^3 kg/m^3)
Unconsolidated			
Clay/silt, dry	0.4–1.0	1.5–1.6	1.8–2.0
Clay/silt, water-saturated	1.1–3.1	2.0–2.8	2.0–2.2
Sand, dry	0.3–0.9	1.3–1.6	1.8–2.2
Sand, water-saturated	2.0–3.0	2.2–2.8	1.9–2.3
Gravel/stones, dry	0.4–0.9	1.3–1.6	1.8–2.2
Gravel/stones, water-saturated	1.6–2.5	2.2–2.6	1.9–2.3
Till/loam	1.1–2.9	1.5–2.5	1.8–2.3
Sedimentary rock			
Clay/silt stone	1.1–3.4	2.1–2.4	2.4–2.6
Sandstone	1.9–4.6	1.8–2.6	2.2–2.7
Conglomerate/breccia	1.3–5.1	1.8–2.6	2.2–2.7
Marlstone	1.8–2.9	2.2–2.3	2.3–2.6
Limestone	2.0–3.9	2.1–2.4	2.4–2.7
Dolomitic rock	3.0–5.0	2.1–2.4	2.4–2.7

Appendix IV – Calculations followed to determine monthly average hot water consumption for a dwelling as is done in the BREDEM method [U]. Some values such as the number of showers and baths taken per day as well as hot and cold water delivery temperatures were taken from the Energy Savings Trust report [reference]. The results from this process are attributed to Q_{HW}.

2.1 The volume and energy content of heated water

Data item	Symbol	Type	Units	Notes
Number of showers per day	n_{shower}	User input / calculated	Showers/day	Step A
Number of occupants	N	User input / calculated	Occupants	From §1 A
Daily hot water requirement for showers	$V_{d,shower}$	Calculated	Litres/day	Step B
Hot water use per shower	V_{PS}	User input / from table	Litres	From Table 6
Number of baths per day	n_{bath}	User input / calculated	Baths/day	Step C
Daily hot water requirement for baths	$V_{d,bath}$	Calculated	Litres/day	Step D
Daily hot water requirement for other uses	$V_{d,other}$	Calculated	Litres/day	Step E
Average daily hot water requirement	$V_{d,ave}$	Calculated	Litres/day	Step F
Daily hot water requirement in month m	$V_{d,m}$	Calculated	Litres/day	Step G
Monthly hot water use factor	f_{hw}	Constants / from table	Dimensionless	From Table 7
Monthly rise in temperature required	ΔT_m	Constants / from table	°C	From Table 8
Monthly energy content of heated water	$Q_{HW,m}$	Calculated	kWh/month	Step H
Number of days in month, m	n_m	Constants	Days	Use 28 for February
Annual energy content of heated water	Q_{HW}	Calculated	kWh/yr	Step I

A. If the number of showers taken per day is known use the actual figure, otherwise
   $n_{shower} = 0.45\ N + 0.65$
B. $V_{d,shower} = n_{shower}\ x\ V_{PS}$
C. If the number of baths taken per day is known use the actual figure, otherwise
   If no shower is present $n_{bath} = 0.35\ N + 0.5$
   If a shower is also present $n_{bath} = 0.13\ N + 0.19$
D. $V_{d,bath}\quad = n_{bath}\ x\ 50.8$
E. $V_{d,other}\ = 9.8N + 14$
F. $V_{d,ave}\quad = V_{d,shower} + V_{d,bath} + V_{d,other}$
G. $V_{d,m}\quad = V_{d,ave}\ x\ f_{hw}$
H. Calculate monthly energy content of the heated water
   $Q_{HW,m}\quad = 4.18\ x\ V_{d,m}\ x\ n_m\ x\ \Delta T_m /3600$
I. $Q_{HW} = \sum Q_{HW,m}$

Table 6: Hot water use per shower

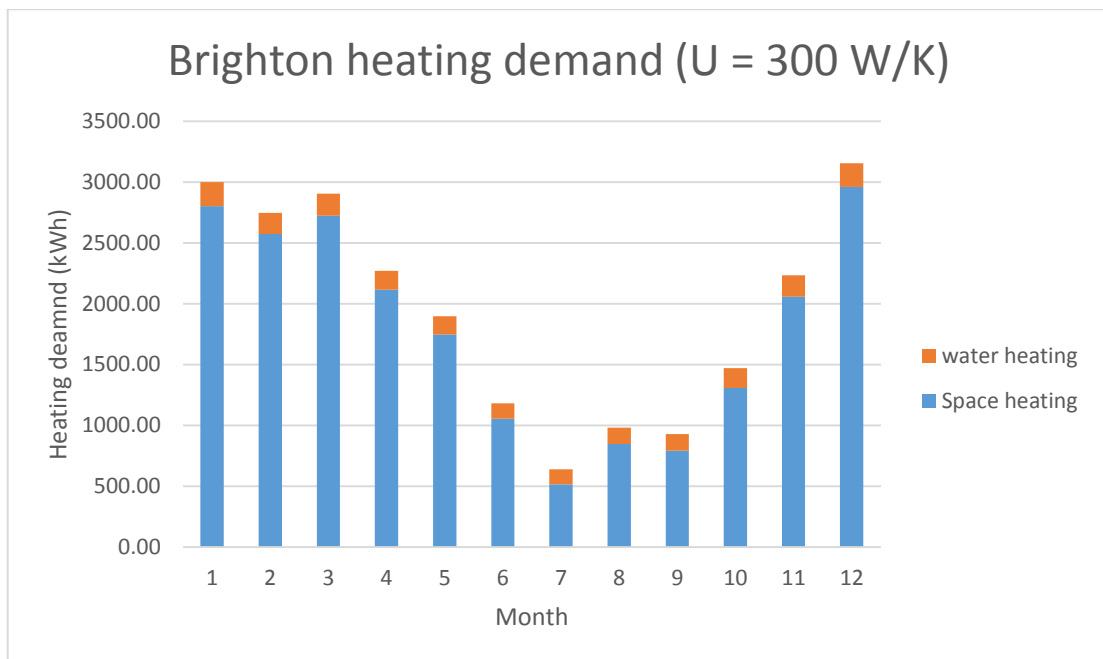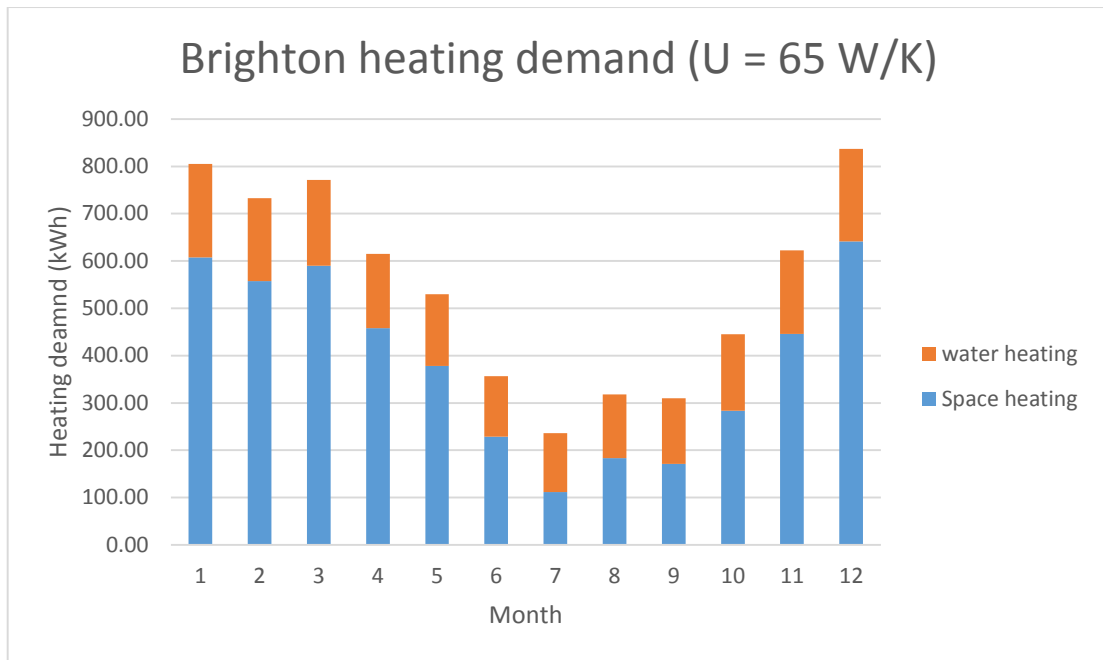| Shower type	Hot water use per shower, V_{PS} (litres)
None	0
Mixer (not combi)	28.8
Mixer (combi)	44.4
Pumped	43.5
Electric	0
Unknown	18.7

If more than one shower type present, choose the one that is used most often.

Table 7: Monthly hot water use factor

Month	Jan	Feb	Mar	Apr	May	Jun	Jul	Aug	Sep	Oct	Nov	Dec
Month factor, f_{hw}	1.10	1.06	1.02	0.98	0.94	0.90	0.90	0.94	0.98	1.02	1.06	1.10

Appendix V – Charts showing the monthly average heating demand for Glasgow and Brighton based dwellings with overall heat loss coefficients of 65 and 300 W/K. Total heating demand is split between water (orange) and space heating (blue).

Glasgow heating demand (U = 65 W/K)

Glasgow heating demand (U = 300 W/K)

Brighton heating demand (U = 65 W/K)

Brighton heating demand (U = 300 W/K)
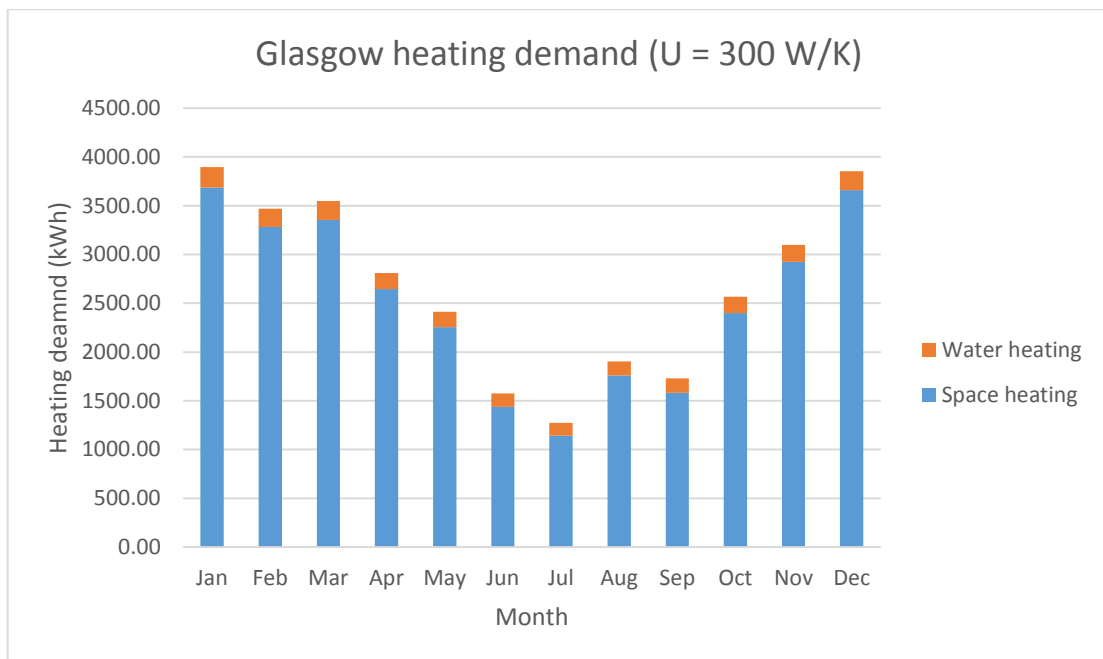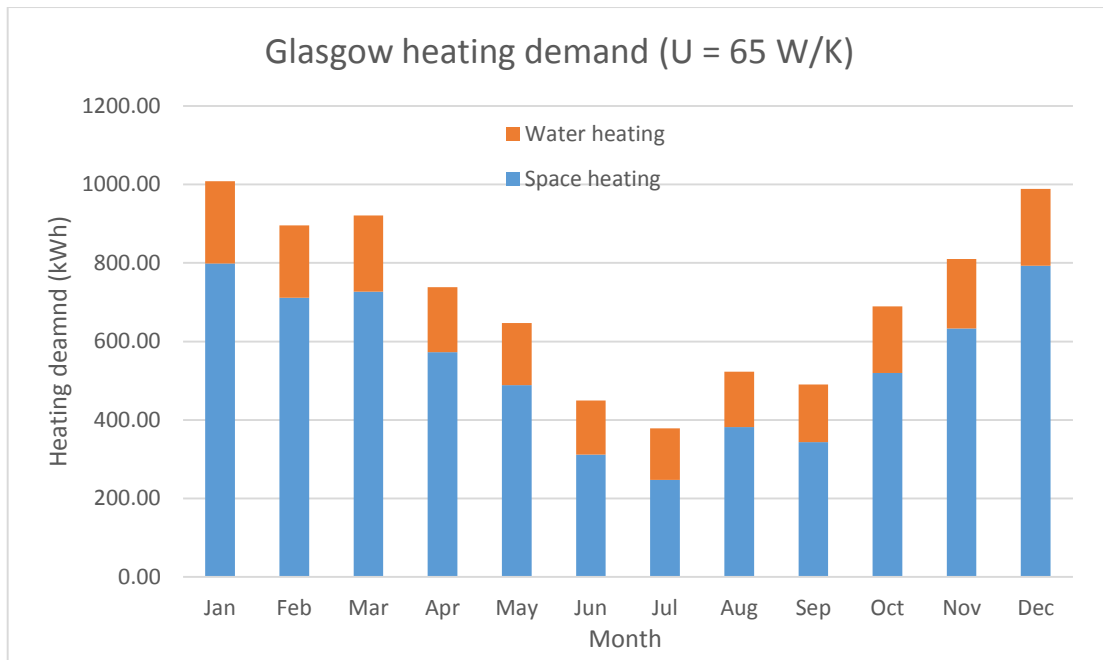
Appendix VI – Image highlighting the far boundaries of the soil and grout to which the boundary conditions were applied of an initial ground temperature of 283.15 K.

Appendix XII – Map legends used when identifying the soil types surround Glasgow (left) [50] and Brighton (right) [51].

National Soil Map of Scotland: Generalised Soil Type

- Alluvial soils
- Brown soils
- Calcareous soils
- Immature soils
- Mineral gleys
- Mineral podzols
- Montane soils
- Peat
- Peaty gleys
- Peaty podzols
- Lochs

- Freely draining slightly acid sandy soils
- Freely draining very acid sandy and loamy soils
- Lime-rich loamy and clayey soils with impeded drainage
- Loamy and clayey floodplain soils with naturally high groundwater
- Loamy and clayey soils of coastal flats with naturally high groundwater
- Loamy and sandy soils with naturally high groundwater and a peaty surface
- Loamy soils with naturally high groundwater
- Naturally wet very acid sandy and loamy soils
- Raised bog peat soils
- Restored soils mostly from quarry and opencast spoil
- Saltmarsh soils
- Sand dune soils
- Shallow lime-rich soils over chalk or limestone
- Shallow very acid peaty soils over rock